1967-09

The analysis of a log-periodic zig-zag antenna

Gonsalves, Victor Manuel Nogueira Novais

Monterey, California. U.S. Naval Postgraduate School

THE ANALYSIS OF A LOG-PERIODIC ZIG-ZAG ANTENNA

VICTOR MANUEL NOGUEIRA NOVAIS GONSALVES

50

[redacted]

THE ANALYSIS OF A LOG-PERIODIC ZIG-ZAG ANTENNA

by

Victor Manuel Nogueira Novais Gonsalves
Lieutenant, Portuguese Navy
B. S., Escola Naval, Alfeite, Portugal, 1957

Submitted in partial fulfillment of the requirements
for the degree of

MASTER OF SCIENCE IN ENGINEERING ELECTRONICS

from the

NAVAL POSTGRADUATE SCHOOL
September 1967

ABSTRACT

During recent years, logarithmically periodic antennas have been widely used due to their frequency response characteristics, simplicity of design and directivity. However, their theory of operation still is in a development phase, and very few models have been fully analyzed. The present paper is an attempt to analyze the operation of a zig-zag model that has the property of being symmetrical, and suitable for operation against ground. The radiation pattern of the antenna is obtained for different models of current distribution, and, finally, the impedance characteristics and an approximate current distribution are obtained, using non-uniform transmission line theory. The results obtained show reasonable agreement with experimental data, and confirm conclusions drawn from physical considerations.

TABLE OF CONTENTS

LIST OF ILLUSTRATIONS

I - LOG-PERIODIC ANTENNAS - HISTORICAL BACKGROUND

1.1 - Frequency Independent Antennas and Log-Periodic Antennas

Frequency independent antennas were originated in 1954, when V. H. Rumsey [14] started the idea that a structure characterized by angles, and without any characteristic length dimension, should behave independently of the frequency of operation. As a practical example, Rumsey proposed an equiangular spiral structure. J. D. Dyson carried out a study of such a structure composed of two plane sheets of metal extending from a central point according to this geometry, and he proved that the model not only had frequency independence characteristics, but also that the interesting part of the antenna was confined to the area inside an "active region," where the dimensions become of the order of half a wavelength. That is, the outward area is not necessary and the structure can be truncated at a convenient size, and will be useful within a range of frequencies whose lower limit is determined by the peripheral dimensions, and whose upper limit is determined by the spacing at the feeding terminals, near the center of the antenna.

A structure like this is bidirectional and has circular polarization. Also, since the active region rotates along the spiral, the polarization rotates too. Strictly speaking, then, not all the characteristics of the antenna are frequency independent, but, instead, they repeat periodically every time the frequency is changed so as to reproduce a reference space condition. The input characteristics, pattern shape and field intensity are constant.

One year later, in 1955, R. H. DuHamel, who was working with Rumsey in broadband antenna development, proposed a structure that, instead of being entirely defined by angles, was interrupted by discontinuities

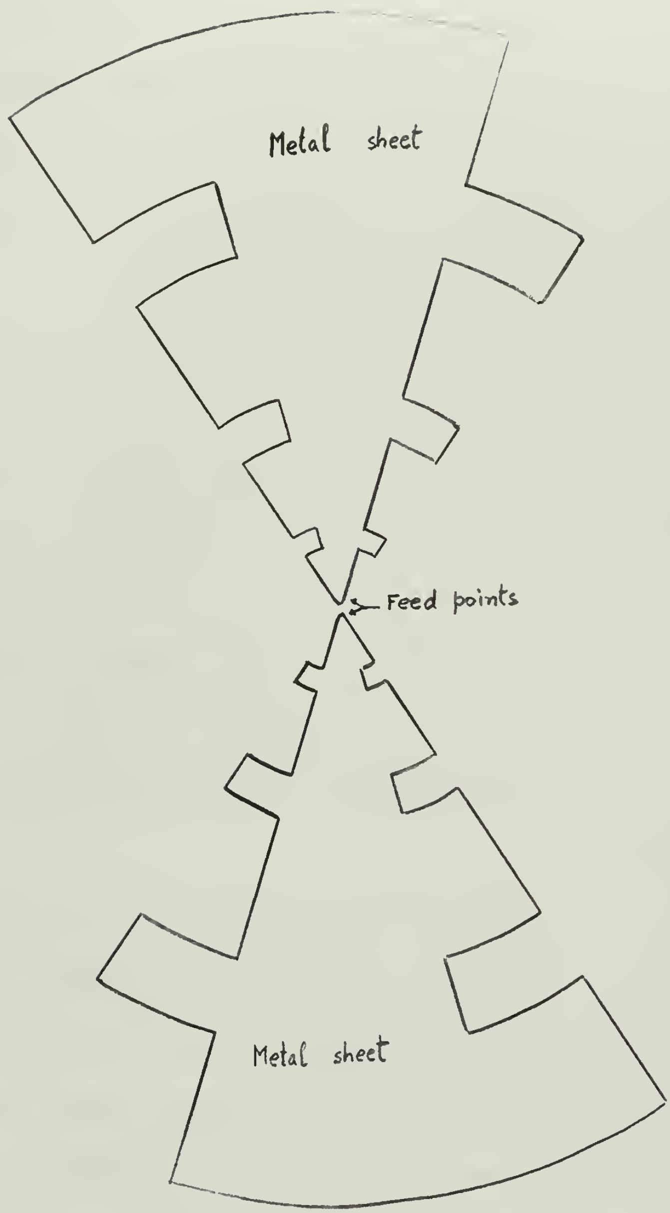

Fig. 1 - DuHamel's log-periodic teeth structure

properly located. The first model built (Fig. 1) was formed by a circular sheet of metal, cut along two symmetrical circular sectors, and with teeth placed along the radial edges. The size of the teeth and their distances to the center, are related by a constant ratio p. It is evident that such a structure, within its size limits, will repeat its radiating characteristics every time the frequency changes by p; that is, for all the set $[p^n f_0]$. A plot of these frequencies in a logarithmic scale will show them equally spaced by log p, and that is the origin of the name log-periodic given to this kind of geometry.

The model shown in Fig. 1 is a bidirectional antenna with large half power beam width. Bending one of the halves of the antenna toward the other, so as to form an acute angle, D. E. Isbell obtained a unidirectional antenna with the surprising characteristic of radiating toward the vertex; that is, backward in relation to the feed. Meanwhile, proceeding with his work in the equiangular spiral antenna, Dyson devised another unidirectional antenna by wrapping the two metal sheets of the planar spiral around a cone. Again, he obtained a backward radiating structure, whose characteristics could be adjusted by means of the cone angle and the spiral rate of growth.

These two pioneer models brought log-periodic antennas to the field of practical application; and they, and their variations, have been extensively used in the VHF band and above. They are particularly suited for military applications where more often than not, a single antenna is required to cover a very large range of frequencies. As it might be expected, these antennas have moderate gains, and for fixed circuit applications they do not match high gain structures. However, when a trade between even performance along a large band, and optimum performance only

at one frequency or narrow band is allowed, the log-periodic models offer the best possibilities.

1.2 - Unidirectional Planar Structures

Traditionally, it is with the lower frequencies that the search for efficient radiating systems has been less successful. Good electrical performance has been obtained at the expense of size, and, although theoretically it would be possible to build optimum systems, the costs involved in the ground occupied and the hardward employed make such attempts prohibitive. In the HF band, the best compromise between size and operational characteristics, during the past three decades, has been the rhombic antenna. Today, the rhombic still is the practical structure with highest gain, and when used with a range of frequencies within a ratio of not more than 3:1, it still might be the best answer for an HF radio link. Its main inconveniences are the size and the variable take-off angle, but the latter can be used with advantage by appropriate selection of frequency according to ionospheric conditions.

The log-periodic models of the type mentioned above are not, in general, feasible for HF long range communications. Besides being too bulky, they employ sheets of metal that would make the cost too high. Two important developments were to come, and solve these two problems.

The first was when DuHamel and his research team verified that only the peripheral strips of the metal sheets are active in the radiation mechanism, so that, essentially, all the structures can be reduced to wire frames.

The second was when Isbell [11] built the first array of log-periodic half-wave dipoles (Fig. 2a). Again, here a surprising fact was verified.

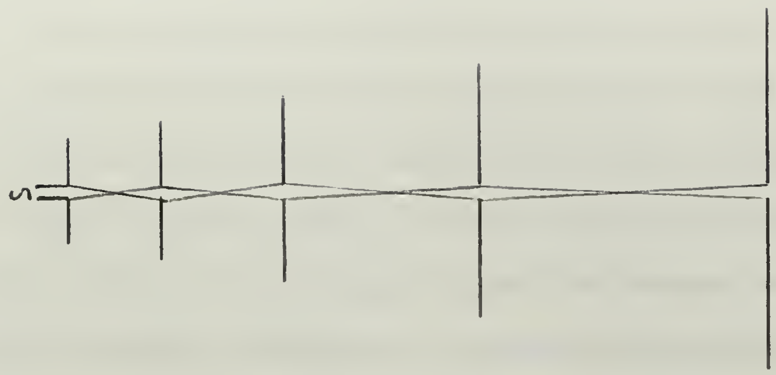

Fig. 2a - Isbell's transverse dipole array

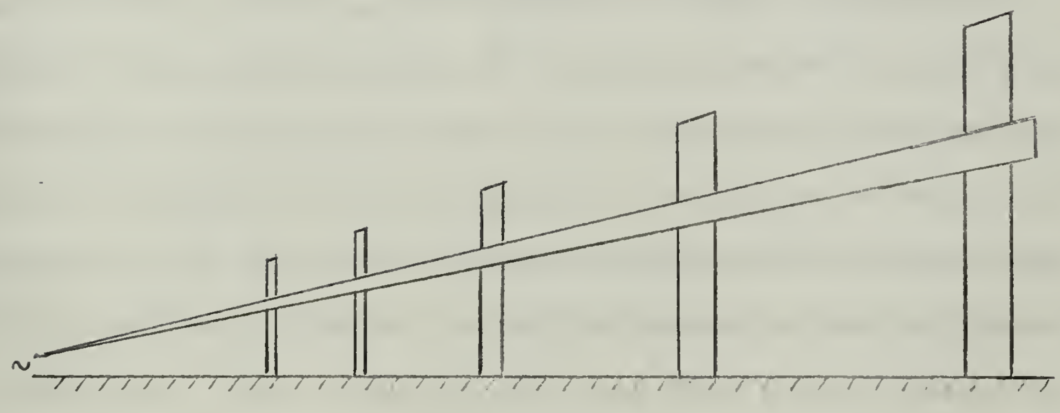

Fig. 2b - A tapered-ladder for operation above ground

The structure, as all log-periodic structures so far realized, radiates backward; but, to obtain proper operation, every other dipole of the array is fed through a reversal of the feed line connections.

This dipole array established the applicability of log-periodics in the HF band. The structure can be built for vertical or horizontal polarization, and in the latter case, by adequate choice of the slope of the feed line, either fixed or variable take-off angles can be obtained. The first models had tubular dipoles, with radius scaled to the structure period. Granger Associates, who might be properly recognized as the pioneers in large scale building of HF log-periodic antennas, have replaced the tubular dipoles by wire triangular elements with appreciable reduction in weight, making it possible to build the rotatable long range log-periodic. This is a steerable antenna, mounted on a pole high enough so that the take-off angles are as low as 10°, and light enough to be rotated by a small electric motor through a 360° azimuth span.

Incidentally, one of the problems that arose with these antennas was the matching of the feeding line. The antenna terminals show a balanced input impedance of the order of 200 ohms, and, typically, a maximum VSWR with respect to 50 Ω below 2:1 through the band of operation. Two hundred ohms is not the most convenient value to carry energy from a distant transmitter, and the problem was that of obtaining a matching device that would enable the use of 50 ohms standard coaxial cable. That need speeded up the research in the area of baluns and matching transformers with outstanding results. Granger Associates have supported their achievements in antenna production, supplying also baluns with the required broadband characteristics, and multicouplers that enable the simultaneous use of one

single antenna with a number of independent transmitters; the total power being the only limitation in the system plus a small separation in the frequencies of operation.

Looking for more and better, the next step in log-periodics was to try to obtain a structure that would use a ground image with the purpose of reducing its size. The reversal in dipole connections excluded that possibility in Isbell's array, except by the use of inverting transformers between radiators, which does not seem to be a very practical idea. The more significant successful structures are the bent log-periodic zig-zag, the tapered ladder, and the monopole array. The bent zig-zag, developed by J. Greiser and P. Mayes [8], [9], will be the main subject of this paper. The tapered ladder, developed by Wickersham, consists of an array of grounded vertical radiators (Fig. 2b) capacitively coupled to an inclined transmission line, the slope of which is adjusted for proper feed of each radiator. A variation of this arrangement, that uses triangular wire radiators, has been commercialized by Granger Associates. The monopole array, developed by D. Berry and F. R. Ore [23] uses phasing stubs between every two radiators, scaled with the structure period. The stubs are horizontal and open-circuited, so that only one wire is actually necessary, since its image provides the other, and the radiators are vertical tubes, of a quarter of a wavelength, for the respective operating frequency.

In general, the half-size structures do not have as good a performance as the transverse dipole, and the recent advances in construction techniques have made the latter a stronger competitor, even for frequencies as low as 2 MHz.

1.3 - Developments in the Theory of Log-Periodic Antennas

The development of log-periodic structures during their first years was mainly the result of good intuition and extensive laboratory testing of a large number of proposed models. As a rule, only after a successful model was obtained, was a theoretical foundation to explain its performance developed, and only relatively recently models based on sound theoretical investigation are being realized.

There have been three main approaches to the problem of analysis of operation of LP's. The first, which we can call the classical approach, uses the theories developed for the components of the antennas and combines them to suit the particular model under consideration. The outstanding example of this approach is Carrell's analysis of the transverse dipole array [10], who described the behavior of the structure in terms of currents, voltages, input impedance and far-field with very close agreement with experiments. This approach usually has the limitation of being valid for a particular structure only.

Another approach, that has been pursued by DuHamel [15], [16], Armstrong [16], Mittra, Jones [17], [18], [19], and others is to develop an adequate body of information and knowledge in log-periodic networks, on which a general theory of the antenna problem could be based. Great progress has been made toward this purpose, and results obtained have helped in a better understanding of log-periodics, and, in some cases, provided new ideas for future realizations.

The third approach, followed by Mayes, Deschamps, Patton [20], Greiser [8], [9], Oliner, Mittra, Jones [22] and others is an application of concepts developed for surface and leaky wave structures, that are typically uniformly periodic structures, to the active region of log-periodics

that can be approximated as a uniformly periodic region for limited purposes. Since such concepts give an excellent insight into the main operational characteristics of these structures, we will briefly review some of its basic points [4], [5], [7].

Consider a structure, such as a waveguide, with a periodic grating in one face, and suppose that the waveguide carries an electromagnetic wave. Due to the discontinuities in the grated face there will be leakage of energy through them, and, also, the fields inside the guide will adjust to this periodic configuration. According to Floquet's theorem, "for a given mode of propagation at a given steady-state frequency, the fields at one cross section differ from those one period away only by a complex constant" [7]. This can be expressed as

$$E_2 = E_1 e^{-\gamma L}$$

where L is the period of the grating and γ is the propagation factor.

Now, if the longitudinal dimension of the guide is made to coincide with the z axis, and we expand the equation in a Fourier series, we get

$$E = E(x,y,z)e^{-\gamma z} = \sum_{\text{all } n} E_n(x,y)e^{-j(2\pi n/L)z}\, e^{-\gamma z}, \tag{1}$$

that is, we obtain a set of n space harmonics, each one having propagation constant

$$\Gamma = \gamma + j\,\frac{2\pi n}{L}\,.$$

If we now assume that the system is lossless, we obtain

$$\beta_n = \beta_0 + \frac{2\pi n}{L} \tag{2}$$

where β_0 is the medium phase constant. Now, we apply this result to the

usual description of waves bounded by guides. In general, the fields are described by the wave numbers and a relation of the form

$$K^2 = K_x^2 + K_y^2 + K_z^2 .$$

When the x = 0 plane is a ground plane, that is the general case of interest for the present purpose, the y number is zero, and, with the assumption of no losses, we have

$$\beta^2 = K^2 + \beta_x^2 + \beta_z^2$$

where $\beta = K$ is the free space phase constant.

If now we recognize that the x and z phase constants are given, for the grated guide, by a series of the form of equation (2), we obtain the general form of the solution. But, before, let us consider an angle θ, as being the angle between the z axis and the direction of a z component wavefront. Then we can relate the x and z wave numbers, or the phase factors as

$$\beta_x = K \sin \theta$$

and

$$\beta_z = K \cos \theta \quad ,$$

so that the direction of leaking energy, that is the direction of the wavefront, is given by

$$\cos \theta = \frac{\beta_z}{K} . \tag{3}$$

Now, according to (2) we recall that β_z can take any discrete value β_n (note that n ranges from all negative values to all positive values), and, being so, the ratio (3) can take an equal number of values, positive or negative. When this ratio falls in the range -1 to +1, that corresponds to a solution of the cos function, and also to real solutions of space harmonics for which there is leaking energy. In particular, when (3) takes the value -1, energy is fired backward, and this corresponds to the mode of interest in the present analysis.

Since the amplitude of the harmonics decreases with increasing order, we would like to have the structure operating in a low order mode. For the n = -1 mode we have

$$\beta_{-1} = \beta_0 - \frac{2\pi}{L}$$

and

$$\cos \theta_{-1} = \frac{\beta_0 - 2\pi/L}{K} \quad .$$

In log-periodic structures, always there is some sort of guide that carries energy from the feed point toward the radiators, and discontinuities placed along the guide force energy to leak away. In the transverse dipole the line is the feeder, a transmission line, and the grating is represented by the dipoles; in the teeth structure of Fig. 1, the plane sheets form the guide and the teeth form the grating; the bent zig-zag is a transmission line deformed by the radiating elements. In each of these models, and, in general, in each log-periodic model, we can consider three distinct regions: the active region comprising the two to five radiating elements near resonance for the operating frequency, the feeding region, between this and the source where radiation is small and in general the radiators can be considered as a capacitive loading, and the end region, that we

assume is not reached by any significant amount of energy, since most of it was radiated by the active region. Since the active region is small, we now assume that it is a uniformly periodic structure, and then apply it to the above results for leaky waves.

Perhaps a clearer picture of such an application is by means of dispersion diagrams. Fig. 3 shows a dispersion diagram for equation (3), assuming that $\beta_0/K > 1$. It is a well-known fact in transmission theory that propagation within boundaries takes place when the phase constant in the medium is larger than the phase constant in the boundary material, i.e., when the propagation velocity in the medium is lower than the propagation velocity in the boundary material. For metallic boundaries the velocity is usually taken as that of free space, and we represent that condition by the phase constant K. This situation is usually identified by the designation of slow waves and it is said that periodic structures have stop bands for fast waves. These fast waves that do not propagate within the structure are the ones that leak away and form the radiated field.

In Fig. 3 we represent the fundamental and the first and second negative harmonics as given by equation (2), and we show the $\pm 45°$ slope lines that separate zones of slow waves from zones of fast waves. We see that the fundamental is a slow wave for all frequencies, and so are all the positive order harmonics. The negative order harmonics are slow waves for low frequencies, but as the frequency increases to near the point B, the first negative harmonic approaches the negative slope line. On the line we have

$$\cos \theta_{-1} = \frac{\beta_{-1}}{K} = \frac{\beta_0 - 2\pi/L}{K} = -1 \quad ,$$

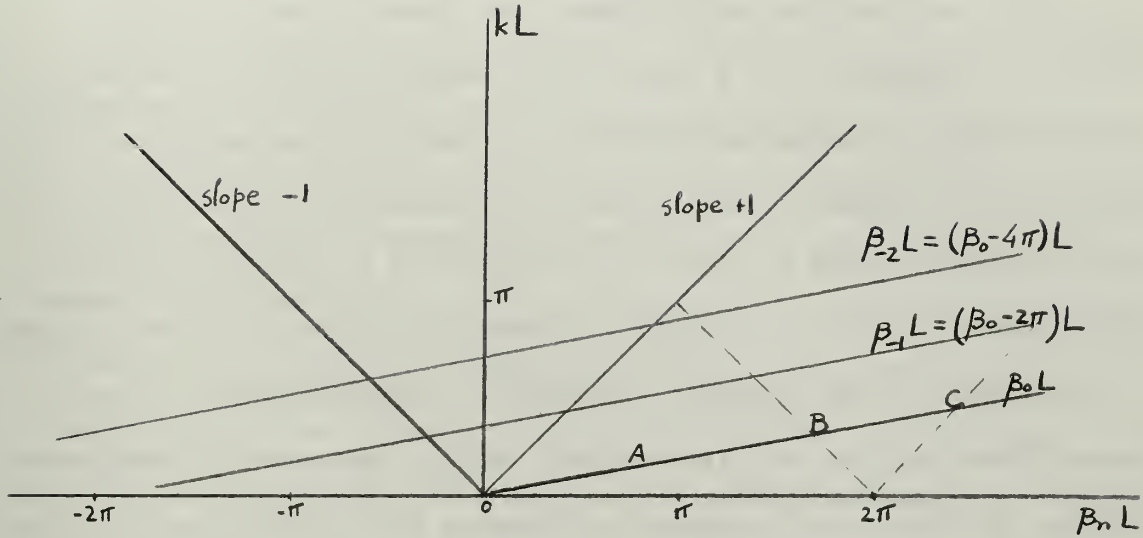

Fig. 3 - Dispersion diagram

that is, we start having radiation backwards; and until the positive slope line is reached the radiation angle rotates from 180° to 0°. Meanwhile, the other negative order harmonics were having similar behavior in the region that we can visualize to the left of the diagram.

Since the analysis is applied to a uniformly periodic structure, we only have well-defined active bands, the first of which is the strongest, separated by stop bands (these have the opposite meaning of the stop bands of transmission theory). However, in log-periodic antennas the structure is scaled almost continuously (typical scale factors range from .80 to .98), so that there is a continuous active band, limited only by the operating frequencies of the first and the last of its elements. The frequency independence characteristics of the antenna depend on how well its discrete scaling approaches a continuous scaling, and the over-all antenna performance can be predicted from this type of analysis. Greiser and Mayes [8], [9] have used this technique with remarkable success, in predicting whether or not different models of bent zig-zag antennas would radiate, and how the radiation characteristics could be improved. Mittra [17] has conducted a similar analysis for the transverse dipole, showing by this method how the phase reversal was necessary to make the dispersion diagrams approach the radiation zone.

Again, there is a remarkable lack of dispersion diagrams developed for the type of structures used in log-periodics, and, as yet, the theory was not really adapted for them, except under the heuristic approach described above. We should note here that, although this application of leaky waves theory in a wired log-periodic structure might, at first sight, seem rather displaced, there is reason to believe that the theory is actually valid. R. L. Bell, C. T. Elfving and R. E. Franks [21]

reported measurements of fields around a log-periodic structure that show the existence of a forward wave progressing from the source along the structure, and a backward wave with a 90 degrees spacial phase difference. The forward wave is supported by the structure; the backward wave is launched by it into space. That is exactly the type of leaky wave behavior used in the above theory.

The mathematical tools developed to deal with the various problems posed by electromagnetic theory, although having in common the basic source given by Maxwell's equations, follow different courses and tend to place in distinct categories, problems that have much in common. It seems to be a marked trend in recent years, to reunite electromagnetic theory in the sense of extending concepts and ideas developed for particular systems to other, apparently different, applications.

As a final remark, we note that, since log-periodics are scaled up from the feeder, the active elements are the ones in the active region together with the smaller ones. Smaller elements in all cases tend to increase the propagation velocity (the feeder approaches a uniform line toward the feed point). If we would attempt to build a log-periodic for forward radiation we would scale the structure in the opposite sense, and would count on positive order waves for the radiation process. However, while in the usual scaling the positive harmonics find a high impedance in the first part of the feeder (they are in the stop band of transmission theory and mismatched to the available radiators), in the opposite scaling the negative harmonics would still reach the end part of the feeder and cause a disturbing radiation from that region.

II - THE BENT LOG-PERIODIC ZIG-ZAG ANTENNA (BLPZZ)

The BLPZZ (Fig. A-1) was developed by Greiser and Mayes using the concepts of dispersion diagrams. As mentioned before, this was one of the first attempts to obtain a LP antenna with symmetrical characteristics that could be fed against ground. For that reason, it seems particularly suited for HF applications.

The basic geometry of the antenna is derived from a zig-zag antenna bent along a convenient line, so as to obtain adequate radiating elements and proper connecting stubs. Since the structure is progressively elevated from ground the connecting stubs are actually radiating, but, for small elevation angles that can be neglected. Their essential function is to provide the proper phase delay between radiators, and they can be, and have been, replaced by other forms of delay line, or even removed, without destroying the basic characteristics of operation of the antenna.

The antenna is usually defined by the radiators spreading angle α_E, the stubs spreading angle α_S, the elevation angle ε, the period p, and the length of a wire, 2b, or the distance of one element to the geometric origin. In Appendix A we develop the relations among these parameters and other useful quantities. We note that the spreading angles and the period are interrelated through the slope of the wires. Although each one of them can be independently changed, that involves a change in the dimensions and inclination of the wires. Also, we note that each element, for small elevation angles, can be compared to a rhombic antenna made of small wires, and with a very large apex angle.

This antenna has the interesting characteristic of being fed in series, i.e., the radiators are part of the feed line. The other planar LP structure so far analyzed--the transverse dipole--has the radiators

fed in parallel, and it might be worthwhile to compare the results obtained. On the other side, this one, also is a structure that seems adequate to analyze with conventional tools.

In the first part of this work we obtain a set of equations for the radiation pattern of the antenna. Then we assign to the wires different types of current distribution, and compare the results with the experimental data obtained by Greiser and Mayes.

In the last part of the work we consider the antenna and its image as a non-uniform transmission line and we obtain an approximation for the input impedance and current distribution.

2.1 - The Radiation Pattern Equations of the BLPZZ

To obtain the radiation pattern of the BLPZZ structure above ground we begin by considering one element at a time. We define as an element, one period of the structure. Since the elements are related by a constant size factor, that is, the period p, the general equations obtained for one element are valid for the other elements as well.

In each element, we assume that the connecting stub does not radiate, and we split the radiating section in two straight wires. Then we obtain the fields due to these two wires and their images, all referred to an element phase center, and add them vectorially.

We make two more assumptions. First, we assume that there is no mutual coupling between elements; second, we assume that the wires carry travelling waves. This corresponds to considering the structure and its image as forming a radiating transmission line properly terminated; that is, without standing waves. Later we will further elaborate on this point.

After obtaining the element's equations we establish an array expression, accounting for spacings and feed currents.

We outline here the development of the equations for one wire, wire 1 in Fig. 4. Details, as well as the work concerning other wires, can be found in Appendix A.

In general, the distant field due to the flow of current along a wire is given by

$$E_{\theta 1} = -j \frac{w\mu_0}{4\pi} e^{-jwt} \int_0^1 \frac{\sin \theta'}{r} e^{-jkr} \mu(s)\, ds \tag{4}$$

where θ', s, 1 and r are defined in Fig. 4, and w, k, μ_0 and π have the usual significance. $\mu(s)$ is the current distribution. In general, this will be given by

$$\mu(s) = I_0\, e^{-(\alpha+j\beta)s} \tag{5}$$

where α is the attenuation factor and β is the propagation factor, along the wire.

For large distances the angle θ and the distance r are essentially independent of the position along the wire, so that we can consider them as constants in regard to s, provided that we account for the phase delay at the far field due to the different points along the wire.

Again, referring to Fig. 4, if we consider the distance R from the center of the wire, we can express r as

$$r = R - s \cos \theta'$$

and, replacing in equation (4), and defining

$$I_0 = \mu(-\tfrac{1}{2})$$

we obtain

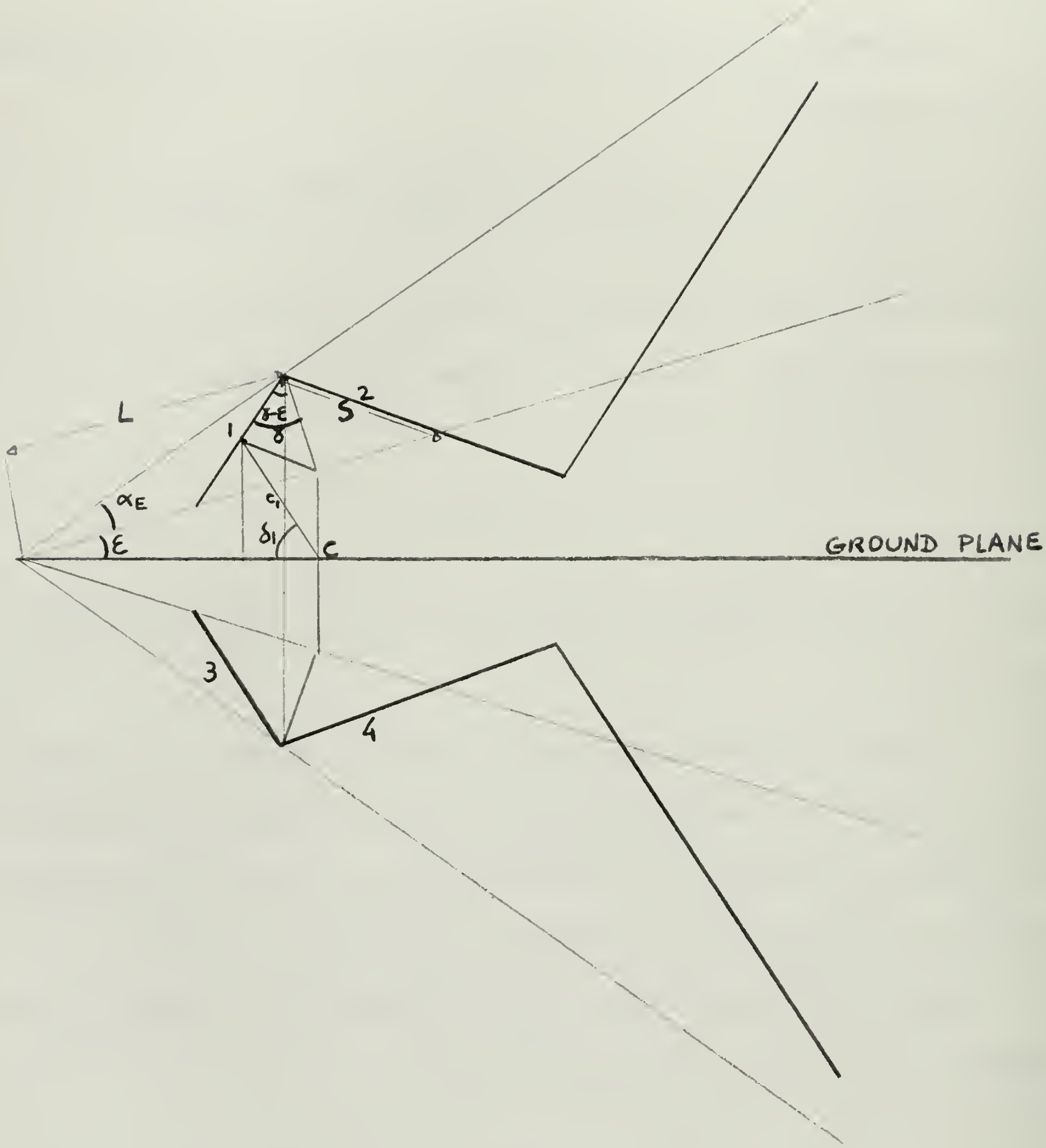

Fig. 5 - Geometrical relations in the BLPZZ

$$E_{\theta'} = -j\,\frac{\omega\mu_0}{4\pi}\, I_0\, \frac{\sin\theta'}{R}\, e^{-j\left[(kR+\omega t)+\frac{\beta\ell}{2}\right]} \int_{-\frac{\ell}{2}}^{\frac{\ell}{2}} e^{-\left[\alpha + jk\left(\frac{\beta}{k} - \cos\theta'\right)\right]s}\, ds \qquad (6)$$

Now we apply this equation to wire 1 in Fig. 5. Here 1 = 2b, and, then

$$\int_{-b}^{b} e^{-\left[\alpha+jk\left(\frac{\beta}{k} - \cos\theta_1'\right)\right]s}\, ds = \frac{e^{\left[\alpha+jk\left(\frac{\beta}{k} - \cos\theta_1'\right)\right]b} - e^{-\left[\alpha+jk\left(\frac{\beta}{k} - \cos\theta_1'\right)\right]b}}{\left[\alpha + jk\left(\frac{\beta}{k} - \cos\theta_1'\right)\right]}$$

Defining

$$F = -\frac{w\mu_0}{2\,K}\,\frac{e^{-j(kR+wt)}}{R} = -\,60\,\frac{e^{-j(kR+wt)}}{R}$$

we obtain

$$E_{\theta_1'} = j\,\frac{kF}{2}\, I_0\, e^{-j\beta b}\, \frac{e^{\left[\alpha+jk\left(\frac{\beta}{k} - \cos\theta_1'\right)\right]b} - e^{-\left[\alpha+jk\left(\frac{\beta}{k} - \cos\theta_1'\right)\right]b}}{\left[\alpha + jk\left(\frac{\beta}{k} - \cos\theta_1'\right)\right]} \qquad (7)$$

Since we are going to use this equation with a digital computer, this is a convenient form.

Now we need to convert this equation to a system of coordinates to be used with all the structure. We choose spherical coordinates, as shown in Fig. 6, and we obtain the following transformation equations (see Appendix A, Parts II and III):

$$\cos \theta_1' = \cos (\gamma-\varepsilon) \cos \theta - \sin (\gamma-\varepsilon) \sin \theta \cos \phi \tag{8}$$

$$E_{\theta 1} = E_{\theta_1'} \frac{\cos (\gamma-\varepsilon) \sin \theta + \sin (\gamma-\varepsilon) \cos \theta \cos \phi}{\sin\theta_1'} \tag{9}$$

$$E_{\phi_1} = E_{\theta_1'} \frac{\sin (\gamma-\varepsilon) \sin \phi}{\sin \theta_1'} \tag{10}$$

At this point it is convenient to introduce the correction to the "phase centers" of the element. Here the designation "phase center" is used to mean the reference point of the element. The actual phase center was not computed, although physical considerations would lead to the point C in Fig. 5, that was chosen.

Again, we assume that the angles θ and ϕ, as well as the distance R are not altered to an appreciable degree, and we only take into account the phase delay in the far field. The distance c_1, from the center of the wire to point C is given by (see Appendix A, Part I)

$$c_1 = \frac{b \sin (\gamma-\varepsilon)}{\cos \delta_1} \tag{11}$$

where

$$\delta_1 = \tan^{-1} \frac{L \sin \varepsilon + b \cos (\gamma-\varepsilon)}{b \sin (\gamma-\varepsilon)}$$

The phase difference in the far field is given by (see Fig. 5)

$$R_1 - R = c_1 \cos \alpha,$$

where

$$\cos \alpha_1 = - [\sin \delta_1 \cos \theta + \cos \delta_1 \sin \theta \cos \phi] ,$$

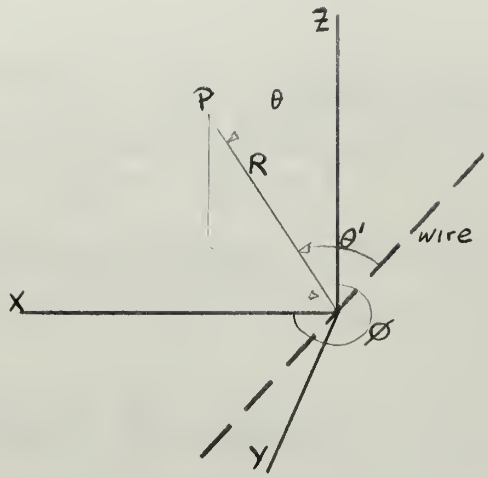

Fig. 6 - Coordinate system

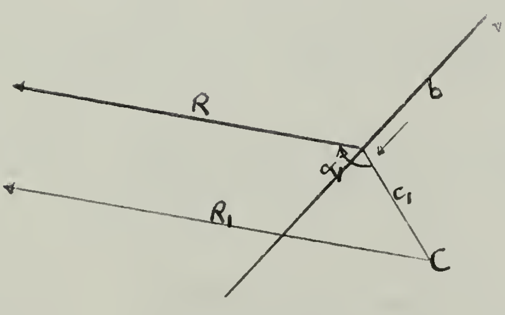

Fig. 7 - Correction for reference point

so that the factor e^{-jkR} in equation (6) becomes becomes $e^{-jk(R+c_1\cos\alpha_1)}$, and, finally, combining equations (7), (8), (9), (10), and this correction, we obtain

$$E_{\theta_1} = j\frac{kF}{2} I_0 e^{-jk\left(\frac{\beta}{k}+c_1\cos\alpha_1\right)} \frac{e^{\left[\alpha+jk\left(\frac{\beta}{k}-\cos\theta_1'\right)\right]b} - e^{-\left[\alpha+jk\left(\frac{\beta}{k}-\cos\theta_1'\right)\right]b}}{\left[\alpha+jk\left(\frac{\beta}{k}-\cos\theta_1'\right)\right]} \times$$

$$\times\left[\cos(\gamma-\varepsilon)\sin\theta+\sin(\gamma-\varepsilon)\cos\theta\cos\phi\right] \tag{12}$$

and

$$E_{\phi_1} = j\frac{kF}{2} I_0 e^{-jk\left(\frac{\beta}{k}+c_1\cos\alpha_1\right)} \frac{e^{\left[\alpha+jk\left(\frac{\beta}{k}-\cos\theta_1'\right)\right]b} - e^{-\left[\alpha+jk\left(\frac{\beta}{k}-\cos\theta_1'\right)\right]b}}{\left[\alpha+jk\left(\frac{\beta}{k}-\cos\theta_1'\right)\right]b} \sin(\gamma-\varepsilon)\sin\phi \tag{13}$$

Now combining these equations with the similar equations obtained for the other three wires (see Appendix B) we have, for each element,

$$E_{\theta_n} = E_{\theta_1} + E_{\theta_2} + E_{\theta_3} + E_{\theta_4} \tag{14a}$$

$$E_{\phi_n} = E_{\phi_1} + E_{\phi_2} + E_{\phi_3} + E_{\phi_4} \tag{14b}$$

For the whole structure we will have

$$E_\theta = \sum_{n=1}^{N} a_n E_{\theta_n} \tag{15a}$$

$$E_\phi = \sum_{n=1}^{N} a_n E_{\phi_n} \tag{15b}$$

where a_n is a factor accounting for the spacing and feed currents, that can be split in the product of two terms, one accounting for each.

The feed current for the n+1 element is the feed current for the order n element delay attenuated by the length of wires 1 and 2 and the connecting stub. As mentioned before, the connecting stub is assumed to be a uniform transmission line, so that it is only responsible for an additional delay.

Referring to Fig. 5, the distance along the wires from the feed point of element 1 to the feed point of element 2 is

$$2b_1 + 2b_1 + 2b_1' + 2b_1' = 4b_1 + 4b_1' = 4(b_1 + b_1')$$

From Appendix A we have

$$b_1' = \frac{b_1}{\sqrt{p}} \frac{\tan \alpha s}{\tan \alpha E}$$

so that the distance becomes

$$d_2 = 4b_1 \left(1 + \frac{\tan \alpha s}{\sqrt{p} \tan \alpha E} \right)$$

The distance to the feed point of element 3 is

$$d_3 = 4b_1 \left(1 + \frac{\tan \alpha s}{\sqrt{p} \tan \alpha E} \right) + 4b_2 \left(1 + \frac{\tan \alpha s}{\sqrt{p} \tan \alpha E} \right) =$$

$$= 4b_1 \left(1 + \frac{\tan \alpha s}{\sqrt{p} \tan \alpha E} \right) \left(1 + \frac{1}{p} \right) \text{, since } b_2 = b_1;$$

and the distance to the order n element is

$$d_n = 4b_1 \left(1 + \frac{\tan \alpha s}{\sqrt{p} \tan \alpha E} \right) \left(1 + \frac{1}{p} + \frac{1}{p^2} + \dots + \frac{1}{p^{n-2}} \right) =$$

$$= 4b_1 \left(1 + \frac{\tan \alpha s}{\sqrt{p} \tan \alpha E} \right) \text{SUM}$$

where SUM $= 1 + \frac{1}{p} + \frac{1}{p^2} + \ldots + \frac{1}{p^{n-2}}$.

If we subtrace $\frac{S}{p}$ from S, where,

$$\frac{S}{p} = \frac{1}{p} + \frac{1}{p^2} + \frac{1}{p^3} + \ldots + \frac{1}{p^{n-1}} ,$$

we get

$$S(1 - \frac{1}{p}) = 1 - \frac{1}{p^{n-1}} \quad \therefore \quad S = \frac{1 - 1/p^{n-1}}{1 - 1/p}$$

and the distance becomes

$$d_n = 4b_1 \left(1 + \frac{\tan \alpha s}{\sqrt{p} \tan \alpha E} \right) \frac{1 - 1/p^{n-1}}{1 - 1/p}$$

If we call β the propagation constant along the radiating wires, and assume that along the stubs the constant is K, as in free space, we have the phase angle of the feeding current given by

$$4b_1 K \left(\frac{\beta}{K} + \frac{\tan \alpha s}{\sqrt{p} \tan \alpha E} \right) \frac{1 - 1/p^{n-1}}{1 - 1/p} \tag{16}$$

We could obtain an analogous expression for the attenuation, assuming that the attenuation factor was constant along the radiating structure; however, physical considerations imply different attenuations along the line, so that we obtain, for the order n element feed current an attenuation given by

$$\sum_{i=1}^{n-1} 4b_i \alpha_i \tag{17}$$

where α_i is the average attenuation for each element.

Then the correction factor for current in the array expression is

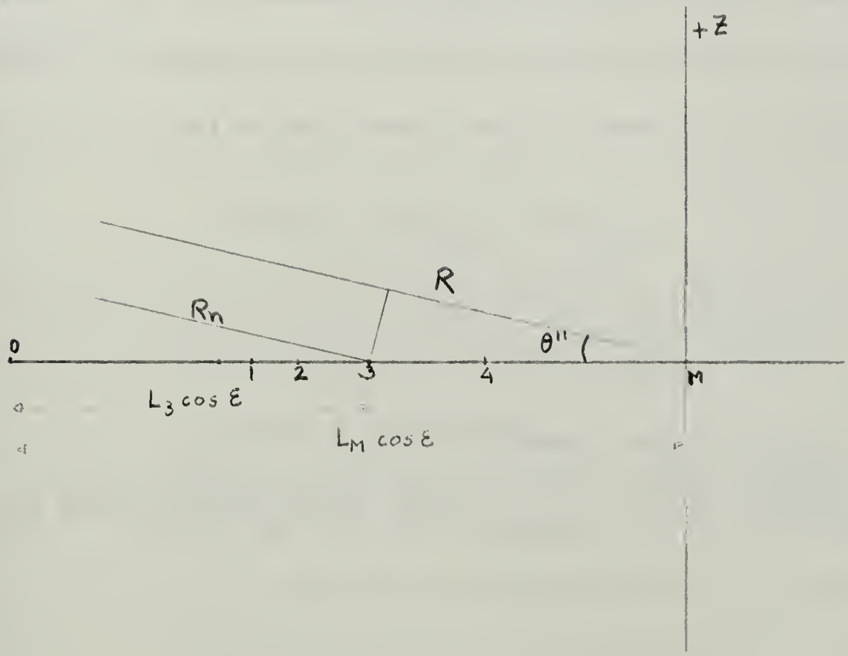

Fig. 8 - Correction for array spacing

$$e^{-\sum_{i=1}^{n-1} 4 b_i \alpha_i - j 4 b_1 k \left(\frac{\beta}{k} + \frac{\tan\alpha_s}{\sqrt{p}\tan\alpha_\varepsilon}\right) \frac{1 - 1/p^{n-1}}{1 - 1/p}} \qquad (18)$$

To introduce now a correction for spacing, we are going to use as the reference point the "phase center" of the array. Again, we do not know exactly where the phase center is, but we expect in that respect a behavior similar to other log periodic structures [10], [21]. Being so, the phase center should lie by the element that is nearest to resonance, and that we call the M element. Then, according to Fig. 8, we obtain

$$R_n = R - (L_M \cos\varepsilon - L_n \cos\varepsilon)\cos\theta''$$

where $\cos\theta'' = \sin\theta\cos\phi$ and

$$R_n = R - (L_M - L_n)\sin\theta\cos\phi\cos\varepsilon \qquad (19)$$

In equation (6), e^{-jkR} becomes $e^{-jkR}\, e^{+jk(L_M - L_n)\sin\theta\cos\phi\cos\varepsilon}$ and we insert in the array expression the factor

$$e^{jk(L_M - L_n)\sin\theta\cos\phi\cos\varepsilon} \qquad (20)$$

Then the total correction a_n is

$$a_n = e^{-\sum_{i=1}^{n-1} 4 b_i \alpha_i - j 4 b_1 k \left(\frac{\beta}{k} + \frac{\tan\alpha_s}{\sqrt{p}\tan\alpha_\varepsilon}\right) \frac{1 - 1/p^{n-1}}{1 - 1/p} + jk(L_M - L_n)\sin\theta\cos\phi\cos\varepsilon} \qquad (21)$$

Finally, the array equations become

$$E_\theta = \sum_{n=1}^{N} e^{-\sum_{i=1}^{n-1} 4b_i\alpha_i - j4b_1k\left(\frac{\beta}{k} + \frac{\tan\alpha_s}{\sqrt{p}\tan\alpha_E}\right)\frac{1-1/p^{n-1}}{1-1/p} + jk(L_M - L_n)\sin\theta\cos\phi\cos\varepsilon} \times E_{\theta_n} \tag{22a}$$

$$E_\phi = \sum_{n=1}^{N} e^{-\sum_{i=1}^{n-1} 4b_i\alpha_i - j4b_1k\left(\frac{\beta}{k} + \frac{\tan\alpha_s}{\sqrt{p}\tan\alpha_E}\right)\frac{1-1/p^{n-1}}{1-1/p} + jk(L_M - L_n)\sin\theta\cos\phi\cos\varepsilon} \times E_{\phi_n} \tag{22b}$$

And from here we obtain the total field E by taking the real parts of E_θ and E_ϕ and combining them vectorially, so that

$$E(\theta,\phi) = \sqrt{[Real(E_\theta)]^2 + [Real(E_\phi)]^2} \;\angle \tan^{-1}\frac{Real(E_\theta)}{Real(E_\phi)}$$

$$= |E| \angle \Psi$$

where Ψ is an angle counted positive in the clockwise sense starting in the direction of the $\bar{a}_\phi$ vector by an observer at the array phase center.

2.2 - Current Distribution - Radiation Diagrams

Before programming the equations obtained in section 2.1 in a computer, we had to decide on the current distribution that would be most closely approximate to the real situation. With that purpose in mind, we made the following considerations:

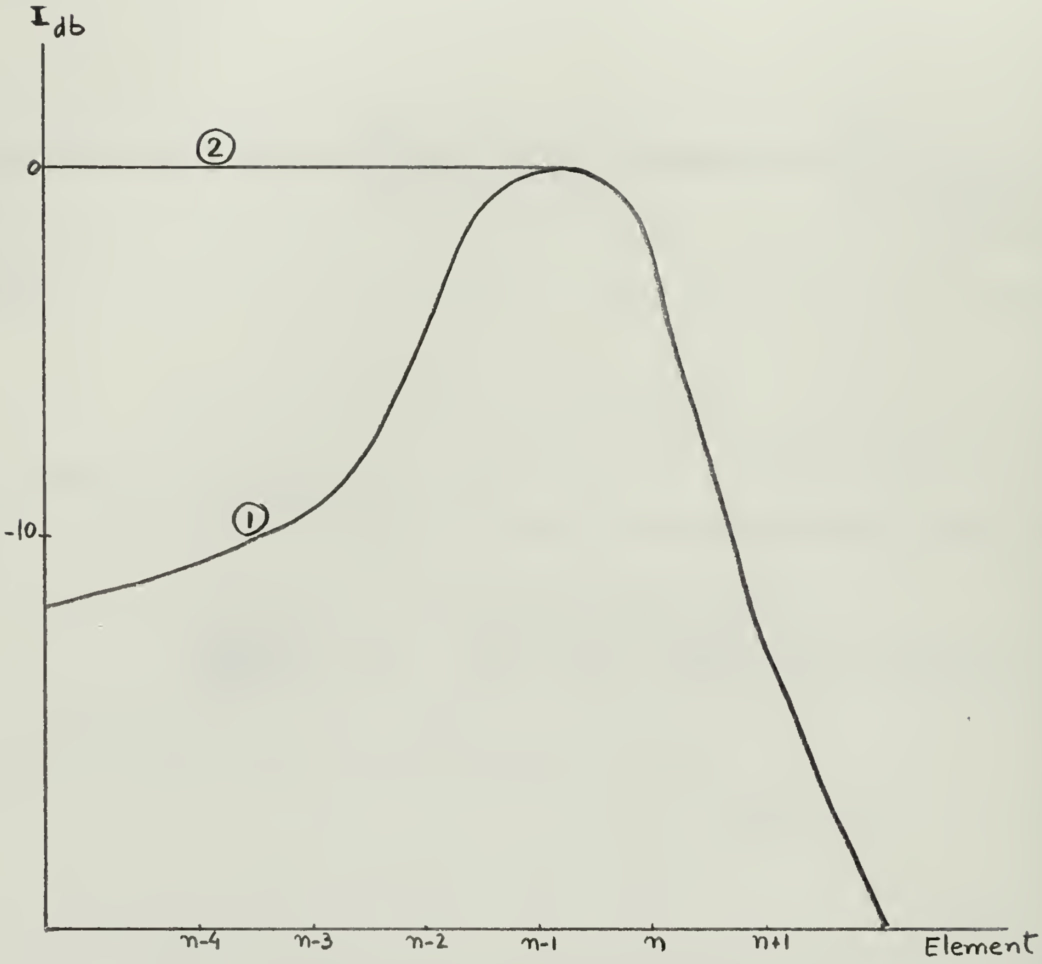

Note: n denotes resonant element

Fig. 9 - Models of current distribution
(1) As obtained in other LP networks
(2) Assuming travelling wave attenuated at active region

(1) The antenna and its image form a radiating transmission line, and since experiments [8], [9] show that its input impedance is mainly resistive and almost constant along the operating band, having a small capacitive reactance probably due to input termination effect, it is reasonable to assume that the line is well terminated.

(2) The elements forming the feed region must see the same impedance toward the end, and that is the input impedance of the antenna. This is so because that impedance does not essentially change with frequency, and a change in frequency is equivalent to a change of antenna. That is, when we decrease the frequency by one period, we move the active region one period toward the end, and that is equivalent to using one antenna "one period larger;" the impedance that was seen by the input terminals must now be seen at the end of the first element. But since the input impedance remains the same, that means the first element is a good match, and so must be all the elements forming the feed region. Then the current along the feed region must be essentially constant, except for a relatively small amount of attenuation.

(3) The energy reaching the end region must be very small. The structure is abruptly terminated without any dissipation load, and it has been shown experimentally [8], [9] that the effect on the radiation pattern of ending the structure by a short or an open circuit is very small, for frequencies well above the lowest frequency of operation. Then, it seems reasonable to assume that the current dies off after the active zone, and is essentially zero at the last elements.

(4) The current distribution at the active zone is more problematic. The non-uniform line forming the antenna is continuous in the sense that its impedance [2] changes without interruption, and has the property of a constant product of reactance times susceptance. We can call this a continuously tapered line, with linear taper, of the type often used to match impedances. Under this point of view it is continuously matching itself.

On the other side, if we think of the line as composed of series sections connected by stubs, then we have to consider the fact that some of these sections (the ones forming the active region) are near their natural resonance frequency and are likely to form standing waves.

The first point of view would lead us to a heavily attenuated travelling wave. The second leads us to the type of current distribution found by Carrel [10] in the dipole array, and by Mittra and Jones [18] for a theoretical line. A point to note here is that both these cases had parallel loads, while the present case is of series loading. Fig. 9 shows the two types of current distribution corresponding to the two points of view.

We started by trying these two models. The results obtained can be summarized with reference to Fig. 10, 11, 12, that show diagrams obtained with the data given for the antenna referred to by BLPZZ 19c in Greiser's and Maye's work. This antenna operates from 500 to 2500 MHZ. Fig. 10, for 2000 Mcs is what can be called the typical pattern. Most computer runs show that kind of diagram. Half power beam widths of the order of 90° in azimuth and 35° in elevation. The directivity, computed by the approximate formula given by Kraus [6], is around 7.5 db. Also, in almost

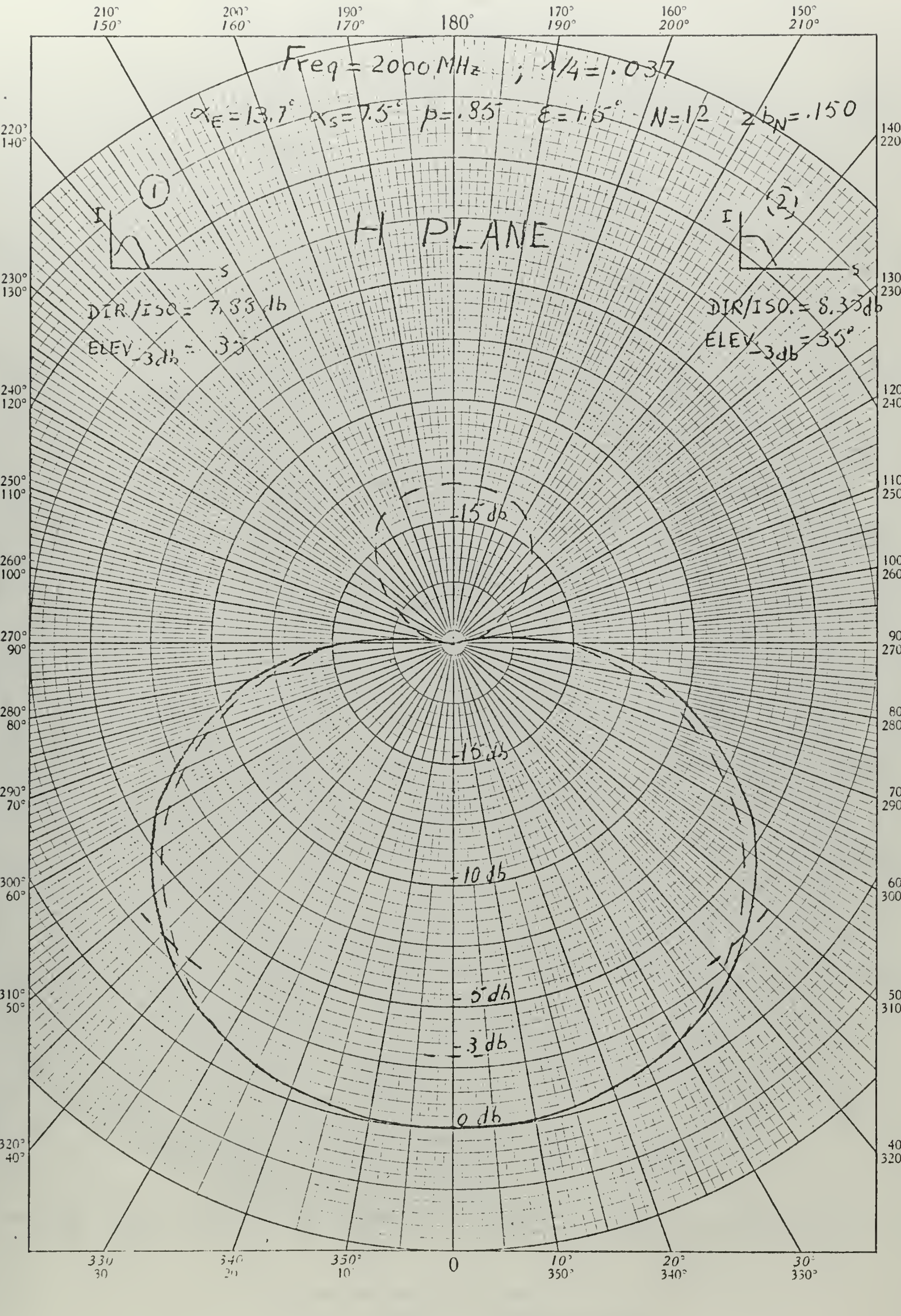

Fig. 10 - Radiation pattern

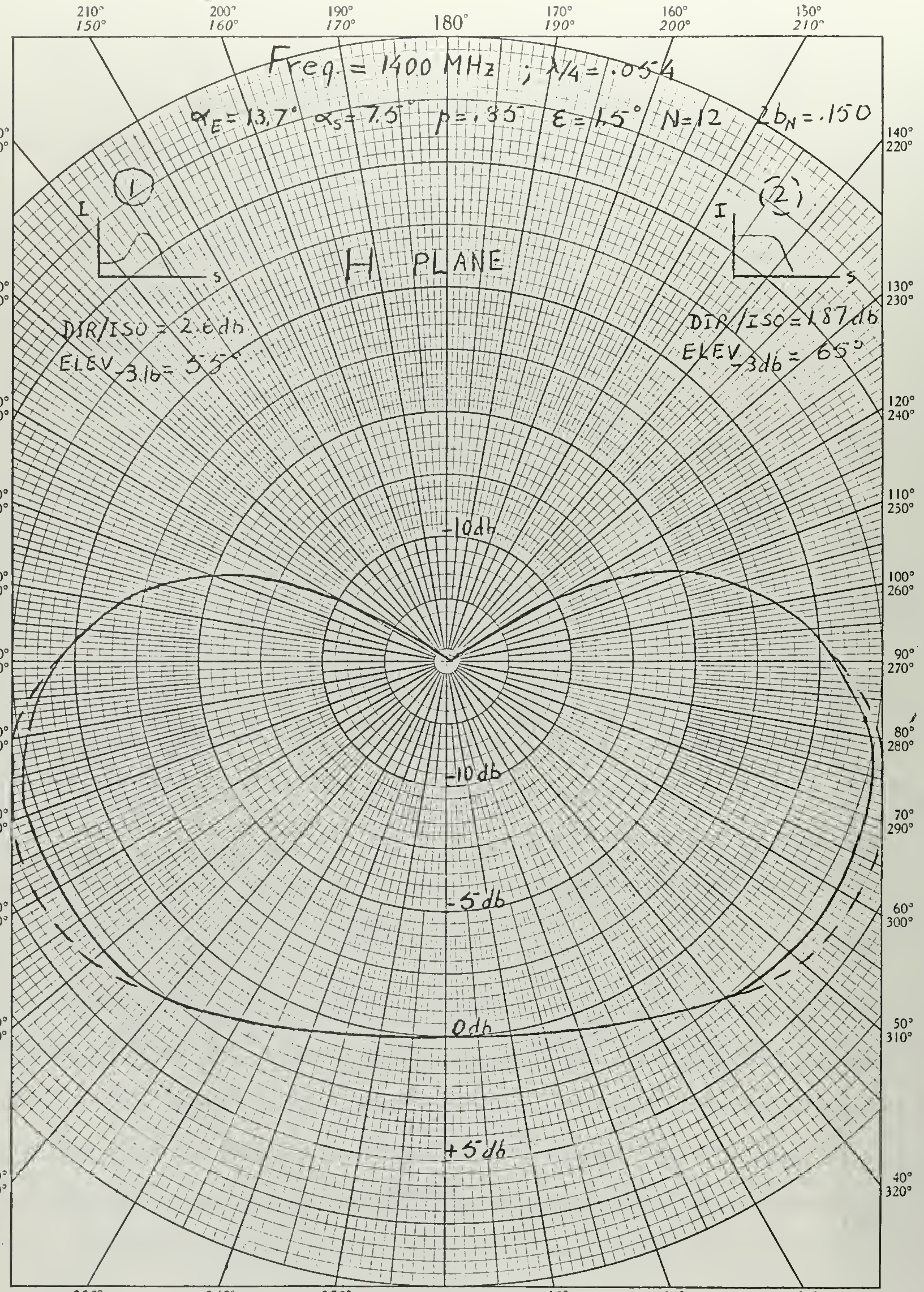

Fig. 11 - Radiation pattern

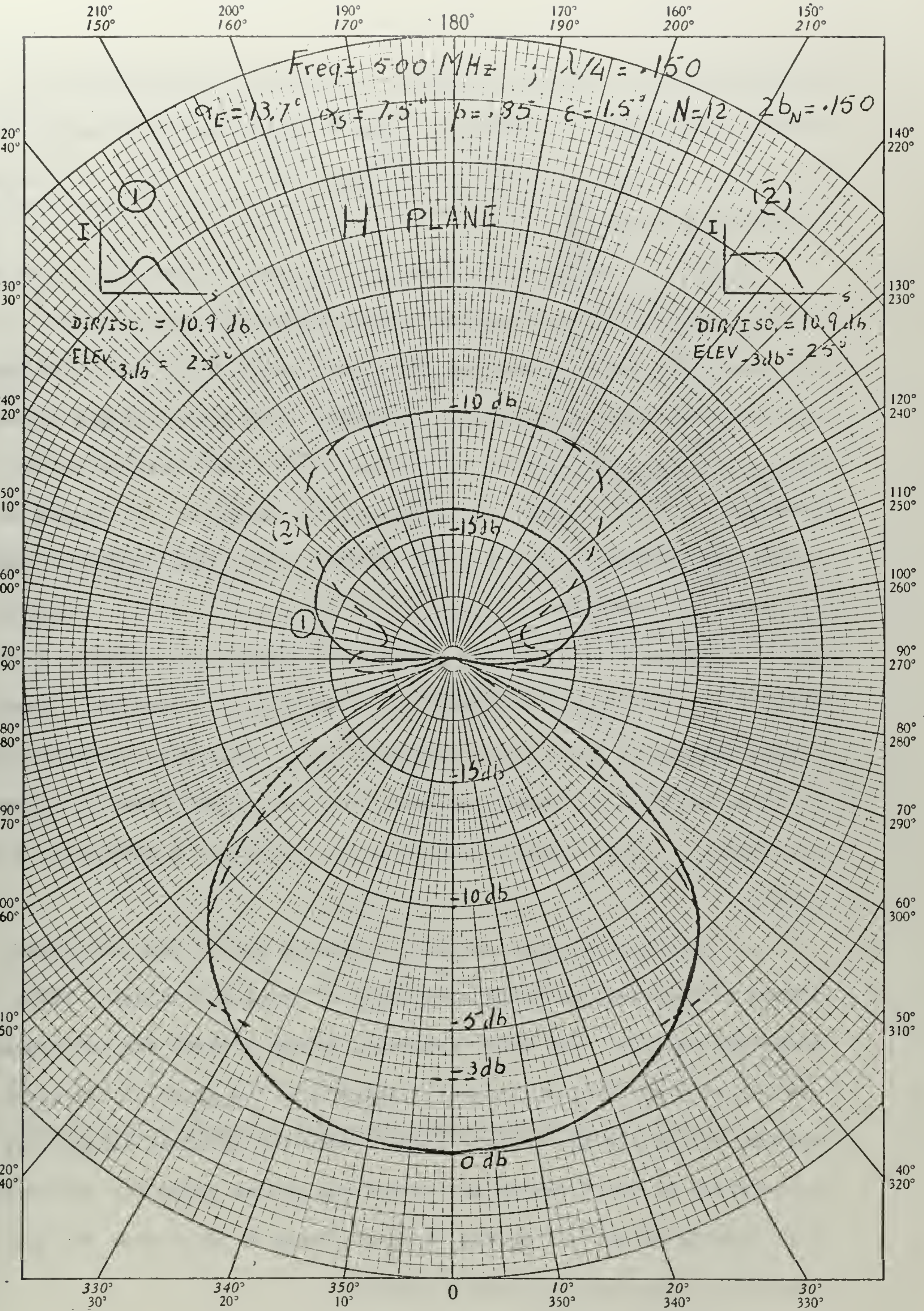

Fig. 12 - Radiation pattern

every case the difference between the results for the two types of current distribution is small, although the distribution of curve 1 in Fig. 9 gives slightly better results, particularly in what concerns the front-to-back ratio.

After an extensive set of runs was obtained, it was found that for certain frequencies the diagrams depart appreciably from what was expected. Two extreme examples are shown in Fig. 11 and 12. The first is "too good," and the second is "too bad." The most likely explanation that we can find for that is in the way the current distribution is processed in the program. The program has a sample of the curves in Fig. 9 and assigns a value to each element. Now, that sample is always the same, but the real situation in the antenna varies with the frequency. When it happens that the wires forming one element have length of one quarter of a wavelength the sample fits exactly, but when that dimension "falls" somewhere between two elements, it is clear that we are doing a rough approximation, because in that case the program takes the element just below it, and treats that element as if it were a quarter of a wavelength.

To explore this point further, we made a set of runs at closely spaced frequencies, covering one period of frequency values. Table I shows the results. For each frequency, column 2 shows the corresponding quarter of a wavelength, columns 3 and 4 show the sizes of the wires nearest to that value, columns 5 and 7 show the obtained directivity and orientation of the E vector all around the ground plane for the current distribution of curve 1 in Fig. 9, and columns 6 and 8 show the same results for the current given by curve 2.

1	2	3	4	5	6	7	8
Freq MHz	λ/4	Wire's length		Current Dist (1) DIR/ISO	 (2) DIR/ISO	Polarization (1)	 (2)
820	.091	.078	.092	5.24	5.00	-90°	-90°
855	.088	.078	.092	1.45	7.05	+90°	+90°
875	.086	.078	.092	6.36	6.06	+90°	+90°
895	.084	.078	.092	5.24	3.9	+90°	+90°
935	.080	.078	.092	8.89	10.9	+90° within ±60° +90° remain. directions	-90° within ±60° +90° remain. directions
970	.077	.067	.078	7.05	7.45	-90° within ±135° +90° remain. directions	-90° within ±130° +90° remain. directions

Table I
Variations in Results Along One Period of Frequency Values

Here it becomes clearer that the current distribution 1 results in a more balanced set of results than distribution 2. It is interesting to see the way the direction of the field vector changes along the period. Actually, this change of frequency is equivalent to moving the structure one period in space, at fixed frequency, and, in any case, we would expect the change in phase that has been observed in all LP's. It has been called the phase rotation principle--the phase of the resultant field changes by 360° with a change of one period, in space or frequency.

2.3 The BLPZZ Antenna as a Non-Uniform Transmission Line

With the purpose of obtaining a better description of the current distribution in the BLPZZ, we consider the structure and its image as forming a non-uniform transmission line. For easier handling of the equations involved, we split the structure in sections, each composed of a radiator element and the following connecting stub. Then we apply to the radiator Schelkunoff's equations for slightly non-uniform lines, and assume that the stubs are uniform lines with characteristic impedance equal to their average impedance. To account for radiation, we introduce in the equations an attenuation factor and a phase factor obtained from the radiation resistance of each element and its average impedance. The value of radiation resistance used is one obtained by Chaney [24] and Klamm [25], for rhombic antennas in free space.

According to Schelkunoff [2] a non-uniform transmission line can be described by equations of the form

$$V(x) = V_0(x) + V_1(x) + V_2(x) + \ldots \tag{25a}$$

$$I(x) = I_0(x) + I_1(x) + I_2(x) + \ldots \tag{25b}$$

where $V_0(x)$ and $I_0(x)$ are the expression for a uniform line with the average characteristics of the line under consideration. When a line or a section of line is slightly non-uniform the terms of order 2 and above can be neglected, without large error. In particular, when the line has the property of having a constant ZY product, where Z is the line reactance and Y is the line susceptance, and Z and Y vary slowly about their average values, the first order term is given by

$$V_1(x) = V_0[B(x)\cosh\Gamma x - A(x)\sinh\Gamma x] - K_0 I_0[A(x)\cosh\Gamma x - B(x)\sinh\Gamma x] \quad (26a)$$

$$I_1(x) = -\frac{V_0}{K_0}[B(x)\sinh\Gamma x - A(x)\cosh\Gamma x] + I_0[A(x)\sinh\Gamma x - B(x)\cosh\Gamma x] \quad (26b)$$

where

$\Gamma = \sqrt{ZY}$ is the propagation factor

$K_0 = \sqrt{Z_0/Y_0}$ is the average impedance of the line

$$A(x) = \frac{1}{K_0}\int_0^x \hat{Z}(s)\cosh 2\Gamma s\, ds$$

$$B(x) = \frac{1}{K_0}\int_0^x \hat{Z}(s)\sinh 2\Gamma s\, ds$$

$$\hat{Z} = Z - Z_{av}$$

$Z_0 = Z_{av}$ is the average reactance of the line

$Y_0 = Y_{av}$ is the average susceptance of the line,

and we assume that the wires are perfect conductors, perfectly isolated, so that there is no resistance or conductance to account for.

The required condition of slow variation of line parameters can be met by considering conveniently small sections of line at a time.

Using the hyperbolic form of the equations for a uniform line, we have

$$V_0(x) = V_0\cosh\Gamma x - K_0 I_0\sinh\Gamma x \quad (27a)$$

$$I_0(x) = -\frac{V_0}{K_0}\sinh\Gamma x + I_0\cosh\Gamma x \quad (27b)$$

and, then,

$$V(x) = V_0 \left[(1+B(x)) \cosh\Gamma x - A(x) \sinh\Gamma x \right] - K_0 I_0 \left[A(x) \cosh\Gamma x + (1-B(x)) \sinh\Gamma x \right] \tag{28a}$$

$$I(x) = \frac{-V_0}{K_0} \left[(1+B(x)) \sinh\Gamma x - A(x) \cosh\Gamma x \right] + I_0 \left[A(x) \sinh\Gamma x + (1-B(x)) \cosh\Gamma x \right] \tag{28b}$$

For the line parameters we use the equations for the inductance and capacitance per unit length of a two wire line, in the logarithmic form, implying the assumption that the radius of the wires is very small compared with their spacing, and, so,

$$Z = j \frac{w\mu}{\pi} \ln \left(\frac{s}{a} \right) = j\ 120k \ln \left(\frac{s}{a} \right) \tag{29}$$

$$Y = j\ w\ \varepsilon\ \pi / \ln \left(\frac{s}{a} \right) = j\ k/120 \ln \left(\frac{s}{a} \right) \tag{30}$$

where

$w = 2\pi$ times the frequency

$\mu = 4\pi \times 10^{-7}$ Henry/m is permeability of free space

$\varepsilon = 10^{-9}/36\pi$ Farad/m is permittivity of free space

s is the spacing between wires, and

a is the wire radius.

The propagation factor, Γ, is a constant if we do not account for losses. If we consider the radiation resistance as a distributed loss resistance, with value Ra per unit length, we can use the following approximations described in the literature for lossy transmission lines, and define an attenuation per unit length.

$$\alpha = \frac{Ra}{2K_0} \tag{31}$$

and an average phase factor

$$\beta = \sqrt{ZY} \left(1 + \frac{1}{8Q^2} \right) = k \left(1 + \frac{1}{8Q^2} \right) \tag{32}$$

where

$$Q = \frac{R_a}{Z_0}$$

k is the free space phase constant, and

$\Gamma = \alpha + j\beta$

As mentioned before, we use for the computation of radiation resistance the equations given by Chaney and Klamm for a rhombic antenna in free space. Those equations were developed for an antenna well terminated, and carrying a travelling wave. Actually, the present structure does not exactly have the rhombic shape, but the elevation angles considered are small enough to allow the assumption that they can be neglected. More daring is the assumption of a travelling wave. However, from the work reported by DuHamel on nonuniform transmission lines [16], we conclude that the value of Q should not be expected to be critical, and that is essentially what would change directly with the value of radiation resistance.

So far we have not accounted for the mutual impedance among radiators, and, naturally, that is due to the large amount of computations needed, that would exceed the time allowed for the present work. After presenting the results obtained with the present assumptions we will try to do a rough estimate of the mutuals effects, based on the values found for current distribution and impedances.

Using equations (28) for the radiators and equations (27) for the stubs, we start from the end of the line, where there is a short-circuit, and proceed toward the feed point computing the input impedances, and the

coefficients of the equations. As a block the equations can be expressed by

$$V(x) = A\, V_0 - K_0\, B\, I_0 \tag{33a}$$

$$I(X) = -\frac{C}{K_0} V_0 + D\, I_0 \tag{33b}$$

and, for each section, we obtain A, B, C and D, and the ratio V_0/I_0. When we reach the feed end of the line ratio V_0/I_0 is its input impedance. Then we assign to the current the value 1.0 + j0.0 and we proceed forward, using the previously computed values of A, B, C and D, obtaining the values of current and voltage along the line, for as many points as the number of sections considered. From these, and using the equations, the complete description of the line can be obtained.

We program these equations into the IBM 360 system, according to the program in Appendix C. Appendix D shows the details of the equations involved.

Sample program SMIGUEL shows the results for the same antenna that was used in sample program AZORES (radiation pattern), for three frequencies within the operation band--1100, 1700 and 2300 MHZ. For each frequency the first run does not account for mutual impedance effects. The second run includes the mutual resistance that would be found between parallel wires with sinusoidal current distribution.

The experimental results obtained by Greiser and Mayes [8], [9], with the BLPZZ fed against ground show that the input impedance has a resistive component varying between 90 and 250 ohms and a reactive component varying between +10 and -100 ohms. Since we are considering a double structure, we would expect the resistance values to be about doubled.

Although the behavior of the reactive component is more difficult to predict, we would expect the same orders of magnitude.

These assertions are confirmed in the results obtained for 2300 MHz. Referring to SMIGUEL the column of ZINR values shows the input impedance seen at the feed end of each radiator, and, not only the input impedance is as expected (291.3-j314.8 ohms), but also, as assumed before, each element essentially provides a match for the next element. The column of CUR values shows the magnitude of the current at the feed end, at the vertex, and at the stub end of each radiator. We note that, for this frequency, element 2 is smaller than a quarter of a wavelength, and that element 3 is larger than that. Up to the third element the current magnitude values are typical of an attenuated standing wave situation. After element 3 the distribution is of a heavily attenuated travelling wave.

As mentioned beofre, the more delicate assumption in this approach was to apply to this structure the radiation resistance given by Chaney and Klamm [24], [25] for the rhombic antenna. It appears from these first results that such assumption is reasonable for the large elements, but it is not adequate for the small elements. Also, for these elements, the effects of mutual impedance become increasingly important, since they are "electrically closer" to each other. These two sources of error become more important as we lower the frequency. At 1700 MHz (the resonance dimension falling between elements 7 and 8) the results obtained for the first 4 elements are inconsistent.

A closer inspection of the results shows that the departures in impedance values are related to extremely high values of Q (above 20), and that fact even more strengthens the idea that the loading due to mutual

effects plays an important part in the behavior of the "feed region" of the antenna.

At this point we found it useful to make some numerical analysis of radiation and mutual resistance values, with the following conclusions:

(1) The radiation resistance of the "rhombic" elements increases steadily with size, from a few ohms at the "feed region" to thousands of ohms at the "end region."

(2) The mutual resistance between parallel wires in adjacent elements with sinusoidal distribution of current, in phase, decreases steadily from hundreds of ohms at the "feed region" to essentially zero at the "end region."

This enables us to obtain a better approximation, by also including the mutual effects, taking two parallel consecutive wires of the structure at a time. Again here, we neglect a few points; namely, that the parallel wires considered do not have the same size, the input currents are not in phase, the current distribution is not exactly sinusoidal, and that there are other interactions to be accounted for, among the non-parallel wires. However, before taking this step we made extensive numerical calculations with different arrangements of wires with different conditions of phase differences and current distributions, and the results obtained were all within the same orders of magnitude.

Essentially, what we are doing here is to introduce a rough correction to lower the Q of the "feed region," and the same result could be obtained if we assigned to it specific (and reasonable) values. As shown in the referenced paper by DuHamel [16] the exact value of Q is relatively unimportant.

We note that, by this procedure

(1) at the "feed region" we are essentially neglecting the travelling wave approach since the rhombic radiation resistance is much smaller than the mutual resistance, and

(2) inversely, at the "end region," we are neglecting the sinusoidal distribution approach.

The results obtained with this procedure apparently prove its soundness. For the three cases previously considered, the input impedance values now fall in the expected range (439.1-j148.5, 562.1-j109.8, and 516.4+j19.9 ohms). The current distribution shows the same features as before but with stronger attentuation, making it resemble more closely an attenuated travelling wave configuration.

The next step would be to obtain a more exact description of the line by considering a larger number of smaller sections, obtaining better approximations for the non-uniformity corrections, and a more detailed picture of the current values. That would enable the application of these results to the radiation equations. Unfortunately the attempts to program this detailed analysis failed due to unknown reasons, related to the difficulties encountered during the "adaptation" phase of the new IBM 360 system, recently installed at the Naval Postgraduate School. Although we have received extensive help from the Computer Facility staff, and undoubtedly the program would eventaully work, there was not time available to pursue the project.

Before closing this subject we note that, due to the method used in deriving the coefficients in equations (33), there is a cumulative source of error in the approximations used. This is so because every new value

is based on another value that had been obtained by an approximation, and only the first value is an exact value. Since we start from the end of the structure, the "end region" coefficients are little affected, but the ones at the "feed region" are likely to be farther away from exactness. This might be another reason for the worse results obtained with the smaller elements. The way to correct, or at least to minimize this error, would be to split the line in more sections, as was attempted.

Finally, we note that the current distribution does not show the marked peak near the resonance region obtained with parallel feed type of structures, or circuits. On one side this seems a reasonable result due to the different physical lay-out of the antenna; but, on the other side, it remains to be explained why the radiation patterns show acceptable results with different current distributions. An inspection of the phase distribution of the current (column CANG) shows that in all cases the current at the feed point of any two consecutive elements is very nearly in phase opposition, except for the element with dimensions closest to the resonance dimension, and the one before that. For these, the phase difference is near 90°, as also happens in other LP structures. This means then that only the "active region" is important for radiation characteristics, and the two models of current distribution previously used are essentially equivalent to each other and to the computed values.

BIBLIOGRAPHY

1. "Electromagnetic Theory," by Y. A. Stratton, McGraw-Hill Book Co., New York, 1941.

2. "Electromagnetic Waves," by S. A. Schelkunoff, D. Van Nostrand Co., Inc., New York, 1948.

3. "Principles of Microwave Circuits," by C. G. Montgomery, et al, McGraw-Hill Book Co., New York, 1948.

4. "Antenna Analysis," by E. A. Wolff, John Wiley and Sons, Inc., New York, 1966.

5. "Antenna Engineering Handbook," by H. Jasik (Ed.), McGraw-Hill Book Co., New York.

6. "Antennas," by J. Kraus, McGraw-Hill Book Co., New York, 1950.

7. "Topics in Electromagnetic Theory," by D. A. Watkins, John Wiley and Sons, Inc., New York, 1951.

8. "Vertically Polarized Log-Periodic Zig-Zag Antennas," by J. W. Greiser and P. E. Mayes, Proc. of the National Elect. Conference, Oct. 1961, pp. 193-204.

9. "The Bent Backfire Zig-Zag--A Vertically Polarized Frequency-Independent Antenna," by J. W. Greiser and P. E. Mayes, IEEE Transactions on Antennas and Propagation, May, 1964, pp. 281-290.

10. "The Design of Log-Periodic Dipole Antennas," by R. Carrel, IRE International Convention Record, 1961, pp. 61-75.

11. "Log-Periodic Dipole Arrays," by D. E. Isbell, IRE Transactions on Antennas and Propagation, May, 1960, pp. 260-267.

12. "A Non-Resonant Endfire Array for VHF and UHF," by W. A. Cumming, IRE Transactions on Antennas and Propagation, April, 1955, pp. 52-58.

13. "The Radiation Characteristics of a Zig-Zag Antenna," by D. L. Sengupta, IRE Transactions on Antennas and Propagation, April, 1958, pp. 191-194.

14. "Developments in Broadband Antennas," by E. C. Jordan, et al, IEEE Spectrum, April, 1964, pp. 58-71.

15. "Log-Periodic Antennas and Circuits," by R. H. DuHamel, "Electromagnetic Theory and Antennas," vol. 2, E. C. Jordan (Ed.), Pergamon Press, New York, 1963.

16. "Log Periodic Transmission Line Circuits--Part I: One Port Circuits," by R. H. DuHamel and M. E. Armstrong, IEEE Transactions on Microwave Theory and Techniques, June 1966, pp. 264-274.

17. "Theoretical Study of a Class of Logarithmically Periodic Circuits," by R. Mittra, University of Illinois Antenna Laboratory, Technical Report No. 59, July, 1962, Urbana, Illinois.

18. "Non-Uniform Transmission Lines with Applications to Log-Periodic Antennas," by R. Mittra and K. E. Jones, Proceedings of the National Electronics Conference, Vol. 20, 1964, pp. 23-28.

19. "Theoretical Brillouin Diagrams for Monopole and Dipole Arrays and Their Application to Log-Periodic Antennas," by R. Mittra and K. E. Jones, IEEE Transactions on Antennas and Propagation, September, 1964, pp. 533-540.

20. "Backward-Wave Radiation from Periodic Structures and Application to the Design of Frequency-Independent Antennas," by P. E. Mayes, G. A. Deschamps, and W. T. Patton, Proceedings of the IRE (Correspondence), May, 1961, pp. 962-963.

21. "Near Field Measurements on a Logarithmically Periodic Antenna," by R. L. Bell, C. T. Elfring and R. E. Franks, Electronic Defense Lab., P. O. Box 205, Mountain View, California, Technical Memo. No. EDL-M231, Dec., 1959.

22. "Resolution of Multimode Data in Periodic Structures and Waveguides," by R. Mittra and K. E. Jones, Proceedings of the IEEE, Feb. 1965, p. 325.

23. "Log Periodic Monopole Array," by D. G. Berry and F. R. Ore, IRE International Convention Record, 1961, pp. 76-85.

24. "Free Space Radiation Impedance of Rhombic Antenna," by J. G. Chaney, U. S. Naval Postgraduate School, Monterey, California, Technical Report No. 4, May, 1952.

25. "A Detailed Integration for the Radiation Impedance of a Rhombic Antenna," by C. F. Klamm, Jr., U. S. Naval Postgraduate School, Monterey, California, Technical Report No. 5, June, 1952.

APPENDIX A

I. Geometric Relations in the BLPZZ

With the aid of Fig. A-1 the following relations are evident:

$$L_n = \frac{L_1}{p^{n-1}} \qquad \text{and} \qquad b_n = \frac{b_1}{p^{n-1}} \tag{A-1}$$

The relation between the length of the radiating wires and the stubs can be obtained in the following way:

$$L_n = \frac{2b_n \cos\gamma}{\tan \alpha E} \qquad L_n' = \frac{2b'_n \cos\gamma}{\tan \alpha s} \tag{A-2}$$

$$L_n - L_{n-1} = \frac{2b_n \cos\gamma}{\tan \alpha E} - \frac{2b_{n-1} \cos\gamma}{\tan \alpha E} = 2b_{n-1}\sin\gamma + 2b_n \sin\gamma + 4b_{n-1}'\sin\gamma$$

$$\frac{\cos\gamma\, b_{n-1}}{\tan \alpha E} \left(\frac{1}{p} - 1\right) = b_{n-1} \sin\gamma \left(1 + \frac{1}{p}\right) + 2b_{n-1}' \sin\gamma$$

$$\frac{b_{n-1}}{\tan \alpha E} (1-p) = b_{n-1} \tan\gamma\, (1+p) + 2b_{n-1}'\, p \tan\gamma$$

$$\frac{b_n}{b_n'} = \frac{2p \tan\gamma \tan \alpha E}{(1-p) - (1+p) \tan\gamma \tan \alpha E} \tag{A-3}$$

Other useful relations are

$$2L'_{n-1} = L_{n-1} + L_{n-1} \tan \alpha E \tan\gamma + L_n - L_n \tan \alpha E \tan\gamma$$

$$= L_{n-1} \left(1 + \frac{1}{p}\right) + L_{n-1} \left(1 - \frac{1}{p}\right) \tan \alpha E \tan\gamma$$

$$= \frac{L_{n-1}}{p} [(1+p) + (p-1) \tan \alpha E \tan\gamma]$$

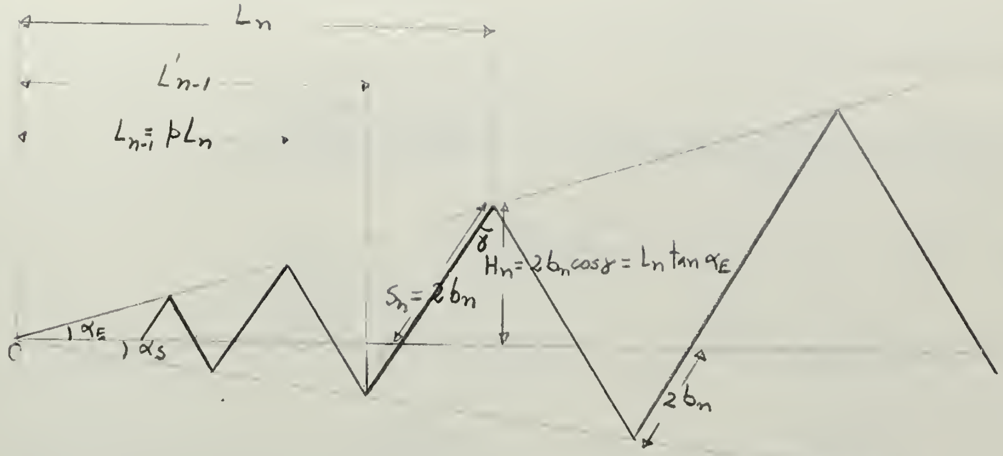

a) Basis structure

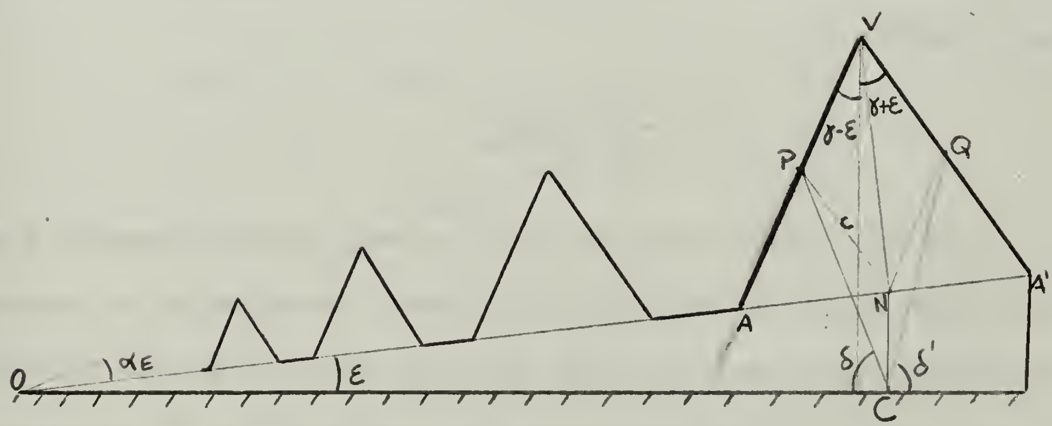

b) Bent structure

Fig A-1 - Geometric Relations in the BLPZZ

from which

$$b'_{n-1} = \frac{L_{n-1}}{4p\cos\gamma}\left[(1+p) - (1-p)\tan\alpha E \tan\gamma\right]\tan\alpha s$$

and combining with (A-3)

$$\frac{b_{n-1}}{\frac{L_{n-1}}{4p\cos\gamma}\left[(1+p)-(1-p)\tan\alpha_E\tan\gamma\right]\tan\alpha_S} = \frac{2p\tan\gamma\tan\alpha_E}{(1-p)-(1+p)\tan\gamma\tan\alpha_E}$$

and, since $$L_{n-1} = \frac{2b_{n-1}\cos\gamma}{\tan\alpha E}$$

$$(1-p)-(1+p)\tan\gamma\tan\alpha_E = (1+p)\tan\gamma\tan\alpha_S - (1-p)\tan\alpha_E\tan\alpha_S\tan^2\gamma$$

$$\tan\gamma = \frac{\left(\frac{1+p}{1-p}\right)(\tan\alpha_E+\tan\alpha_S) - \sqrt{\left(\frac{1+p}{1-p}\right)^2(\tan\alpha_E+\tan\alpha_S)^2 - 4\tan\alpha_E\tan\alpha_S}}{2\tan\alpha_E\tan\alpha_S} \qquad \text{(A-4)}$$

Since the structure is usually defined by the parameters αE, αs, p, b for the last element and the number of elements, equation (A-4) gives the next parameter, γ, and equations (A-1) and (A-2) define the rest of the structure. The length of the stubs can be obtained with (A-3), or approximately by

$$b'_n = \frac{b_n}{\sqrt{p}}\,\frac{\tan\alpha s}{\tan\alpha E} \qquad \text{(A-5)}$$

This equation is exact when $\alpha s = \alpha E$, but it can be used as a good approximation for the typical values used. The equation is obtained by inspection of Fig. A-1, with the help of a sort of "optical illusion." In fact, when $\alpha s = \alpha E$ the structure repeats itself at $\sqrt{p}$ increments, with an upside down rotation. When $\alpha s \neq \alpha E$, however, the rate of change of b' with αs is not linear and the equation is not true.

The relations concerning the "phase center" of the element are obtained from Fig. 3, by inspection

$$\tan \delta_1 = \frac{L_n \sin \varepsilon + b_n \cos(\gamma - \varepsilon)}{b_n \sin(\gamma - \varepsilon)} \quad \text{(A-6)}$$

$$\tan \delta_2 = \frac{L_n \sin \varepsilon + b_n \cos(\gamma + \varepsilon)}{b_n \sin(\gamma + \varepsilon)} \quad \text{(A-7)}$$

$$c_1 = \frac{b_n \sin(\gamma - \varepsilon)}{\cos \delta_1} \quad \text{(A-8)}$$

$$c_2 = \frac{b_n \sin(\gamma + \varepsilon)}{\cos \delta_2} \quad \text{(A-9)}$$

II. Transformations of Coordinates

Expressions for the angle between a wire and a direction $-\theta'$. Considering Fig. A-2, that is a planification of the Y=0 and Z=0 planes, we obtain the following relations:

$$\cos a \sin b = \cos\theta$$

$$\cos a \cos b = \sin\theta \cos \phi_1 \qquad \phi_1 = 180-\phi$$

$$\begin{aligned} R \cos\theta' &= R \cos a \cos (\beta - b) \\ &= R [\cos \beta \cos a \cos b + \sin \beta \cos a \sin b] \\ &= R [\cos \beta \sin \theta \cos \phi_1 + \sin \beta \cos \theta] \\ &= R [\sin \beta \cos \theta - \cos \beta \sin \theta \cos \phi] \end{aligned}$$

The wire in the figure corresponds to wire 1 in a BLPZZ element, and the angle β is given by (see Fig. A-1)

$$\beta = \varepsilon + 90° - \gamma = 90° - (\gamma - \varepsilon)$$

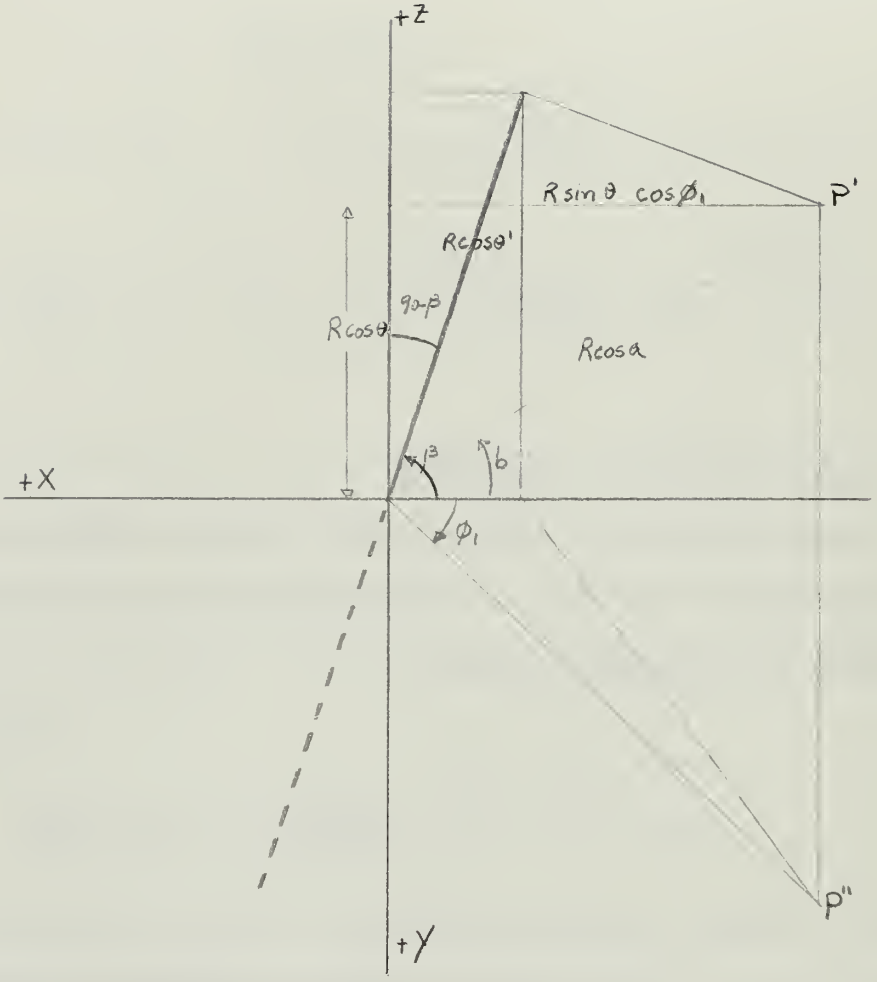

Fig. A-2 - Transformation of coordinates

so that, for wire 1

$$\cos\theta_1' = \cos(\gamma-\varepsilon)\cos\theta - \sin(\gamma-\varepsilon)\sin\theta\cos\phi \tag{A-10}$$

For wire 2 we have instead of an angle β, and angle $-\beta$, given by

$$-\beta = -(90 - (\gamma+\varepsilon))$$

and using the equation for $\cos\theta_1'$ we get

$$\cos\theta_2' = -\cos(\gamma+\varepsilon)\cos\theta - \sin(\gamma+\varepsilon)\sin\theta\cos\phi \tag{A-11}$$

For wire 3, we obtain (see Fig. A-3)

$$\cos a \sin b = \cos\theta$$

$$\cos a \cos b = \sin\theta\cos\phi.$$

$$\begin{aligned}\cos\theta_3' &= \cos a \cos(\beta-b)\\ &= \cos a\cos b\cos\beta + \cos a\sin b\sin\beta\\ &= \cos\theta\sin\beta + \sin\theta\cos\beta\cos\phi_1\end{aligned}$$

and, with $\phi_1 = \phi$ and $\beta = 90 - (\gamma-\varepsilon)$

$$\cos\theta_3' = \cos\theta\cos(\gamma-\varepsilon) + \sin\theta\sin(\gamma-\varepsilon)\cos\phi \tag{A-12}$$

For wire 4, we note that the only difference is again the direction of the angle $\beta = 90 - (\gamma+\varepsilon)$, so that

$$\cos\theta_4' = -\cos\theta\cos(\gamma+\varepsilon) + \sin\theta\sin(\gamma+\varepsilon)\cos\phi \tag{A-13}$$

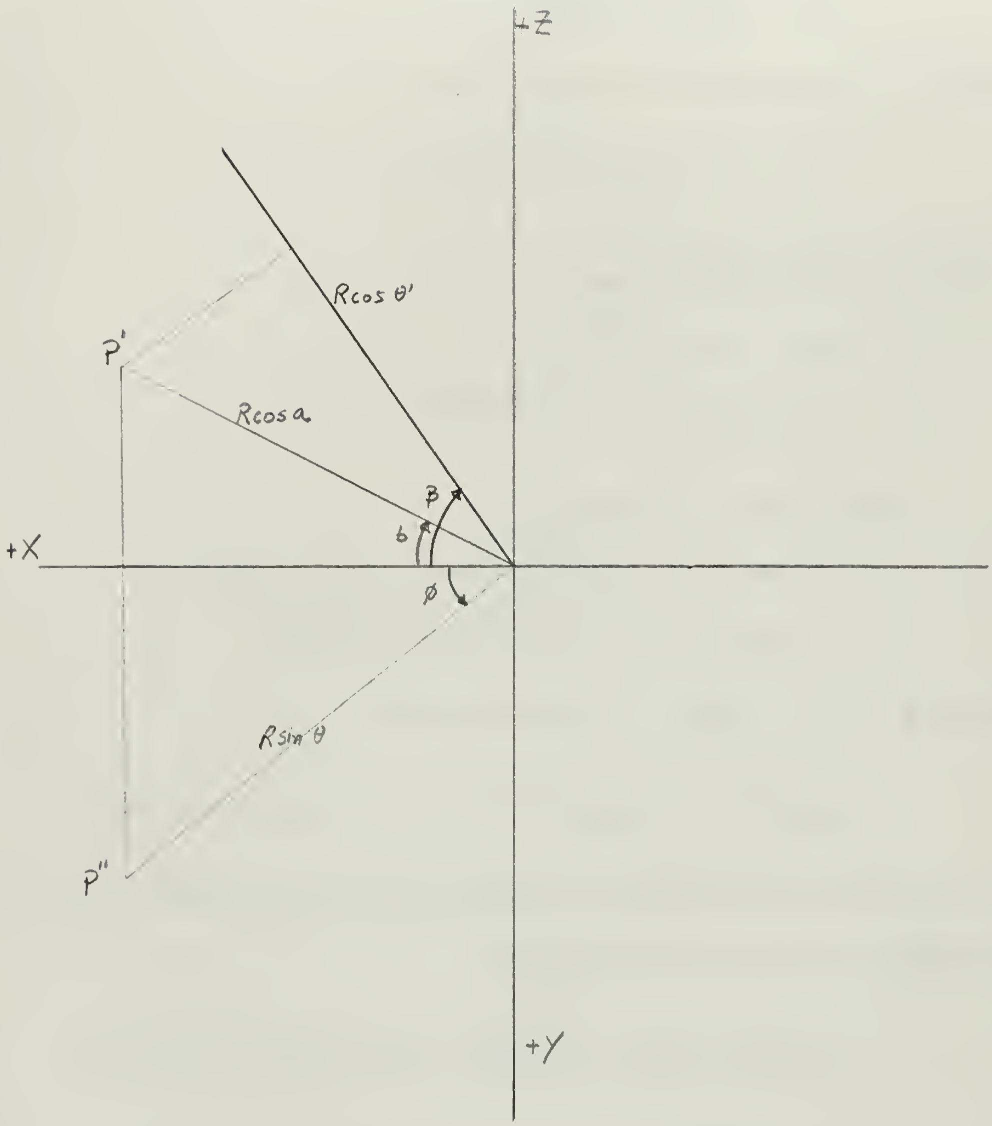

Fig. A-3 - Transformation of Coordinates - Wire 3

III. <u>The Components of the E_θ' Vector in Spherical Coordinates</u>

According to Fig. A-4, we obtain the following relations, for wire 1

$$E_{\theta_1} = E_{\theta_1'} \cos A_1 \tag{A-14a}$$

$$E_{\phi_1} = E_{\theta_1'} \sin A_1 \tag{A-14b}$$

Using the expression from spherical trigonometry

$$\cos A_1 = \frac{\cos a - \cos b \cos c}{\sin b \sin e}$$

we obtain

$$\cos A_1 = \frac{\cos(90-\beta) - \cos\theta_1' \cos\theta}{\sin\theta_1' \sin\theta} = \frac{\sin\beta - \cos\theta(\sin\beta\cos\theta - \cos\beta\sin\theta\cos\phi)}{\sqrt{1-\cos^2\theta_1'}\ \sin\theta}$$

$$= \frac{\sin\beta - \sin\beta\cos^2\theta + \cos\beta\sin\theta\cos\theta\cos\phi}{\sqrt{1-\cos^2\theta_1'}\ \sin\theta} = \frac{\sin\beta(1-\cos^2\theta) + \cos\beta\sin\theta\cos\theta\cos\phi}{\sqrt{1-\cos^2\theta_1'}\ \sin\theta}$$

$$= \frac{\sin\beta\sin\theta + \cos\beta\cos\theta\cos\phi}{\sqrt{1-\cos^2\theta_1'}}$$

and, since $\beta = 90 - (\gamma-\varepsilon)$,

$$\cos A_1 = \frac{\cos(\gamma-\varepsilon)\sin\theta + \sin(\gamma-\varepsilon)\cos\theta\cos\phi}{\sqrt{1-\cos^2\theta_1'}} \tag{A-15a}$$

We have the denomination in the form $\sqrt{1-\cos^2\theta_1'}$ because in the field expression we have a $\sin\theta'$ in numerator that cancels with this. Now we obtain, from here, sin A

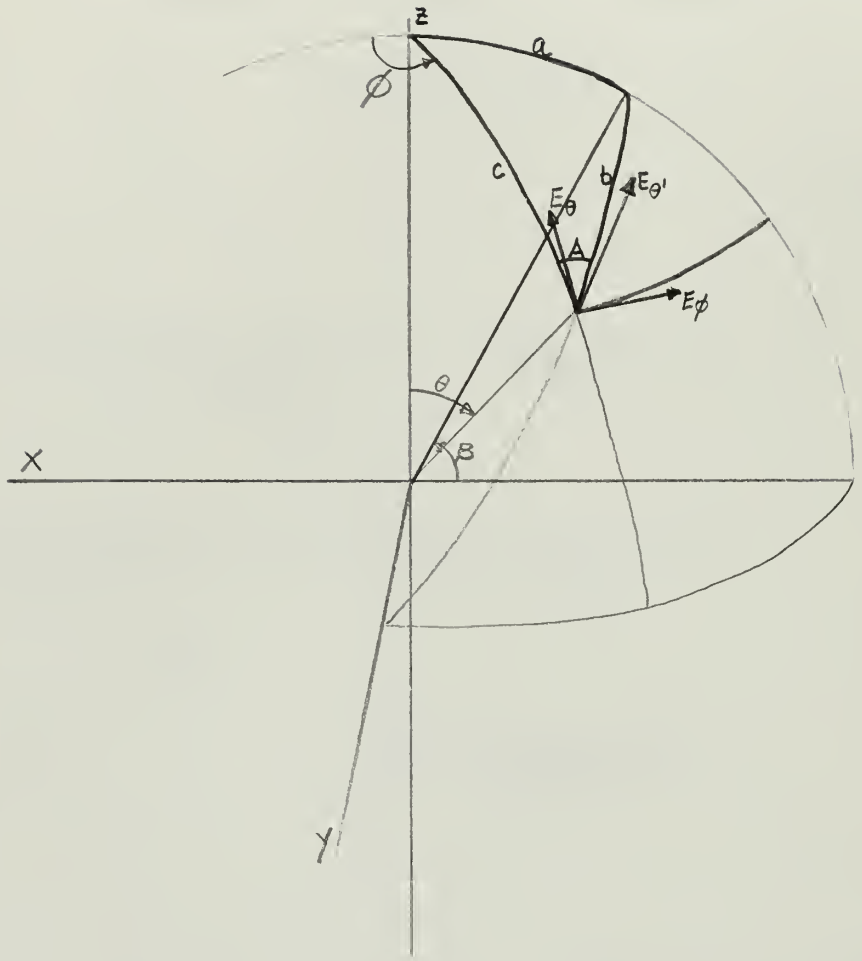

Fig. A-4 - Components of the field vector

$$\sin^2 A_1 = 1-\cos^2 A_1 = \frac{1-(\sin^2\beta\cos^2\theta+\cos^2\beta\sin^2\theta\cos^2\phi-2\sin\beta\cos\beta\sin\theta\cos\theta\cos\phi)}{\sin^2\theta_1'} -$$

$$-\frac{(\sin^2\beta\sin^2\theta+\cos^2\beta\cos^2\theta\cos^2\phi+2\sin\beta\cos\beta\sin\theta\cos\theta\cos\phi)}{\sin^2\theta_1'}$$

that reduces to

$$\sin^2 A_1 = \frac{1-\sin^2\beta-\cos^2\phi(1-\sin^2\beta)}{\sin^2\theta_1'} = \frac{(1-\sin^2\beta)(1-\cos^2\phi)}{\sin^2\theta_1'} = \frac{\cos^2\beta\sin^2\phi}{\sin^2\theta_1'}$$

and

$$\sin A_1 = \frac{\cos\beta\sin\phi}{\sin\theta_1'} = \frac{\sin(\gamma-\varepsilon)\sin\phi}{\sin\theta_1'} \tag{A-15b}$$

The procedure is analogous for the other wires, and the results are for wire 2

$$E_{\theta_2} = -E_{\theta'}\cos A_2 \tag{A-16a}$$

$$E_{\theta_2} = E_{\theta'}\sin A_2 \tag{A-16b}$$

$$\cos A_2 = \frac{\cos(\gamma+\varepsilon)\sin\theta-\sin(\gamma+\varepsilon)\cos\theta\cos\phi}{\sin\theta_2'} \tag{A-17a}$$

$$\sin A_2 = \frac{\sin(\gamma+\varepsilon)\sin\phi}{\sin\theta_2'} \tag{A-17b}$$

for wire 3

$$E_{\theta_3} = E_{\theta_3'} \cos A_3 \qquad \text{(A-18a)}$$

$$E_{\phi_3} = - E_{\theta_3'} \sin A_3 \qquad \text{(A-18b)}$$

$$\cos A_3 = \frac{\cos(\gamma-\varepsilon)\sin\theta - \sin(\gamma-\varepsilon)\cos\theta\cos\phi}{\sin\theta_3'} \qquad \text{(A-19a)}$$

$$\sin A_3 = \frac{\sin(\gamma-\varepsilon)\sin\phi}{\sin\theta_3'} \qquad \text{(A-19b)}$$

and for wire 4

$$E_{\theta_4} = - E_{\theta_4'} \cos A_4 \qquad \text{(A-20a)}$$

$$E_{\phi_4} = E_{\theta_4'} \sin A_4 \qquad \text{(A-20b)}$$

$$\cos A_4 = \frac{\cos(\gamma+\varepsilon)\sin\theta + \sin(\gamma+\varepsilon)\cos\theta\cos\phi}{\sin\theta_4'} \qquad \text{(A-21a)}$$

$$\sin A_4 = \frac{\sin(\gamma+\varepsilon)\sin\phi}{\sin\theta_4'} \qquad \text{(A-21b)}$$

IV. The Angle α for the Correction of Reference Point

This is the angle between the direction of c (see Fig. 3) and the direction to a point in the far field. Since c is in the same vertical plane as the wires, we can use the relations developed for the conversion of the angle θ' to spherical coordinates, with δ in place of β, and we obtain the following relations:

$$\cos \alpha_1 = -[\sin \delta_1 \cos \theta + \cos \delta_1 \sin \theta \cos \phi] \qquad \text{(A-22)}$$

$$\cos \alpha_2 = \sin \delta_1 \cos \theta - \cos \delta_1 \sin \theta \cos \phi \qquad \text{(A-23)}$$

$$\cos \alpha_3 = \sin \delta_1 \cos \theta - \cos \delta_1 \sin \theta \cos \phi \qquad \text{(A-24)}$$

$$\cos \alpha_4 = \sin \delta_2 \cos \theta + \cos \delta_2 \sin \theta \cos \phi \qquad \text{(A-25)}$$

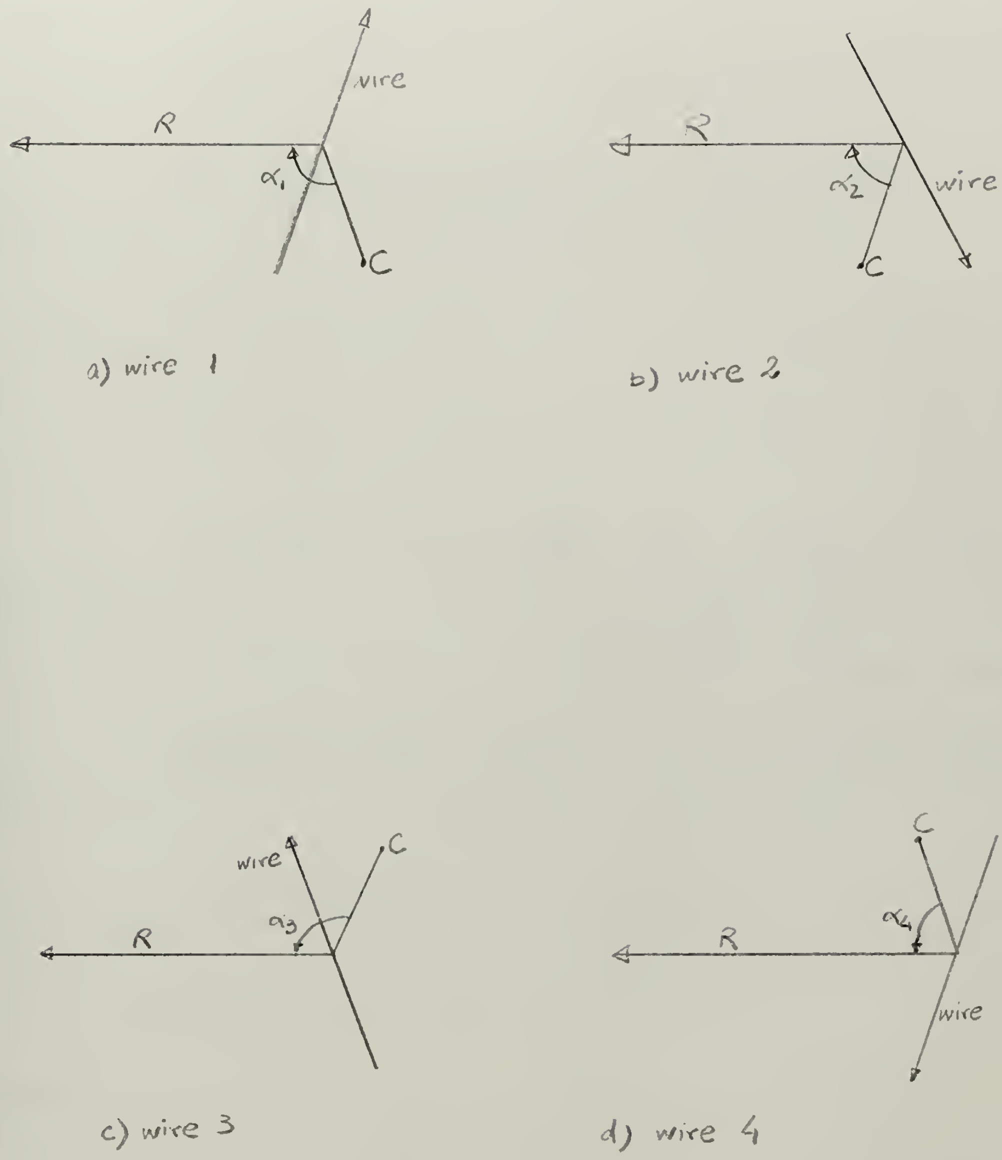

Fig. A-5 - Reference point and direction angles

The angles δ_1 and δ_2 are shown in Fig. 3, and given by equations (A-6) and (A-7). Fig. A-5 shows the way how the α angles are defined.

APPENDIX B

Field Equations for Wires 2, 3 and 4

I - Wire 2

Since wire 2 (see Fig. 5) is in series with wire 1, we need to add in the exponent a factor corresponding to the length of wire 1 - 2b - and we get from (7)

$$E_{\theta_2'} = \frac{kF}{2} I_o e^{-j3\beta b} \frac{e^{\left[\alpha + jk\left(\frac{\beta}{k} - \cos\theta_2'\right)\right]b} - e^{-\left[\alpha + jk\left(\frac{\beta}{k} - \cos\theta_2'\right)\right]b}}{\left[\alpha + jk\left(\frac{\beta}{k} - \cos\theta_2'\right)\right]} \tag{B-1}$$

Now, using equations (A-11), (A-16), (A-17) and (A-23), we obtain

$$E_{\theta_2} = -\frac{kF}{2} I_o e^{-jk\left[3\frac{\beta}{k} b + c_2 \cos\alpha_2\right]} \frac{e^{\left[\alpha + jk\left(\frac{\beta}{k} - \cos\theta_2'\right)\right]b} - e^{-\left[\alpha + jk\left(\frac{\beta}{k} - \cos\theta_2'\right)\right]b}}{\left[\alpha + jk\left(\frac{\beta}{k} - \cos\theta_2'\right)\right]} \times \left[\cos(\gamma+\varepsilon)\sin\theta - \sin(\gamma+\varepsilon)\cos\theta\cos\phi\right] \tag{B-2}$$

$$E_{\phi_2} = \frac{k}{2} F I_o e^{-jk\left[3\frac{\beta}{k} b + c_2 \cos\alpha_2\right]} \frac{e^{\left[\alpha + jk\left(\frac{\beta}{k} - \cos\theta_2'\right)\right]b} - e^{-\left[\alpha + jk\left(\frac{\beta}{k} - \cos\theta_2'\right)\right]b}}{\left[\alpha + jk\left(\frac{\beta}{k} - \cos\theta_2'\right)\right]} \times \sin(\gamma+\varepsilon)\sin\phi \tag{B-3}$$

where the factor $e^{-jk\, c_2 \cos\alpha_2}$ is the correction for the reference point, being c_2 and $\cos\alpha_2$ given by equations (A-9) and (A-23).

II - Wire 3

Here we consider the current flowing upward, but to use the same exponential representation for the current, we consider the distance as negative away from the source. This is the usual representation for transmission lines, inherent in the present assumption of a travelling wave in the antenna. Then

$$I_3 = I_0 \, e^{-j\beta s}$$

and

$$E_{\theta_3'} = \frac{Fk}{2} I_0 \sin\theta_3' \, e^{-j\beta b} \, \frac{e^{[\alpha+jk(\frac{\beta}{k}+\cos\theta_3')]b} - e^{-[\alpha+jk(\frac{\beta}{k}+\cos\theta_3')]b}}{[\alpha+jk(\frac{\beta}{k}+\cos\theta_3')]} \qquad \text{(B-4)}$$

Now, using equations (A-12), (A-18), (A-19) and (A-24), we obtain

$$E_{\theta_3} = \frac{Fk}{2} I_0 \, e^{-jk[\frac{\beta}{k}b + c_3\cos\alpha_3]} \, \frac{e^{[\alpha+jk(\frac{\beta}{k}+\cos\theta_3')]b} - e^{-[\alpha+jk(\frac{\beta}{k}+\cos\theta_3')]b}}{[\alpha+jk(\frac{\beta}{k}+\cos\theta_3')]} \times$$

$$\times [\cos(\gamma-\varepsilon)\sin\theta - \sin(\gamma-\varepsilon)\cos\theta\cos\phi] \qquad \text{(B-5)}$$

$$E_{\phi_3} = -\frac{Fk}{2} I_0 \, e^{-jk[\frac{\beta}{k}b + c_3\cos\alpha_3]} \, \left(e^{[\alpha+jk(\frac{\beta}{k}+\cos\theta_3')]b} - e^{-[\alpha+jk(-\frac{\beta}{k}+\cos\theta_3')]b} \right) \times$$

$$\times \sin(\gamma-\varepsilon)\sin\phi \qquad \text{(B-6)}$$

where c_3 and α_3 are given by equations (A-8) and (A-24). Note that $c_3 = c_1$, and $c_4 = c_2$ (Fig. 5).

III. <u>Wire 4</u>

This wire is in series with wire 3, so that the procedure is analogous to wire 2 that was in series with wire 1

$$E_{\theta_4'} = \frac{Fk}{2} I_0 \sin\theta_4' \, e^{-j\beta 3b} \, \frac{e^{[\alpha+jk(\frac{\beta}{k}+\cos\theta_4')]b} - e^{-[\alpha+jk(\frac{\beta}{k}+\cos\theta_4')]b}}{[\alpha+jk(\frac{\beta}{k}+\cos\theta_4')]} \qquad \text{(B-7)}$$

Now, using equations (A-13), (A-20), (A-21) and (A-25), we obtain

$$E_{\theta_4} = -\frac{Fk}{2} I_0 \, e^{-jk[\frac{\beta}{k}3b + c_4\cos\alpha_4]} \, \frac{e^{[\alpha+jk(\frac{\beta}{k}+\cos\theta_4')]b} - e^{-[\alpha+jk(\frac{\beta}{k}+\cos\theta_4')]b}}{[\alpha+jk(\frac{\beta}{k}+\cos\theta_4')]} \times$$

$$\times [\cos(\gamma+\varepsilon)\sin\theta + \sin(\gamma+\varepsilon)\cos\theta\cos\phi] \qquad \text{(B-8)}$$

$$E_{\phi_{4_1}} = -\frac{Fk}{2} I_0 \, e^{-jk\left[\frac{\beta}{k} 3b + c_4 \cos\alpha_{4_1}\right]} \, \frac{e^{\left[\alpha + jk\left(\frac{\beta}{k} + \cos\theta_4'\right)\right]b} - e^{-\left[\alpha + jk\left(\frac{\beta}{k} + \cos\theta_4'\right)\right]b}}{\left[\alpha + jk\left(\frac{\beta}{k} + \cos\theta_4'\right)\right]} \times \tag{B-9}$$

$$\times \sin(\gamma + \varepsilon) \sin\phi$$

APPENDIX C

Equations for Non-Uniform Line

I. Line Parameters

Neglecting wire resistance and conductance between wires, the line parameters are

$$Z = j\ 120\ k\ \ln\ (s/a)$$

and

$$Y = j\ k/\ (120\ \ln\ (s/a))$$

as given by equations.

From here we obtain the line impedance

$$K = \sqrt{Z/Y} = 120\ \ln\ (s/a) = \frac{Z}{jk}$$

and the propagation factor not accounting for losses

$$\Gamma = \sqrt{ZY} = jk$$

In terms of the structure defining dimensions and angles (see Fig. A-1a), we obtain the following equations

For the radiators

$$Z(x) = j\ 120k\ (B + \ln\ (A + x)) \qquad \text{for } 0 \leq x < 2b \qquad \text{(C-1a)}$$

$$Z(x) = j\ 120k\ (C + \ln\ (D - x)) \qquad \text{for } 2b \leq x \leq 4b \qquad \text{(C-1b)}$$

where

$$A = \frac{1 - 2b\ \sin\gamma}{\cos\ (\gamma-\varepsilon)}\ \sin\varepsilon$$

$$B = \ln \frac{2\ \cos\ (\gamma-\varepsilon)}{a}$$

$$C = \ln \frac{2 \cos (\gamma+\epsilon)}{a}$$

$$D = \frac{L - 2b \sin \gamma}{\cos (\gamma+\epsilon)} \sin\epsilon + \frac{2b \cos (\gamma-\epsilon)}{\cos (\gamma+\epsilon)} + 2b$$

For the stubs

$$z(x) = j120K\left(E + \ln (F+x) \right) \tag{C-2}$$

where

$$E = \ln \frac{2\sin \gamma \sin \epsilon}{a}$$

$$F = \frac{L}{\sqrt{p} \sin \gamma} - \frac{2b \tan \alpha_s}{\sqrt{p} \tan \alpha_E}$$

and the quantities involved are as defined in Fig. A-1a

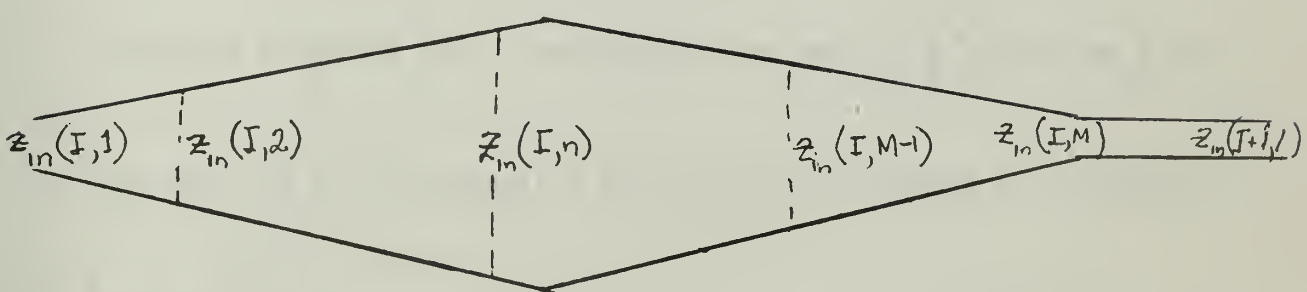

Fig. C-1 Input Impedance.

II. Radiation Resistance

According to Chaney and Klamm [24], [25], the radiation resistance of a rhombic antenna in free space is given by

$$R_r = 120 \Big\{ 1.1544 + 2 \ln (2 kl \sin^2 a) + 2 \mathrm{Ci} (2kl) - 2 \mathrm{Ci}(2kl \sin a)$$

$$- \mathrm{Ci} (2kl (1 + \cos a) - \mathrm{Ci}\Big(2kl (1 - \cos a) \Big)$$

$$+ \cos\Big(2kl \sin^2 a \Big)\Big[\mathrm{Ci}\Big(2kl \cos a (1 - \cos a) \Big) + \mathrm{Ci}\Big(2kl \sin a (1 - \sin a) \Big)$$

$$+ \mathrm{Ci}\Big(2kl \cos a(1+\cos a)\Big) + \mathrm{Ci}\Big(2 kl \sin a(1+\sin a)\Big) - 2\mathrm{Ci}\Big(2 kl \cos^2 a \Big)$$

$$- 2\mathrm{Ci}\Big(2kl \sin^2 a \Big)\Big]$$

$$+ \sin\Big(2kl \sin^2 a\Big)\Big[\mathrm{Si}\Big(2kl \cos a (1-\cos a)\Big) - \mathrm{Si}\Big(2kl \sin a (1-\sin a)\Big)$$

$$- \mathrm{Si}\Big(2kl \cos a (1+\cos a)\Big) + \mathrm{Si}\Big(2kl \sin a (1+\sin a) \Big) + 2 \mathrm{Si}\Big(2kl \cos^2 a \Big)$$

$$- 2 \mathrm{Si}\Big(2kl \sin^2 a \Big)\Big]\Big\}$$

where l is the wire length - 2b - , a is the vertex angle $90^{\circ} - \gamma$, Ci is the cosine integral

$$\mathrm{ci}(x) = \int_{\infty}^{x} \frac{\cos v}{v}\, dv$$

and Si is the sine integral

$$\mathrm{Si}(x) = \int_0^x \frac{\sin v}{v}\, dv$$

III. Input Impedance and Current Distribution

Using equations (33) and dividing the line in sections as shown in Fig. D-1, we obtain for each section

$$Z_{in}(I,n) = \mathrm{Kave}(I,n)\, \frac{\mathrm{Kave}(I,n)\ B(I,n) + \mathrm{Zin}(I,n+1)\ D(I,n)}{\mathrm{Zin}(I,n+1)\ C(I,n) + \mathrm{Kave}(I,n)\ A(I,n)}$$

Each stub counts as only one section of uniform line. The number M of divisions within each radiation depends on the degree of approximation desired, but it is convenient to use for M an even number, to avoid the relatively faster rate of change of characteristics at the middle point.

APPENDIX D

Computer Programming

I. Program AZORES

This program is written in code FORTRAN IV and it was prepared for the IBM 360 system that is operating at the Naval Postgraduate School.

The program uses two subroutines. The main program reads the data, computes and writes the physical characteristics of the antenna, selects the current distribution for the antenna wires, controls the coordinates of the desired pattern, prints the results, and calls for the subroutines.

The pattern computation is made by subroutine CORVO, that is given the antenna parameters, the elevation and azimuth angles, and the current distribution. In output, CORVO gives the two components of the electric field.

The program computes each pattern twice, for two different models of current distribution. Model 1 (see Fig. 9) is fed in data cards; Model 2 is generated by the main program.

The use of a large number of comment cards, hopefully makes the program self-explanatory. As much as possible, the names given to algebraic and geometric symbols have the same phonetics as the ones used in the text. The only remarkable exception is the symbol TAU, that stands for p, the structure scaling factor.

The following pages contain the programming statements and the output print of a sample program.

```
C
C
C        SAMPLE PRCGRAM AZORES - MAIN
C
C
C     COMPUTATION CF DIMENSIONS OF THE STRUCTURE
C
      AMEDA=(3.0*(1C.0**8))/FR
      SRES=AMEDA/4.0
      PI=3.14159
      RACIO1=.0005
      ALFAS=(2.0*PI*ALPAS)/360.0
      ALFAE=(2.0*PI*ALPAE)/360.0
      SAN=TAN(ALFAS)/TAN(ALFAE)
      TNT=2.0*TAN(ALFAE)*TAN(ALFAS)
      GNT=(TAN(ALFAE)+TAN(ALFAS))*((1.0+TAU)/(1.0-TAU))
      GANT=ATAN((GNT-SQRT(GNT**2-2.0*TNT))/TNT)
      GAMA=GANT
      B1=SDE*(TAU**(DE-1.0))/2.0
      EL1=B1*2.0*CCS(GAMA)/TAN(ALFAE)
      GAMA=360.0*GAMA/(2.0*PI)
      NDE=DE
      NDD=DE
      DO 18 NN=1,NCD
      D(NN)=2.0*B1/(TAU**(NN-1))
   18 CONTINUE
C
C     PRINTING OF WORKING PARAMETERS
C       B1 -THE HALF LENGTH OF A WIRE OF THE FIRST ELEMENT
C       EL1-DISTANCE FROM THE CENTER OF FIRST ELEMENT
C           TO THE GEOMETRIC ORIGIN OF THE STRUCTURE
C       GAMA-THE HALF ANGLE AT THE VERTEX OF EACH ELEMENT
C       SAN- TAN(ALFAS)/TAN(ALFAE)
C       LAMEDA-WAVELENGTH
C       INPUT DATA
C       SRES-QUARTER OF A WAVELENGTH
C       D - THE LENGTH OF THE RADIATORS WIRES
C
C
      WRITE(6,22) ALPAE,ALPAS,TAU,FR,SDE,DE,EPSLON,B1,EL1,GAMA,SAN,AMEDA
      WRITE(6, 24) SRES,(D(NN),NN=1,NDD)
C
C     PREPARATION CF CCNSTANT VALUES TO BE USED BY CORVO
      GAMA=2.0*PI*GAMA/360.0
      EPSLCN=2.0*PI*EPSLON/360.0
```

```
C
C
C      SAMPLE PROGRAM AZCRES - MAIN
C
C
      DIMENSION BE(30),ELE(30),RAD1(30),RAD2(30),CUR(30),CURP(30)
     1,CAR(30),C(30),EA(20,40)
     2,ELEV(20),AZIM(40)
     3,BECA(30),ATEN(30)
     4,RADIO(30)
      COMPLEX ZCI,ZCIA,E1TETA,E1TETP,E1FI,E1FIP,ZCI2,ZCI2A,E2TETA,
     1E2TETP,E2FI,E2FIP,ENTETA,ENFI,ZCURR,ZDIST,ENTETC,ENFIC,ENTETS,
     2ENFIS
C
C     THIS PROGRAM COMPUTES THE RADIATION PATTERN OF A
C     LOG-PERIODIC BENT ZIG-ZAG ANTENNA.
C
C     THE DATA REQUIRED ARE THE FOLLOWING
C        ALFAE-ANGLE OF SPREAD OF THE RADIATORS
C        ALFAS-ANGLE OF SPREAD OF THE STUBS
C        TAU-THE PERIOD OF THE STRUCTURE
C        FR-FREQUENCY OF OPERATION
C        SDE-THE LENGTH OF A WIRE OF THE LAST ELEMENT
C        DE-THE NUMBER OF ELEMENTS
C        EPSLON-THE ELEVATION ANGLE OF THE STRUCTURE
C
C     IF DESIRED A CURRENT DISTRIBUTION CAN BE ASSIGNED
C     AND FED IN THE DATA CARDS
C
C     THE PROGRAM USES THE FOLLOWING SUBROUTINES:
C         CORVO - COMPUTES THE RADIATION PATTERN
C         POLA  - CONVERTS COMPLEX NUMBERS INTO POLAR FORM
C
C     READING OF ASSIGNED CURRENT DISTRIBUTION
C
C
      READ(5,10 ) (CAR(IX),IX=1,30)
C
      READ(5,12)K
C     K IS THE NUMBER OF RUNS DESIRED
      DO 510 KK=1,K
C
C     READING OF ANTENNA DATA
      READ (5,14) ALPAE,ALPAS,TAU,FR,SDE,DE,EPSLON
C
```

```
C
C
C
C          SAMPLE PRCGRAM AZORES - MAIN
C
C
      CAPA=2.0*PI/AMEDA
      GAMEP=GAMA-EPSLON
      GAPEP=GAMA+EPSLON
      DELTA1=  ATAN((EL1*SIN(EPSLON)+B1*COS(GAMEP))/(B1*SIN(GAMEP)))
      DELTA2=  ATAN((EL1*SIN(EPSLON)+B1*COS(GAPEP))/(B1*SIN(GAPEP)))
      RAD11  =B1*SIN(GAMEP)/COS(DELTA1)
      RAD21  =B1*SIN(GAPEP)/COS(DELTA2)
C
      FRL=3.0*(10.C**8)/(4.C*SDE)
      FRH=3.0*(10.C**8)/(8.0*B1)
      HH=SDE*COS(GAMEP)+EL1*SIN(EPSLON)/(TAU**(NDE-1))
      HL=EL1*SIN(EPSLON)
      SIZE=2.0*B1*(SIN(GAMEP)+SIN(GAPEP)/(TAU**(NDE-1)))+EL1*
     1(1.0/(TAU**(NDE-1))-1.0)
C
C     PRINTING THE OVERALL CHARACTERISTICS OF THE ANTENNA
      WRITE(6,25)FRH,FRL,HH,SIZE,HL
C
      DO 33 IP=1,3C
      ATEN(IP)=0.C
   33 BECA(IP)=CAPA
C
C     PREPARATICN CF CURRENT DISTRIBUTION
C     EACH CASE IS WORKED WITH TWO MODELS OF CURRENT DISTRIBUTION
C        -THE ASSIGNED VALUES GIVEN IN DATA
C        -THESE MODIFIED FOR AMPLITUDE 1.0 UP TO THE ACTIVE REGION
C
      DO 502 KV=1,2
      GO TO (100,2C0),KV
  100 EN=DE
  105 WRITE(6,1105) FR
  120 DO 126 M=1,NCE
      AM=M
      S=(2.0*B1)/(TAU**(M-1))
  123 IF(S-SDE) 124,127,127
  124 IF(S-(AMEDA/4.0)/(COS(GAMA))) 126,127,127
  126 CONTINUE
  127 M=AM-1.0
  128 MM=15-M
  129 DO 132 MV=1,NDE
```

```
C
C
C
C         SAMPLE PROGRAM AZORES - MAIN
C
C
  130 CUR(MV)=CAR(MM+MV)
  131 CURP(MV)=CUR(MV)
  132 CONTINUE
      MF=M
      GO TO 275
  200 M=AM-1.0
      MF=M
      MI=M -1
  205 WRITE(6,1205) FR
      DO 208 MY=1,MI
      CUR(MY)=1.0
      CURP(MY)=1.0
  208 CONTINUE
  275 CONTINUE
C
C
C     COMPUTATION OF PATTERN
C     IN THE PRESENT FORM THE PROGRAM COMPUTES PATTERNS
C     IN THE HORIZONTAL AND VERTICAL PLANS, AND REFERS THEM
C     TO THE (0,0) VALUE OF ODB.
C     THE RESULTS ARE PRINTED AS THEY ARE COMPUTED AND SHOW
C          ELEVATION ANGLE
C          AZIMUTH ANGLE
C          RESULTANT
C          ANGLE FROM THE FI UNIT VECTOR
C          RELATIVE INTENSITY IN DB
C          DIRECTIVITY OVER ISOTROPIC ASSUMING A WELL-BEHAVED
C          PATTERN
C          HORIZONTAL AND VERTICAL HALF-POWER ANGLES
C
  290 WRITE(6,1290)
  295 TETA=PI/2.0
      FI=0.0
      CALL CCRVO  (B1,EL1,TAU,AMEDA,GAMA,EPSLON,DE,TETA,FI,SAN,ETETA,
     1EFI,GAMEP,GAPEP,DELTA1,DELTA2,EN,RAD11,RAD21,CAPA,CUR,CURP,MF,
     1ATEN,BECA)
      CALL PCLA(ETETA,EFI,E,PSI)
      EREF=E
C
  300 JFI=1
```

SAMPLE PROGRAM AZORES - MAIN

```
      FI=0.0
      FIG=0.0
      DO 315 ITETA=1,9,1
      TETAG=(90-10*(ITETA-1))
      TETA=(2.0*PI*TETAG)/360.0
      CALL CCRVO  (B1,EL1,TAU,AMEDA,GAMA,EPSLON,DE,TETA,FI,SAN,ETETA,
     1EFI,GAMEP,GAPEP,DELTA1,DELTA2,EN,RAD11,RAD21,CAPA,CUR,CURP,MF,
     1ATEN,BECA)
      CALL POLA(ETETA,EFI,E,PSI)
      EA(ITETA,JFI)=E
      EDB=20.0*ALOG10(E/EREF)
      PELEV=90.0-TETAG
      WRITE(6,1350) PELEV,FIG,E,PSI,EDB
      ELEV(ITETA)=EDB
  315 CONTINUE
C
  320 JFI=37
      FI=PI
      FIG=180.0
      DO 335 ITETA=10,19,1
      TETAG=(10*(ITETA-10))
      TETA=(2.0*PI*TETAG)/360.0
      CALL CCRVO  (B1,EL1,TAU,AMEDA,GAMA,EPSLON,DE,TETA,FI,SAN,ETETA,
     1EFI,GAMEP,GAPEP,DELTA1,DELTA2,EN,RAD11,RAD21,CAPA,CUR,CURP,MF,
     1ATEN,BECA)
      CALL POLA(ETETA,EFI,E,PSI)
      EA(ITETA,JFI)=E
      EDB=20.0*ALOG10(E/EREF)
      PELEV=90.0-TETAG
      WRITE(6,1350) PELEV,FIG,E,PSI,EDB
      ELEV(ITETA)=EDB
  335 CONTINUE
      ITETA=1
      TETA=PI/2.0
      TETAG=90.0
      DO 355 JFI=1,37,1
      FIG=5*JFI-5
      FI=(2.0*PI*FIG)/360.0
      CALL CCRVO  (B1,EL1,TAU,AMEDA,GAMA,EPSLON,DE,TETA,FI,SAN,ETETA,
     1EFI,GAMEP,GAPEP,DELTA1,DELTA2,EN,RAD11,RAD21,CAPA,CUR,CURP,MF,
```

```
C
C
C         SAMPLE PRCGRAM AZCRES - MAIN
C
C
     1ATEN,BECA)
      CALL PCLA(ETETA,EFI,E,PSI)
      EA(ITETA,JFI)=E
      EDB=20.0*ALCG1C(E/EREF)
      PELEV=90.0-TETAG
      WRITE(6,135C) PELEV,FIG,E,PSI,FDB
      AZIM(JFI)=EDB
  355 CCNTINUE
C
      DC 386 ITETA=1,9,1
      RTI=EREF/EA(ITETA,1)
      IF(1.414-RTI) 387,387,386
  386 CCNTINUE
  387 PELEV=10*(ITETA-1) -5
  388 DO 392 JFI=1,37,1
      RTJ=EREF/EA(1,JFI)
      IF(1.414-RTJ) 397,397,391
  391 IF(ITETA-37) 392,395,395
  392 CONTINUE
C
  395 WRITE(6,1395)
  397 PFI=5*JFI-7
      DIR=10.0*ALOG10(41253.0/(4.0*PELEV*PFI))
  399 WRITE(6,1399)
      WRITE(6,401) DIR,PFI,PELEV
  500 WRITE(6,150C)
  502 CCNTINUE
  510 CONTINUE
   10 FCRMAT(8F1C.3)
   12 FORMAT (I10)
   14 FORMAT (3F10.3,E10.3,3F10.3)
   22 FORMAT(1H1,/,/,/,/,/,/,/,/,/,
     1             15X,17HALL UNITS ARE MKS,/,/,16X,11H-INPUT DATA,/
     2,/,18X,5HALFAE,1X,1H=,F10.4,/,18X,5HALFAS,1X,1H=,F10.4,/,18X,
     37HTAU   =,F1C.4,/,18X,7HFREQ  =,E10.3,/,18X,7HSDE    =,F10.4,/,18X
     4,7HDE    =,F1C.4,/,18X,7HEPSLON=,F10.4,/,/,16X,14H-COMPUTED DATA,
     5/,/,18X,7HB1     =,F1C.4,/,18X,7HL1     =,F10.4,/,18X,7HGAMA  =,
     6F10.4,/,18X,7HSAN    =,F10.4,/,18X,7HLAMEDA=,F10.4)
   24 FORMAT(1H0,17X,7HSRES  =,F10.4,/,18X,15HLENGTH OF WIRES,/,
     111(18X,3F1C.4,/))
```

SAMPLE PRCGRAM AZORES - MAIN

```
   25 FCRMAT(1HO,14X,28HMAX. FREQUENCY OF OPERATION ,E10.3,/,/,
     115X,28HMIN. FREQLENCY OF OPERATION ,E10.3,/,/,
     215X,24HHEIGHT  OF LAST ELEMENT ,4X,F10.3,/,/,
     315X,27HOVERALL LENGTH OF STRUCTURE ,1X,F10.3,/,/,
     415X,2CHHEIGHT OF FEED POINT ,8X,F10.3)
  401 FORMAT(1H ,14X,F7.3,2HDB,5X,F5.0,6X,F5.0)
 1105 FORMAT(1H1,/,/,/,/,/,/,/,/,/,
     1               15X,22HCURRENT DISTRIBUTION 1,5X,5HFREQ=,E10.3)
 1205 FCRMAT(1H1,/,/,/,/,/,/,/,/,/,
     1               15X,22HCURRENT DISTRIBUTION 2,5X,5HFREQ=,E10.3)
 1290 FORMAT(19X,4HELEV,5X,2HFI,11X,1HE,8X,3HPSI,8X, 3HEDB)
 1350 FORMAT(15X,2F8.0,4X,3F10.3)
 1395 FORMAT(1HO,1CX,13HNON DIRECTIVE)
 1399 FORMAT(1HO,15X,15HDIRECTIVITY/ISO,5X,6HFI 3DB,5X,8HELEV 3DB)
 1500 FORMAT(1HO,15X,36HTHIS DIRECTIVITY FIGURE WAS COMPUTED  ,/,18X,
     1   42HASSUMING THAT THE PATTERN IS WELL-BEHAVED. ,/,18X,
     2   43HIT HAS NO MEANING IF THERE ARE SIDE-LOBES. )
      END
```

```
C
C
C       SAMPLE PRCGRAM AZORES - SUBROUTINE CORVO
C
C
      SUBROUTINE CCRVO  (B1,EL1,TAU,AMEDA,GAMA,EPSLON,DE,TETA,FI,SAN,
     1ETETA,EFI,GAMEP,GAPEP,DELTA1,DELTA2,EN,RAD11,RAD21,CAPA,CUR,CURP,
     2MF,ATEN,BECA)
      DIMENSION BE(30),ELE(3C),RAD1(30),RAD2(30),CUR(30)   ,CURP(30)
     1,ATEN(30),BECA(3C)
      CCMPLEX ZCI,ZCIA,E1TETA,E1TETP,E1FI,E1FIP,ZCI2,ZCI2A,E2TETA,E2TETP
     1,E2FI,E2FIP,ENTETA,ENFI,ZCURR,ZDIST,ENTETC,ENFIC,ENTETS,ENFIS
     2,EXPO1,EXPC1A,EXPO2,EXPO2A,SIN1,SIN1A,SIN2,SIN2A
     3,UM
C
C       CORVC CCMPUTES THE RADIATION EQUATIONS
C       THE DATA REQUIRED ARE
C
C         THE DIMENSICNS OF THE STRUCTURE
C         THE FRECUENCY
C         THE AZIMUTH AND POLAR ANGLE
C         THE CURRENT DISTRIBUTION
C         THE PROPAGATION FACTORS (ATENUATION AND PHASE VEL.)
C             FCR EACH ELEMENT
C
C
C       THE OUTPUT IS
C         ETETA - THE REAL PART OF THE TETA COMPONENT OF THE FIELD
C         EFI   - THE REAL PART OF THE FI COMPONENT OF THE FIELD
C
C
      PI=3.14159
      UM=CMPLX(0.C,-1.C)
      ELE(1)=EL1
      BE(1)=B1
      ENTETS=CMPLX(C.0,0.0)
      ENFIS=CMPLX(C.0,C.0)
      RAD1(1)=RAD11
      RAD2(1)=RAD21
C
      ALFA1 =-(SIN(DELTA1)*COS(TETA)+COS(DELTA1)*SIN(TETA)*COS(FI))
      ALFA1A= (SIN(DELTA1)*COS(TETA)-COS(DELTA1)*SIN(TETA)*COS(FI))
      ALFA2 =-(SIN(DELTA2)*COS(TETA)-COS(DELTA2)*SIN(TETA)*COS(FI))
      ALFA2A= (SIN(DELTA2)*COS(TETA)+COS(DELTA2)*SIN(TETA)*COS(FI))
  132 C1=COS(GAMEP)*COS(TETA)
```

SAMPLE PRCGRAM AZORES - SUBROUTINE CORVO

```
C
      S1=SIN(GAMEP)*SIN(TETA)*COS(FI)
      C1S=COS(GAMEP)*SIN(TETA)
      S1C=SIN(GAMEP)*CCS(TETA)*COS(FI)
  136 S1S=SIN(GAMEP)*SIN(FI)
  137 C2=COS(GAPEP)*COS(TETA)
      S2=SIN(GAPEP)*SIN(TETA)*COS(FI)
      C2S=COS(GAPEP)*SIN(TETA)
      S2C=SIN(GAPEP)*CCS(TETA)*COS(FI)
      S2S=SIN(GAPEP)*SIN(FI)
  142 NDE=EN
C
  15C DO 295 N=1,NDE
      BE(N+1)=BE(N)/TAU
      B=BE(N)
      CURP(N)=CUR(N)
      ATT=ATEN(N)
      BETA=BECA(N)
      BC=BETA/CAPA
      COT1 =C1-S1
      COT1A=C1+S1
      COT2 =-C2-S2
      COT2A=-C2+S2
      EXPO1 =B*CMPLX(ATT,(BETA-CAPA*COT1 ))
      EXPO1A=B*CMPLX(ATT,(BETA+CAPA*COT1A))
      EXPO2 =B*CMPLX(ATT,(BETA-CAPA*COT2 ))
      EXPO2A=B*CMPLX(ATT,(BETA+CAPA*COT2A))
      SIN1 =CAPA*B*(CEXP(EXPO1 )-CEXP(-EXPO1 ))/EXPO1 /2.0
      SIN1A=CAPA*B*(CEXP(EXPO1A)-CEXP(-EXPO1A))/EXPO1A/2.0
      SIN2 =CAPA*B*(CEXP(EXPO2 )-CEXP(-EXPO2 ))/EXPO2 /2.0
      SIN2A=CAPA*B*(CEXP(EXPO2A)-CEXP(-EXPO2A))/EXPO2A/2.0
      ELE(N+1)=ELE(N)/TAU
      EL=ELE(N)
  181 RAD1(N+1)=RAD1(N)/TAU
      RADD1=RAD1(N)
  190 CI =-CAPA*( BC*B+RADD1*ALFA1 )
      CIA=-CAPA*( BC*B+RADD1*ALFA1A)
  200 ZCI=CMPLX(COS(CI), SIN(CI))
  201 ZCIA=CMPLX(CCS(CIA), SIN(CIA))
      E1TETA=SIN1*(C1S+S1C)*ZCI
      E1TETP=SIN1A*(C1S-S1C)*ZCIA
```

```
C
C
C         SAMPLE PROGRAM AZORES - SUBROUTINE CORVO
C
C
      E1FI=SIN1*S1S*ZCI
      E1FIP=-SIN1A*S1S*ZCIA
      RAD2(N+1)=RAD2(N)/TAU
      RADD2=RAD2(N)
  240 CI2 =-CAPA*( 3.0*BC*B+RADD2*ALFA2 )
      CI2A=-CAPA*( 3.0*BC*B+RADD2*ALFA2A)
      ZCI2=CMPLX(COS(CI2), SIN(CI2))
      ZCI2A=CMPLX(COS(CI2A), SIN(CI2A))
      E2TETA=-(SIN2)*(C2S-S2C)*ZCI2
      E2TETP=-(SIN2A)*(C2S+S2C)*ZCI2A
      E2FI=SIN2*S2S*ZCI2
      E2FIP=-SIN2A*S2S*ZCI2A
  260 ENTETA=(E1TETA+E1TETP)*CUR(N)+(E2TETA+E2TETP)*CURP(N)
      ENFI=(E1FI+E1FIP)*CUR(N)+(E2FI+E2FIP)*CURP(N)
C
  270 CURR=4.*B1*(BETA+CAPA*SAN/SQRT(TAU))*((1.0-1.0/(TAU**(N-1)))/
     1(1.0-1.0/TAU))
      ZCURR=CMPLX(COS(CURR),-SIN(CURR))
  280 ELEN=EL1/(TAU**(MF-1))
      DIST=CAPA*(ELEN-EL)*SIN(TETA)*COS(FI)*COS(EPSLON)
      ZDIST=CMPLX(COS(DIST), SIN(DIST))
  290 ENTETC=ENTETA*ZCURR*ZDIST*UM
      ENFIC=ENFI*ZCURR*ZDIST *UM
      ENTETS=ENTETS+ENTETC
      ENFIS=ENFIS+ENFIC
  295 CONTINUE
C
  300 ETETA=REAL(ENTETS)
      EFI=REAL(ENFIS)
      RETURN
      END
```

```
C
C
C           SAMPLE PRCGRAM AZORES - SUBROUTINE POLA
C
C
      SUBROUTINE PCLA (ETETA,EFI,E,PSI)
C
C    POLA FINDS THE RESULTANT OF ETETA AND EFI
C     AND CCUNTS THE ANGLE FROM EFI + UP I. E.
C     CLOCKWISE FCR AN OBSERVER LOOKING FROM THE ANTENNA
C
      PI=3.14159
   60 E=SQRT((ETETA**2)+(EFI**2))
      IF(EFI) 63,69,61
   61 PSI=  ATAN(ETETA/EFI)
      GO TO 75
   63 IF(ETETA) 64,66,68
   64 PSI=ATAN(ETETA/EFI)-PI
      GC TO 75
   66 PSI=PI
      GC TO 75
   68 PSI=ATAN(ETETA/EFI)+PI
      GC TO 75
   69 IF(ETETA)7C,72,74
   70 PSI=-PI/2.0
      GC TO 75
   72 PSI=0.0
      GC TO 75
   74 PSI=PI/2.0
   75 PSI=(360.0)*PSI/(2.0*PI)
      RETURN
      END
```

```
ALL UNITS ARE MKS

 -INPUT CATA

   ALFAE =    13.700C
   ALFAS =     7.50CC
   TAU   =     0.85CC
   FREQ  = 0.500E C9
   SDE   =     0.150C
   DE    =    12.000C
   EPSLON=     1.500C

 -COMPUTED DATA

   B1    =     0.0126
   L1    =     0.1006
   GAMA  =    12.2C75
   SAN   =     0.54C1
   LAMEDA=     0.60CC

   SRES  =     0.15CC
   LENGTH OF WIRES
       0.0251     0.C295     0.0347
       0.0409     C.C481     0.0566
       0.0666     0.C783     0.0921
       0.1084     0.1275     0.1500

MAX. FREQUENCY OF CPERATION  0.299E 10

MIN. FREQUENCY OF OPERATION  0.500E 09

HEIGHT  OF LAST ELEMENT          0.163

OVERALL LENGTH OF STRUCTURF      0.541

HEIGHT OF FEED PCINT             0.003
```

CURRENT DISTRIBUTION 1   FREQ= 0.500E 09

ELEV	FI	E	PSI	EDB
0.0	0.0	0.674	-90.000	-0.000
10.	0.0	0.647	-90.000	-0.351
20.	0.0	0.572	-90.000	-1.423
30.	0.0	0.462	-90.000	-3.272
40.	0.0	0.337	-90.000	-6.015
50.	0.0	0.217	-90.000	-9.851
60.	0.0	0.119	-90.000	-15.093
70.	0.0	0.052	-90.000	-22.210
80.	0.0	0.017	-90.000	-31.859
90.	180.	0.004	90.000	-43.757
80.	180.	0.004	90.000	-45.171
70.	180.	0.011	90.000	-35.923
60.	180.	0.026	90.000	-28.260
50.	180.	0.049	90.000	-22.717
40.	180.	0.076	90.000	-18.902
30.	180.	0.102	90.000	-16.425
20.	180.	0.121	90.000	-14.938
10.	180.	0.132	90.000	-14.165
0.0	180.	0.136	90.000	-13.927
0.0	0.0	0.674	-90.000	0.0
0.0	5.	0.669	-90.000	-0.062
0.0	10.	0.655	-90.000	-0.248
0.0	15.	0.631	-90.000	-0.565
0.0	20.	0.599	-90.000	-1.021
0.0	25.	0.559	-90.000	-1.630
0.0	30.	0.510	-90.000	-2.412
0.0	35.	0.456	-90.000	-3.394
0.0	40.	0.396	-90.000	-4.615
0.0	45.	0.333	-90.000	-6.129
0.0	50.	0.268	-90.000	-8.019
0.0	55.	0.203	-90.000	-10.421
0.0	60.	0.141	-90.000	-13.591
0.0	65.	0.084	-90.000	-18.133
0.0	70.	0.033	-90.000	-26.299
0.0	75.	0.011	90.000	-36.072
0.0	80.	0.046	90.000	-23.394
0.0	85.	0.073	90.000	-19.352
0.0	90.	0.093	90.000	-17.244
0.0	95.	0.107	90.000	-16.003
0.0	100.	0.117	90.000	-15.221
0.0	105.	0.124	90.000	-14.694
0.0	110.	0.130	90.000	-14.306
0.0	115.	0.134	90.000	-13.997
0.0	120.	0.139	90.000	-13.741
0.0	125.	0.142	90.000	-13.535
0.0	130.	0.144	90.000	-13.384
0.0	135.	0.146	90.000	-13.294
0.0	140.	0.146	90.000	-13.268
0.0	145.	0.146	90.000	-13.301
0.0	150.	0.144	90.000	-13.381
0.0	155.	0.143	90.000	-13.493
0.0	160.	0.140	90.000	-13.618
0.0	165.	0.139	90.000	-13.739
0.0	170.	0.137	90.000	-13.839
0.0	175.	0.136	90.000	-13.904
0.0	180.	0.136	90.000	-13.927

DIRECTIVITY/ISO	FI 3DB	ELEV 3DB
10.969DB	33.	25.

THIS DIRECTIVITY FIGURE WAS COMPUTED
ASSUMING THAT THE PATTERN IS WELL-BEHAVED.
IT HAS NO MEANING IF THERE ARE SIDE-LOBES.

CURRENT DISTRIBUTION 2 FREQ= 0.500E 09

ELEV	FI	E	PSI	EDB
0.0	0.0	0.668	-90.000	-0.000
10.	0.0	0.642	-90.000	-0.348
20.	0.0	0.567	-90.000	-1.433
30.	0.0	0.452	-90.000	-3.393
40.	0.0	0.315	-90.000	-6.529
50.	0.0	0.179	-90.000	-11.434
60.	0.0	0.071	-90.000	-19.472
70.	0.0	0.010	-90.000	-36.778
80.	0.0	0.007	90.000	-39.533
90.	180.	0.002	-90.000	-52.310
80.	180.	0.004	90.000	-43.891
70.	180.	0.009	90.000	-37.003
60.	180.	0.028	90.000	-27.481
50.	180.	0.069	90.000	-19.740
40.	180.	0.122	90.000	-14.736
30.	180.	0.172	90.000	-11.764
20.	180.	0.208	90.000	-10.153
10.	180.	0.226	90.000	-9.403
0.0	180.	0.232	90.000	-9.191
0.0	0.0	0.668	-90.000	0.0
0.0	5.	0.663	-90.000	-0.062
0.0	10.	0.649	-90.000	-0.249
0.0	15.	0.625	-90.000	-0.573
0.0	20.	0.592	-90.000	-1.050
0.0	25.	0.549	-90.000	-1.705
0.0	30.	0.497	-90.000	-2.578
0.0	35.	0.435	-90.000	-3.724
0.0	40.	0.366	-90.000	-5.226
0.0	45.	0.291	-90.000	-7.213
0.0	50.	0.213	-90.000	-9.914
0.0	55.	0.136	-90.000	-13.815
0.0	60.	0.064	-90.000	-20.413
0.0	65.	0.000	-89.954	-75.435
0.0	70.	0.051	90.000	-22.317
0.0	75.	0.088	90.000	-17.601
0.0	80.	0.110	90.000	-15.636
0.0	85.	0.120	90.000	-14.907
0.0	90.	0.121	90.000	-14.863
0.0	95.	0.117	90.000	-15.145
0.0	100.	0.113	90.000	-15.427
0.0	105.	0.113	90.000	-15.424
0.0	110.	0.119	90.000	-14.985
0.0	115.	0.131	90.000	-14.153
0.0	120.	0.148	90.000	-13.103
0.0	125.	0.167	90.000	-12.029
0.0	130.	0.187	90.000	-11.066
0.0	135.	0.204	90.000	-10.285
0.0	140.	0.219	90.000	-9.708
0.0	145.	0.228	90.000	-9.323
0.0	150.	0.234	90.000	-9.104
0.0	155.	0.237	90.000	-9.013
0.0	160.	0.237	90.000	-9.011
0.0	165.	0.235	90.000	-9.060
0.0	170.	0.234	90.000	-9.122
0.0	175.	0.232	90.000	-9.172
0.0	180.	0.232	90.000	-9.191

DIRECTIVITY/ISO	FI 3DB	ELEV 3DB
10.969DB	33.	25.

THIS DIRECTIVITY FIGURE WAS COMPUTED
ASSUMING THAT THE PATTERN IS WELL-BEHAVED.
IT HAS NO MEANING IF THERE ARE SIDE-LOBES.

```
ALL UNITS ARE MKS

 -INPUT DATA

   ALFAE  =    13.7000
   ALFAS  =     7.5000
   TAU    =     0.8500
   FREQ   =  0.1100E 10
   SDE    =     0.1500
   DE     =    12.0000
   EPSLON=      1.5000

 -COMPUTED DATA

   B1     =     0.0126
   L1     =     0.1006
   GAMA   =    12.2075
   SAN    =     0.5401
   LAMEDA=      0.2727

   SRES   =     0.0682
   LENGTH OF WIRES
        0.0251     0.0295     0.0347
        0.0409     0.0481     0.0566
        0.0666     0.0783     0.0921
        0.1084     0.1275     0.1500

MAX. FREQUENCY OF OPERATION   0.299E 10

MIN. FREQUENCY OF OPERATION   0.500E 09

HEIGHT  OF LAST ELEMENT           0.163

OVERALL LENGTH OF STRUCTURE       0.541

HEIGHT OF FEED POINT              0.003
```

CURRENT DISTRIBUTION 1 FREQ= 0.110E 10

ELEV	FI	F	PSI	FDB
0.0	0.0	3.228	90.000	-0.000
10.	0.0	3.143	90.000	-0.232
20.	0.0	2.900	90.000	-0.930
30.	0.0	2.537	90.000	-2.093
40.	0.0	2.104	90.000	-3.720
50.	0.0	1.653	90.000	-5.816
60.	0.0	1.225	90.000	-8.416
70.	0.0	0.846	90.000	-11.636
80.	0.0	0.525	90.000	-15.768
90.	180.	0.270	-90.000	-21.539
80.	180.	0.082	-89.999	-31.878
70.	180.	0.043	89.999	-37.485
60.	180.	0.117	90.000	-28.789
50.	180.	0.156	90.000	-26.308
40.	180.	0.174	90.000	-25.358
30.	180.	0.182	90.000	-24.974
20.	180.	0.186	90.000	-24.793
10.	180.	0.188	90.000	-24.690
0.0	180.	0.189	90.000	-24.653
0.0	0.0	3.228	90.000	0.0
0.0	5.	3.224	90.000	-0.012
0.0	10.	3.211	90.000	-0.047
0.0	15.	3.189	90.000	-0.106
0.0	20.	3.158	90.000	-0.190
0.0	25.	3.119	90.000	-0.300
0.0	30.	3.070	90.000	-0.437
0.0	35.	3.011	90.000	-0.605
0.0	40.	2.941	90.000	-0.808
0.0	45.	2.860	90.000	-1.052
0.0	50.	2.765	90.000	-1.344
0.0	55.	2.656	90.000	-1.694
0.0	60.	2.531	90.000	-2.114
0.0	65.	2.389	90.000	-2.616
0.0	70.	2.230	90.000	-3.213
0.0	75.	2.056	90.000	-3.920
0.0	80.	1.869	90.000	-4.748
0.0	85.	1.673	90.000	-5.707
0.0	90.	1.475	90.000	-6.802
0.0	95.	1.280	90.000	-8.034
0.0	100.	1.094	90.000	-9.397
0.0	105.	0.923	90.000	-10.877
0.0	110.	0.770	90.000	-12.449
0.0	115.	0.638	90.000	-14.079
0.0	120.	0.528	90.000	-15.722
0.0	125.	0.439	90.000	-17.325
0.0	130.	0.369	90.000	-18.829
0.0	135.	0.316	90.000	-20.184
0.0	140.	0.276	90.000	-21.350
0.0	145.	0.247	90.000	-22.310
0.0	150.	0.227	90.000	-23.064
0.0	155.	0.212	90.000	-23.633
0.0	160.	0.203	90.000	-24.046
0.0	165.	0.196	90.000	-24.331
0.0	170.	0.192	90.000	-24.516
0.0	175.	0.190	90.000	-24.619
0.0	180.	0.189	90.000	-24.653

DIRECTIVITY/ISO	FI 3DB	ELEV 3DB
6.368DB	68.	35.

THIS DIRECTIVITY FIGURE WAS COMPUTED
ASSUMING THAT THE PATTERN IS WELL-BEHAVED.
IT HAS NO MEANING IF THERE ARE SIDE-LOBES.

CURRENT DISTRIBUTION 2 FREQ= 0.110E 10

ELEV	FI	E	PSI	EDB
0.0	0.0	2.951	90.000	0.0
10.	0.0	2.879	90.000	-0.216
20.	0.0	2.675	90.000	-0.852
30.	0.0	2.377	90.000	-1.878
40.	0.0	2.029	90.000	-3.254
50.	0.0	1.664	90.000	-4.976
60.	0.0	1.297	90.000	-7.142
70.	0.0	0.930	90.000	-10.028
80.	0.0	0.580	90.000	-14.132
90.	180.	0.284	-90.000	-20.345
80.	180.	0.079	-89.999	-31.488
70.	180.	0.031	89.999	-39.676
60.	180.	0.078	90.000	-31.517
50.	180.	0.109	90.000	-28.629
40.	180.	0.149	90.000	-25.949
30.	180.	0.197	90.000	-23.494
20.	180.	0.243	90.000	-21.678
10.	180.	0.275	90.000	-20.611
0.0	180.	0.286	90.000	-20.264
0.0	0.0	2.951	90.000	0.0
0.0	5.	2.949	90.000	-0.006
0.0	10.	2.943	90.000	-0.024
0.0	15.	2.934	90.000	-0.052
0.0	20.	2.921	90.000	-0.088
0.0	25.	2.906	90.000	-0.133
0.0	30.	2.889	90.000	-0.184
0.0	35.	2.869	90.000	-0.244
0.0	40.	2.845	90.000	-0.317
0.0	45.	2.814	90.000	-0.413
0.0	50.	2.772	90.000	-0.544
0.0	55.	2.713	90.000	-0.731
0.0	60.	2.632	90.000	-0.996
0.0	65.	2.522	90.000	-1.365
0.0	70.	2.380	90.000	-1.867
0.0	75.	2.205	90.000	-2.531
0.0	80.	1.999	90.000	-3.384
0.0	85.	1.768	90.000	-4.448
0.0	90.	1.524	90.000	-5.742
0.0	95.	1.277	90.000	-7.275
0.0	100.	1.042	90.000	-9.045
0.0	105.	0.829	90.000	-11.030
0.0	110.	0.647	90.000	-13.177
0.0	115.	0.502	90.000	-15.388
0.0	120.	0.393	90.000	-17.512
0.0	125.	0.318	90.000	-19.351
0.0	130.	0.272	90.000	-20.720
0.0	135.	0.248	90.000	-21.525
0.0	140.	0.239	90.000	-21.817
0.0	145.	0.241	90.000	-21.749
0.0	150.	0.249	90.000	-21.488
0.0	155.	0.258	90.000	-21.164
0.0	160.	0.267	90.000	-20.853
0.0	165.	0.275	90.000	-20.597
0.0	170.	0.281	90.000	-20.412
0.0	175.	0.285	90.000	-20.301
0.0	180.	0.286	90.000	-20.264

DIRECTIVITY/ISO	FI 3DB	ELEV 3DB
5.772DB	78.	35.

THIS DIRECTIVITY FIGURE WAS COMPUTED
ASSUMING THAT THE PATTERN IS WELL-BEHAVED.
IT HAS NO MEANING IF THERE ARE SIDE-LOBES.

```
ALL UNITS ARE MKS

 -INPUT DATA

   ALFAE =    13.7000
   ALFAS =     7.5000
   TAU   =     0.8500
   FREQ  = 0.170E 10
   SDE   =     0.1500
   DE    =    12.0000
   EPSLON=     1.5000

 -COMPUTED DATA

   B1    =     0.0126
   L1    =     0.1006
   GAMA  =    12.2075
   SAN   =     0.5401
   LAMEDA=     0.1765

   SRES  =     0.0441
   LENGTH OF WIRES
       0.0251     0.0295     0.0347
       0.0409     0.0481     0.0566
       0.0666     0.0783     0.0921
       0.1084     0.1275     0.1500

MAX. FREQUENCY OF OPERATION  0.299E 10

MIN. FREQUENCY OF OPERATION  0.500E 09

HEIGHT  OF LAST ELEMENT          0.163

OVERALL LENGTH OF STRUCTURE      0.541

HEIGHT OF FEED POINT             0.003
```

CURRENT DISTRIBUTION 1 FREQ= 0.170E 10

ELEV	FI	E	PSI	EDB
0.0	0.0	2.330	90.000	0.0
10.	0.0	2.257	90.000	-0.275
20.	0.0	2.052	90.000	-1.103
30.	0.0	1.749	90.000	-2.493
40.	0.0	1.394	90.000	-4.462
50.	0.0	1.035	90.000	-7.051
60.	0.0	0.708	90.000	-10.344
70.	0.0	0.437	90.000	-14.533
80.	0.0	0.233	90.000	-20.013
90.	180.	0.097	-90.000	-27.627
80.	180.	0.025	-90.000	-39.335
70.	180.	0.005	-89.999	-53.477
60.	180.	0.016	-90.000	-43.384
50.	180.	0.035	-90.000	-36.506
40.	180.	0.045	-90.000	-34.311
30.	180.	0.040	-90.000	-35.350
20.	180.	0.024	-90.000	-39.586
10.	180.	0.009	-90.000	-48.263
0.0	180.	0.003	-90.000	-58.853
0.0	0.0	2.330	90.000	0.0
0.0	5.	2.322	90.000	-0.029
0.0	10.	2.299	90.000	-0.118
0.0	15.	2.259	90.000	-0.269
0.0	20.	2.203	90.000	-0.486
0.0	25.	2.132	90.000	-0.773
0.0	30.	2.043	90.000	-1.140
0.0	35.	1.939	90.000	-1.595
0.0	40.	1.819	90.000	-2.149
0.0	45.	1.685	90.000	-2.817
0.0	50.	1.537	90.000	-3.614
0.0	55.	1.378	90.000	-4.560
0.0	60.	1.212	90.000	-5.680
0.0	65.	1.040	90.000	-7.005
0.0	70.	0.868	90.000	-8.575
0.0	75.	0.700	90.000	-10.445
0.0	80.	0.540	90.000	-12.699
0.0	85.	0.392	90.000	-15.474
0.0	90.	0.261	90.000	-19.029
0.0	95.	0.147	90.000	-23.981
0.0	100.	0.054	90.000	-32.655
0.0	105.	0.018	-90.001	-42.158
0.0	110.	0.071	-90.000	-30.357
0.0	115.	0.105	-90.000	-26.922
0.0	120.	0.123	-90.000	-25.516
0.0	125.	0.129	-90.000	-25.138
0.0	130.	0.125	-90.000	-25.442
0.0	135.	0.113	-90.000	-26.278
0.0	140.	0.097	-90.000	-27.579
0.0	145.	0.080	-90.000	-29.327
0.0	150.	0.062	-90.000	-31.547
0.0	155.	0.045	-90.000	-34.306
0.0	160.	0.030	-90.000	-37.736
0.0	165.	0.018	-90.000	-42.058
0.0	170.	0.010	-90.000	-47.606
0.0	175.	0.004	-90.000	-54.423
0.0	180.	0.003	-90.000	-58.852

DIRECTIVITY/ISO	FI 3DB	ELEV 3DB
7.881DB	48.	35.

THIS DIRECTIVITY FIGURE WAS COMPUTED
ASSUMING THAT THE PATTERN IS WELL-BEHAVED.
IT HAS NO MEANING IF THERE ARE SIDE-LOBES.

CURRENT DISTRIBUTICN 2   FREQ= 0.170E 10

ELEV	FI	E	PSI	EDB
0.0	0.0	2.235	90.000	0.0
10.	0.0	2.176	90.000	-0.233
20.	0.0	2.009	90.000	-0.927
30.	0.0	1.760	90.000	-2.079
40.	0.0	1.461	90.000	-3.693
50.	0.0	1.144	90.000	-5.820
60.	0.0	0.831	90.000	-8.598
70.	0.0	0.541	90.000	-12.327
80.	0.0	0.295	90.000	-17.600
90.	180.	0.116	-90.000	-25.686
80.	180.	0.023	-90.000	-39.767
70.	180.	0.014	-90.000	-43.819
60.	180.	0.066	-90.000	-30.559
50.	180.	0.140	-90.000	-24.072
40.	180.	0.200	-90.000	-20.971
30.	180.	0.229	-90.000	-19.789
20.	180.	0.231	-90.000	-19.724
10.	180.	0.221	-90.000	-20.101
0.0	180.	0.216	-90.000	-20.317
0.0	0.0	2.235	90.000	0.0
0.0	5.	2.231	90.000	-0.019
0.0	10.	2.216	90.000	-0.075
0.0	15.	2.192	90.000	-0.171
0.0	20.	2.157	90.000	-0.311
0.0	25.	2.111	90.000	-0.499
0.0	30.	2.052	90.000	-0.742
0.0	35.	1.981	90.000	-1.049
0.0	40.	1.895	90.000	-1.432
0.0	45.	1.795	90.000	-1.907
0.0	50.	1.678	90.000	-2.490
0.0	55.	1.545	90.000	-3.206
0.0	60.	1.397	90.000	-4.081
0.0	65.	1.235	90.000	-5.153
0.0	70.	1.061	90.000	-6.470
0.0	75.	0.880	90.000	-8.099
0.0	80.	0.695	90.000	-10.144
0.0	85.	0.513	90.000	-12.787
0.0	90.	0.338	90.000	-16.404
0.0	95.	0.177	90.000	-22.045
0.0	100.	0.033	90.000	-36.655
0.0	105.	0.090	-90.000	-27.934
0.0	110.	0.189	-90.000	-21.466
0.0	115.	0.264	-90.000	-18.554
0.0	120.	0.316	-90.000	-16.989
0.0	125.	0.347	-90.000	-16.173
0.0	130.	0.360	-90.000	-15.850
0.0	135.	0.359	-90.000	-15.880
0.0	140.	0.347	-90.000	-16.172
0.0	145.	0.328	-90.000	-16.657
0.0	150.	0.306	-90.000	-17.276
0.0	155.	0.282	-90.000	-17.968
0.0	160.	0.260	-90.000	-18.672
0.0	165.	0.242	-90.000	-19.322
0.0	170.	0.227	-90.000	-19.850
0.0	175.	0.219	-90.000	-20.196
0.0	180.	0.216	-90.000	-20.317

DIRECTIVITY/ISO	FI 3DB	ELEV 3DB
7.451DB	53.	35.

THIS DIRECTIVITY FIGURE WAS COMPUTED
ASSUMING THAT THE PATTERN IS WELL-BEHAVED.
IT HAS NO MEANING IF THERE ARE SIDE-LOBES.

```
ALL UNITS ARE MKS

 -INPUT DATA

   ALFAE  =    13.7000
   ALFAS  =     7.5000
   TAU    =     0.8500
   FREQ   =  0.200E 10
   SDE    =     0.1500
   DE     =    12.0000
   EPSLON=      1.5000

 -COMPUTED DATA

   B1     =     0.0126
   L1     =     0.1006
   GAMA   =    12.2075
   SAN    =     0.5401
   LAMEDA=      0.1500

   SRES   =     0.0375
   LENGTH OF WIRES
        0.0251     0.0295     0.0347
        0.0409     0.0481     0.0566
        0.0666     0.0783     0.0921
        0.1084     0.1275     0.1500

MAX. FREQUENCY OF OPERATION  0.299E 10

MIN. FREQUENCY OF OPERATION  0.500E 09

HEIGHT  OF LAST ELEMENT          0.163

OVERALL LENGTH OF STRUCTURE      0.541

HEIGHT OF FEED POINT             0.003
```

TUP

CURRENT DISTRIBUTICN 1 FREQ= 0.200E 10

ELEV	FI	E	PSI	EDB
0.0	0.0	2.581	-90.000	-0.000
10.	0.0	2.494	-90.000	-0.297
20.	0.0	2.249	-90.000	-1.196
30.	0.0	1.889	-90.000	-2.710
40.	0.0	1.475	-90.000	-4.861
50.	0.0	1.067	-90.000	-7.672
60.	0.0	0.714	-90.000	-11.161
70.	0.0	0.440	-90.000	-15.363
80.	0.0	0.247	-90.000	-20.384
90.	180.	0.120	90.000	-26.630
80.	180.	0.040	90.000	-36.114
70.	180.	0.012	-90.001	-46.740
60.	180.	0.052	-90.000	-33.987
50.	180.	0.089	-90.000	-29.259
40.	180.	0.128	-90.000	-26.067
30.	180.	0.169	-90.000	-23.684
20.	180.	0.205	-90.000	-21.993
10.	180.	0.231	-90.000	-20.982
0.0	180.	0.240	-90.000	-20.645
0.0	0.0	2.581	-90.000	0.0
0.0	5.	2.572	-90.000	-0.032
0.0	10.	2.543	-90.000	-0.129
0.0	15.	2.496	-90.000	-0.293
0.0	20.	2.429	-90.000	-0.527
0.0	25.	2.344	-90.000	-0.836
0.0	30.	2.242	-90.000	-1.225
0.0	35.	2.122	-90.000	-1.702
0.0	40.	1.987	-90.000	-2.275
0.0	45.	1.838	-90.000	-2.952
0.0	50.	1.677	-90.000	-3.743
0.0	55.	1.509	-90.000	-4.660
0.0	60.	1.337	-90.000	-5.712
0.0	65.	1.165	-90.000	-6.910
0.0	70.	0.997	-90.000	-8.263
0.0	75.	0.838	-90.000	-9.776
0.0	80.	0.691	-90.000	-11.450
0.0	85.	0.560	-90.000	-13.276
0.0	90.	0.447	-90.000	-15.226
0.0	95.	0.354	-90.000	-17.248
0.0	100.	0.281	-90.000	-19.249
0.0	105.	0.228	-90.000	-21.092
0.0	110.	0.191	-90.000	-22.608
0.0	115.	0.170	-90.000	-23.649
0.0	120.	0.160	-90.000	-24.153
0.0	125.	0.160	-90.000	-24.178
0.0	130.	0.165	-90.000	-23.867
0.0	135.	0.175	-90.000	-23.375
0.0	140.	0.186	-90.000	-22.826
0.0	145.	0.198	-90.000	-22.298
0.0	150.	0.209	-90.000	-21.832
0.0	155.	0.219	-90.000	-21.446
0.0	160.	0.226	-90.000	-21.143
0.0	165.	0.232	-90.000	-20.917
0.0	170.	0.236	-90.000	-20.764
0.0	175.	0.239	-90.000	-20.674
0.0	180.	0.240	-90.000	-20.645

DIRECTIVITY/ISO	FI 3DB	ELEV 3DB
7.881DB	48.	35.

THIS DIRECTIVITY FIGURE WAS COMPUTED
ASSUMING THAT THE PATTERN IS WELL-BEHAVED.
IT HAS NO MEANING IF THERE ARE SIDE-LOBES.

CURRENT DISTRIBUTION 2 FREQ= 0.200E 10

ELEV	FI	E	PSI	EDB
0.0	0.0	2.288	-90.000	-0.000
10.	0.0	2.201	-90.000	-0.335
20.	0.0	1.959	-90.000	-1.351
30.	0.0	1.607	-90.000	-3.071
40.	0.0	1.210	-90.000	-5.530
50.	0.0	0.835	-90.000	-8.757
60.	0.0	0.527	-90.000	-12.745
70.	0.0	0.308	-90.000	-17.409
80.	0.0	0.171	-90.000	-22.546
90.	180.	0.090	90.000	-28.079
80.	180.	0.038	90.000	-35.573
70.	180.	0.010	-90.001	-47.134
60.	180.	0.069	-90.000	-30.415
50.	180.	0.143	-90.000	-24.070
40.	180.	0.228	-90.000	-20.013
30.	180.	0.314	-90.000	-17.245
20.	180.	0.388	-90.000	-15.423
10.	180.	0.437	-90.000	-14.385
0.0	180.	0.454	-90.000	-14.048
0.0	0.0	2.288	-90.000	0.0
0.0	5.	2.278	-90.000	-0.040
0.0	10.	2.246	-90.000	-0.160
0.0	15.	2.194	-90.000	-0.363
0.0	20.	2.123	-90.000	-0.651
0.0	25.	2.032	-90.000	-1.031
0.0	30.	1.923	-90.000	-1.509
0.0	35.	1.798	-90.000	-2.093
0.0	40.	1.659	-90.000	-2.791
0.0	45.	1.509	-90.000	-3.615
0.0	50.	1.351	-90.000	-4.574
0.0	55.	1.190	-90.000	-5.682
0.0	60.	1.028	-90.000	-6.947
0.0	65.	0.872	-90.000	-8.380
0.0	70.	0.725	-90.000	-9.984
0.0	75.	0.592	-90.000	-11.750
0.0	80.	0.475	-90.000	-13.651
0.0	85.	0.379	-90.000	-15.625
0.0	90.	0.303	-90.000	-17.555
0.0	95.	0.249	-90.000	-19.257
0.0	100.	0.216	-90.000	-20.506
0.0	105.	0.201	-90.000	-21.124
0.0	110.	0.202	-90.000	-21.084
0.0	115.	0.215	-90.000	-20.528
0.0	120.	0.238	-90.000	-19.674
0.0	125.	0.265	-90.000	-18.715
0.0	130.	0.296	-90.000	-17.778
0.0	135.	0.326	-90.000	-16.933
0.0	140.	0.354	-90.000	-16.208
0.0	145.	0.379	-90.000	-15.610
0.0	150.	0.401	-90.000	-15.132
0.0	155.	0.418	-90.000	-14.760
0.0	160.	0.432	-90.000	-14.482
0.0	165.	0.442	-90.000	-14.282
0.0	170.	0.449	-90.000	-14.148
0.0	175.	0.453	-90.000	-14.072
0.0	180.	0.454	-90.000	-14.048

DIRECTIVITY/ISO	FI 3DB	ELEV 3DB
9.820DB	43.	25.

THIS DIRECTIVITY FIGURE WAS COMPUTED
ASSUMING THAT THE PATTERN IS WELL-BEHAVED.
IT HAS NO MEANING IF THERE ARE SIDE-LOBES.

```
ALL UNITS ARE MKS

 -INPUT DATA

   ALFAE =    13.7000
   ALFAS =     7.5000
   TAU   =     0.8500
   FREQ  =  0.2300E 10
   SDE   =     0.1500
   DE    =    12.0000
   EPSLON=     1.5000

 -COMPUTED DATA

   B1    =     0.0126
   L1    =     0.1006
   GAMA  =    12.2075
   SAN   =     0.5401
   LAMEDA=     0.1304

   SRES  =     0.0326
   LENGTH OF WIRES
        0.0251     0.0295     0.0347
        0.0409     0.0481     0.0566
        0.0666     0.0783     0.0921
        0.1084     0.1275     0.1500

MAX. FREQUENCY OF OPERATION  0.299E 10

MIN. FREQUENCY OF OPERATION  0.500E 09

HEIGHT  OF LAST ELEMENT           0.163

OVERALL LENGTH OF STRUCTURE       0.541

HEIGHT OF FEED POINT              0.003
```

CURRENT DISTRIBUTION 1 FREQ= 0.230E 10

ELEV	FI	E	PSI	EDB
0.0	0.0	2.470	90.000	-0.000
10.	0.0	2.400	90.000	-0.250
20.	0.0	2.201	90.000	-1.002
30.	0.0	1.903	90.000	-2.266
40.	0.0	1.547	90.000	-4.064
50.	0.0	1.178	90.000	-6.435
60.	0.0	0.831	90.000	-9.467
70.	0.0	0.532	90.000	-13.341
80.	0.0	0.295	90.000	-18.447
90.	180.	0.128	-90.000	-25.722
80.	180.	0.029	-89.999	-38.723
70.	180.	0.010	89.999	-48.285
60.	180.	0.001	90.000	-72.899
50.	180.	0.037	-90.000	-36.419
40.	180.	0.086	-90.000	-29.140
30.	180.	0.133	-90.000	-25.396
20.	180.	0.169	-90.000	-23.306
10.	180.	0.191	-90.000	-22.228
0.0	180.	0.199	-90.000	-21.894
0.0	0.0	2.470	90.000	0.0
0.0	5.	2.463	90.000	-0.027
0.0	10.	2.440	90.000	-0.107
0.0	15.	2.402	90.000	-0.244
0.0	20.	2.348	90.000	-0.441
0.0	25.	2.278	90.000	-0.704
0.0	30.	2.192	90.000	-1.039
0.0	35.	2.089	90.000	-1.454
0.0	40.	1.971	90.000	-1.960
0.0	45.	1.838	90.000	-2.567
0.0	50.	1.692	90.000	-3.288
0.0	55.	1.535	90.000	-4.135
0.0	60.	1.369	90.000	-5.124
0.0	65.	1.200	90.000	-6.274
0.0	70.	1.029	90.000	-7.606
0.0	75.	0.862	90.000	-9.145
0.0	80.	0.702	90.000	-10.928
0.0	85.	0.553	90.000	-13.005
0.0	90.	0.417	90.000	-15.455
0.0	95.	0.296	90.000	-18.418
0.0	100.	0.192	90.000	-22.178
0.0	105.	0.105	90.000	-27.470
0.0	110.	0.032	90.000	-37.619
0.0	115.	0.025	-90.000	-39.817
0.0	120.	0.070	-90.000	-30.901
0.0	125.	0.105	-90.000	-27.426
0.0	130.	0.131	-90.000	-25.500
0.0	135.	0.150	-90.000	-24.305
0.0	140.	0.165	-90.000	-23.520
0.0	145.	0.175	-90.000	-22.988
0.0	150.	0.183	-90.000	-22.618
0.0	155.	0.188	-90.000	-22.358
0.0	160.	0.192	-90.000	-22.173
0.0	165.	0.195	-90.000	-22.044
0.0	170.	0.197	-90.000	-21.959
0.0	175.	0.198	-90.000	-21.910
0.0	180.	0.199	-90.000	-21.894

DIRECTIVITY/ISO	FI 3DB	ELEV 3DB
7.881DB	48.	35.

THIS DIRECTIVITY FIGURE WAS COMPUTED
ASSUMING THAT THE PATTERN IS WELL-BEHAVED.
IT HAS NO MEANING IF THERE ARE SIDE-LOBES.

↑ UP

CURRENT DISTRIBUTION 2 FREQ= 0.230E 10

ELEV	FI	E	PSI	EDB
0.0	0.0	2.470	90.000	-0.000
10.	0.0	2.400	90.000	-0.250
20.	0.0	2.201	90.000	-1.002
30.	0.0	1.903	90.000	-2.266
40.	0.0	1.547	90.000	-4.064
50.	0.0	1.178	90.000	-6.435
60.	0.0	0.831	90.000	-9.467
70.	0.0	0.532	90.000	-13.341
80.	0.0	0.295	90.000	-18.447
90.	180.	0.128	-90.000	-25.722
80.	180.	0.029	-89.999	-38.723
70.	180.	0.010	89.999	-48.285
60.	180.	0.001	90.000	-72.899
50.	180.	0.037	-90.000	-36.419
40.	180.	0.086	-90.000	-29.140
30.	180.	0.133	-90.000	-25.396
20.	180.	0.169	-90.000	-23.306
10.	180.	0.191	-90.000	-22.228
0.0	180.	0.199	-90.000	-21.894
0.0	0.0	2.470	90.000	0.0
0.0	5.	2.463	90.000	-0.027
0.0	10.	2.440	90.000	-0.107
0.0	15.	2.402	90.000	-0.244
0.0	20.	2.348	90.000	-0.441
0.0	25.	2.278	90.000	-0.704
0.0	30.	2.192	90.000	-1.039
0.0	35.	2.089	90.000	-1.454
0.0	40.	1.971	90.000	-1.960
0.0	45.	1.838	90.000	-2.567
0.0	50.	1.692	90.000	-3.288
0.0	55.	1.535	90.000	-4.135
0.0	60.	1.369	90.000	-5.124
0.0	65.	1.200	90.000	-6.274
0.0	70.	1.029	90.000	-7.606
0.0	75.	0.862	90.000	-9.145
0.0	80.	0.702	90.000	-10.928
0.0	85.	0.553	90.000	-13.005
0.0	90.	0.417	90.000	-15.455
0.0	95.	0.296	90.000	-18.418
0.0	100.	0.192	90.000	-22.178
0.0	105.	0.105	90.000	-27.470
0.0	110.	0.032	90.000	-37.619
0.0	115.	0.025	-90.000	-39.817
0.0	120.	0.070	-90.000	-30.901
0.0	125.	0.105	-90.000	-27.426
0.0	130.	0.131	-90.000	-25.500
0.0	135.	0.150	-90.000	-24.305
0.0	140.	0.165	-90.000	-23.520
0.0	145.	0.175	-90.000	-22.988
0.0	150.	0.183	-90.000	-22.618
0.0	155.	0.188	-90.000	-22.358
0.0	160.	0.192	-90.000	-22.173
0.0	165.	0.195	-90.000	-22.044
0.0	170.	0.197	-90.000	-21.959
0.0	175.	0.198	-90.000	-21.910
0.0	180.	0.199	-90.000	-21.894

DIRECTIVITY/ISO	FI 3DB	ELEV 3DB
7.881DB	48.	35.

THIS DIRECTIVITY FIGURE WAS COMPUTED
ASSUMING THAT THE PATTERN IS WELL-BEHAVED.
IT HAS NO MEANING IF THERE ARE SIDE-LOBES.

II. Program SMIGUEL

This program also is written in code FORTRAN IV for the IBM 360 system.

The program uses seven subroutines, as explained in SAMPLE PROGRAM SMIGUEL that follows. The subroutines supply to the main program the characteristics of the line and the non-uniformity corrections. The main program uses equations 33, first to find the input impedance, and then to find the current distribution.

For each set of input data the impedance and current distribution are computed twice--one time without accounting for mutual impedance effects, and a second time accounting for them.

Again, the program has a large number of comment cards that, hopefully, make it self-explanatory.

```
C
C
C     SAMPLE PROGRAM SMIGUEL - MAIN
C
C
      DIMENSION BE(30),ELE(30),D(30),RADIO(30),AP(30),APA(30)
     1,BP(30),BPB(30),CP(30),CPC(30),DP(30),DPD(30),AKR(30)
     2,SEL(30),AK(30),ZINS(30),ZINT(30),ZINR(30),QIL(30),VIL(30)
      COMPLEX Z,AI,BI,UM,ZIN, AA,BB,CC,DD,ZOUT,QIL,VIL,QI,VI,QIX,VIX,
     1ZXR,ZAVR,ZRA,Z11,Z12,ZINR,ZINT,ZINS,QIM,VIM,
     2  AP,APA,BP,BPB,CP,CPC,DP,DPD
C
C   THIS PROGRAM COMPUTES THE CURRENTS AND VOLTAGES ALONG THE WIRES OF ONE
C   ZIG/ZAG ELEMENT , USING THE EQUATIONS FOR SLIGHTLY NON-UNIFORM TRANSMIS
C   SION LINES
C
C     THE PROGRAM USES THE FOLLOWING SUBROUTINES
C          FAIAL  - PRINTS LINE CHARACTERISTIC VALUES AND MUTUAL
C                   RESISTANCE FOR EACH ELEMENT
C          FLORES - COMPUTES MUTUAL RESISTANCE BETWEEN TWO PARALLEL
C                   WIRES WITH SINUSOIDAL CURRENT DISTRIBUTION
C          IMPRAD - COMPUTES CHARACTERISTIC VALUES OF TRANSMIS-
C                   SION LINE FORMED BY RADIATORS
C          IMPSTU - DOES THE SAME FOR STUBS
C          QSF    - THIS IS A IBM SUBROUTINE THAT PERFORMS
C                   INTEGRATION OF A GIVEN FUNCTION BY
C                   SYMPSON'S RULE
C          RADIA  - COMPUTES RADIATION RESISTANCE OF RHOMBIC ELEMENTS
C          SICI   - COMPUTES VALUES OF SIN AND COS INTEGRALS
C          SJORGE - COMPUTES NON-UNIFORM LINE CORRECTIONS
C
C
C  PREPARATION OF DATA
      N1=1
      N2=2
      DUM=1.0
   15 READ(5,1015) K
   20 DO 159 KK=1,K
   21 READ(5,1021) ALPAE,ALPAS,TAU,FR,SDE,DF,EPSLON
      AMEDA=(3.0*(10.0**8))/FR
      UM=CMPLX(0.0,1.0)
      PI=3.14159
      CAPA=2.0*PI/AMEDA
      SRES=AMEDA/4.0
      ALFAS=(2.0*PI*ALPAS)/360.0
      ALFAE=(2.0*PI*ALPAE)/360.0
```

```
C
C
C
C      SAMPLE PROGRAM SMIGUFL - MAIN
C
C
C
      SAN=TAN(ALFAS)/TAN(ALFAE)
      GAMA=ATAN((1.0-SQRT(TAU))/(SQRT(TAU)*TAN(ALFAE)+TAN(ALFAS)))
      B1=SDE*(TAU**(DE-1.0))/2.0
      EL1=B1*2.0*COS(GAMA)/TAN(ALFAE)
      NDD=DE
      NDE=DE
      RADIO1=.0005
C
   30 DO 35  NN=1,NDD
      BE(NN)=B1/(TAU**(NN-1))
      ELE(NN)=EL1/(TAU**(NN-1))
      D(NN)=2.0*BE(NN)
      RADIO(NN)=RADIO1/(TAU**(NN-1))
      SEL(NN)=4.0*BE(NN)*SAN/SQRT(TAU)
   35 CONTINUE
      GAMA=360.0*GAMA/(2.0*PI)
      WRITE(6,22) ALPAE,ALPAS,TAU,FR,SDE,DE,EPSLON,B1,EL1,GAMA,SAN,AMEDA
      WRITE(6, 24) SRES,(D(NN),NN=1,NDD)
   45 EPSLON=(2.0*PI*EPSLON)/360.0
      GAMA=2.0*PI*GAMA/360.0
      GAMEP=GAMA-EPSLON
      GAPEP=GAMA+EPSLON
      FRL=3.0*(10.0**8)/(4.0*SDE)
      FRH=3.0*(10.0**8)/(8.0*B1)
      HH=SDE*COS(GAMEP)+EL1*SIN(EPSLON)/(TAU**(NDE-1))
      HL=EL1*SIN(EPSLON)
      SIZE=2.0*B1*(SIN(GAMEP)+SIN(GAPEP)/(TAU**(NDE-1)))+EL1*
     1(1.0/(TAU**(NDE-1))-1.0)
C
C     PRINTING THE OVERALL CHARACTERISTICS OF THE ANTENNA
      WRITE(6,25)FRH,FRL,HH,SIZE,HL
C
C
      CALL FAIAL (BE,ELE,EPSLON,RADIO,GAMA,AMEDA,NDE,TAU,SAN)
      DO 159 JJ=1,2
C
C      JJ IS A REFERENCE INDEX. WHEN JJ=1 THE MUTUAL IMPEDANCE
C      ARE NEGLECTED. THEY ARE ACCOUNTED FOR WHEN JJ =2
C
      GO TO (47,48),JJ
```

```
C
C
C      SAMPLE PROGRAM SMIGUEL - MAIN
C
C
C
   47 WRITE(6,1047) FR
      GO TO 49
   48 WRITE(6,1048) FR
   49 WRITE(6,1160)
      WRITE(6,1049)
   50 DO 159 IR=1,2
C
C     WHEN IR=1 THE LOOP FINDS INPUT IMPEDANCE ,AND
C     STORES THE VALUES OF NON-UNIFORM LINE CORRECTIONS
C     IN THE ARRAYS,AP,BP,CP AND DP.
C     WHEN IR=2 THE LOOP FINDS CURRENTS AND VOLTAGES
C     ALONG THE LINE AND PRINTS THEM TOGETHER WITH
C     -QU      - THE AVERAGE Q FOR EACH RADIATOR
C     -ZINR    - THE IMPEDANCE SEEN AT A PARTICULAR POINT
C     -ELEMENT- THE ORDER OF THE ELEMENT
C     -POINT   - THE REFERENCE POINT.NO REF. MEANS THE FEED
C                POINT, 1 IS AT THE VERTEX,2 IS AT THE END
C      THE VALUES OF V AND I ARE GIVEN AS MAGNITUDE AND ANGLE
C      IN RELATION TO THE INPUT SOURCE CURRENT= 1.0+J0.0
C
      DO 159 III=1,NDE
      GO TO (52,54) ,IR
   52 I=NDE-III+1
   53 GO TO 55
   54 I=III
   55 CONTINUE
      B=BE(I)
      EL=ELE(I)
      A=RADIO(I)
      ARG=B/250.0
      X=0.0
      CALL IMPRAD(B,EL,EPSLON,A,GAMA,AMEDA,X,ZXR,ZAVR,AVKR)
      AKR(I)=AVKR
      CALL RADIA (B,CAPA,GAMA,ZRA)
      RA=REAL(ZRA)/(4.0*B)
      GO TO (64,62),JJ
   62 BS=(BE(I)+BE(I+1))/2.0
      RS=(ELE(I+1)-ELE(I))*COS(GAMA)
      CALL FLORES(BS,RS,CAPA,RM)
      RA=RA+RM/B
```

```
C
C
C
C     SAMPLE PROGRAM SMIGUEL - MAIN
C
C
C
   64 CONTINUE
      XA=AIMAG(ZRA)/(4.0*B)
      ATT=RA/(2.0*AVKR)
      QU=AIMAG(ZAVR)/RA
      BETA=CAPA*(1.0+1.0/(8.0*(QU**2)))
C
C BETA IS THE NEW VALUE OF CAPA DUE TO NON UNIFORMITY OF LINE
C
   70 GO TO (72,91) ,IR
   72 CONTINUE
      CALL IMPSTU(EL,B,EPSLON,A,GAMA,X,AMEDA,ZAV,AVK,YAV,ZX,YX,TAU,SAN)
      ZINR(NDE+1)=CMPLX(0.0,0.0)
      ZINS(I)=AVK*(ZINR(I+1)*COS(CAPA*SEL(I))+UM*AVK*SIN(CAPA*SEL(I)))
     1/(AVK*COS(CAPA*SEL(I))+UM*ZINR(I+1)*SIN(CAPA*SEL(I)))
      ZINS(NDE)=CMPLX(0.0,0.0)
      AK(I)=AVK
      AIN=2.0*B+ARG
      MSD=500
      CALL SJORGE(B,EL,EPSLON,A,GAMA,AMEDA,ATT,BETA,MSD,AIN,
     1ARG,AA,BB,CC,DD)
      AP(I)=AA
      BP(I)=BB
      CP(I)=CC
      DP(I)=DD
      ZINT(I)=AVKR*(AVKR*BB+ZINS(I)*DD)/(ZINS(I)*CC+AVKR*AA)
      AIN=ARG
      CALL SJORGE(B,EL,EPSLON,A,GAMA,AMEDA,ATT,BETA,MSD,AIN,
     1ARG,AA,BB,CC,DD)
      APA(I)=AA
      BPB(I)=BB
      CPC(I)=CC
      DPD(I)=DD
      ZINR(I)=AVKR*(AVKR*BB+ZINT(I)*DD)/(ZINT(I)*CC+AVKR*AA)
   90 GO TO (159,91),IR
   91 QIL(I)=CMPLX(1.0,0.0)
      VIL(I)=ZINR(I)
      CALL POLAR (VIL(I),VOLT,VANG)
      CALL POLAR (QIL(I),QIC,QANG)
   96 WRITE(6,1096) I,VOLT,VANG,QIC,QANG,QU,ZINR(I)
      QIM=-VIL(I)*CPC(I)/AKR(I)+QIL(I)*DPD(I)
```

```
C
C
C
C     SAMPLE PROGRAM SMIGUEL - MAIN
C
C
      VIM=VIL(I)*APA(I)-AKR(I)*QIL(I)*BPB(I)
      CALL POLAR (VIM,VOLT,VANG)
      CALL POLAR (QIM,QIC,QANG)
      L=1
  148 WRITE (6,1148) I,L,VOLT,VANG,QIC,QANG
      QIX=-VIM*CP (I)/AKR(I)+QIM*DP (I)
      VIX=VIM*AP (I)-AKR(I)*QIM*BP (I)
      CALL POLAR(VIX,VOLT,VANG)
      CALL POLAR(QIX,QIC,QANG)
      L=2
      WRITE (6,1148) I,L,VOLT,VANG,QIC,QANG
  151 VIL(I+1)=VIX*COS(CAPA*SEL(I))-AK(I)*UM*QIX    *SIN(CAPA*SEL(I))
      QIL(I+1)=-VIX*SIN(CAPA*SEL(I))*UM/AK(I)+QIX*COS(CAPA*SEL(I))
  159 CONTINUE
C
   22 FORMAT(1H1,/,/,/,/,/,/,/,/,
     1                15X,17HALL UNITS ARE MKS,/,/,16X,11H-INPUT DATA,/
     2,/,18X,5HALFAE,1X,1H=,F10.4,/,18X,5HALFAS,1X,1H=,F10.4,/,18X,
     37HTAU    =,F10.4,/,18X,7HFREQ   =,E10.3,/,18X,7HSDE    =,F10.4,/,18X
     4,7HDE     =,F10.4,/,18X,7HEPSLON=,F10.4,/,/,16X,14H-COMPUTED DATA,
     5/,/,18X,7HB1     =,F10.4,/,18X,7HL1     =,F10.4,/,18X,7HGAMA   =,
     6F10.4,/,18X,7HSAN    =,F10.4,/,18X,7HLAMEDA=,F10.4)
   24 FORMAT(1H0,17X,7HSRFS   =,F10.4,/,18X,15HLENGTH OF WIRES,/,
     111(18X,3F10.4,/))
   25 FORMAT(1H0,14X,28HMAX. FREQUENCY OF OPERATION ,E10.3,/,/,
     115X,28HMIN. FREQUENCY OF OPERATION ,E10.3,/,/,
     215X,24HHEIGHT  OF LAST ELEMENT ,4X,F10.3,/,/,
     315X,27HOVERALL LENGTH OF STRUCTURE ,1X,F10.3,/,/,
     415X,20HHEIGHT OF FEED POINT ,8X,F10.3)
 1015 FORMAT(I10)
 1021 FORMAT(3F10.3,E10.3,3F10.3)
 1047 FORMAT(1H1,/,/,/,/,/,/,/,/,
     1                15X,5HFREQ=,E10.3,3X,30HWITHOUT ACCOUNTING FOR MUTU
     2ALS)
 1048 FORMAT(1H1,/,/,/,/,/,/,/,/,
     1                15X,5HFREQ=,E10.3,3X,22HACCOUNTING FOR MUTUALS)
 1049 FORMAT(    15X,4HELEM,1X,5HPOINT,3X,4HVOLT,5X,4HVANG,7X,3HCUR,6X,
     14HCANG,8X,1HQ,12X,4HZINR)
 1096 FORMAT(15X,I2,7X,7F10.3)
 1148 FORMAT(15X,I2,2X,I2,3X,4F10.3)
```

```
C
C
C
C      SAMPLE PROGRAM SMIGUEL - MAIN
C
C
 1160 FORMAT(15X,42HNOTE - SEE MAIN PROGRAM AFTER STATEMENT 50,/,22X,
     128HFOR PRINT OUT INTERPRETATION)
      END
```

```
C
C
C
C     SAMPLE PROGRAM SMIGUEL - SUBROUTINE FAIAL
C
C
      SUBROUTINE FAIAL (BE,ELE,EPSLON,RADIO,GAMA,AMEDA,NDF,TAU,SAN)
      DIMENSION BE(30),ELE(30),RADIO(30)
      COMPLEX ZXR,ZAVR,ZAV,YAV,ZX,YX
C
C        FAIAL PRINTS THE CHARACTERISTIC VALUES OF THE LINE
C        FORMED BY THE ANTENNA AND ITS IMAGE
C        THE REQUIRED INPUT DATA ARE THE PHYSICAL PARAMETERS
C        OF THE ANTENNA,AND THE WAVELENGTH(AMEDA)
C        FAIAL USES SUBROUTINES IMPRAD AND IMPSTU
C
      CAPA=6.28318/AMEDA
      JL=1
      B=BE(JL)
      EL=ELE(JL)
      A=RADIO(JL)
      DO 159 IX=1,3
      XI=IX-1
      X=XI*2.0*BE(JL)
      CALL IMPRAD(B,EL,EPSLON,A,GAMA,AMEDA,X,ZXR,ZAVR,AVKR)
      X=X*SAN/SQRT(TAU)
      CALL IMPSTU(EL,B,EPSLON,A,GAMA,X,AMEDA,ZAV,AVK,YAV,ZX,YX,TAU,SAN)
   90 IF(JL-1) 159,91,159
   91 GO TO (92,95,97),IX
   92 WRITE(6,1091) AVKR,AVK,ZAVR,ZAV
   93 WRITE(6,1093) ZXR,ZX
   94 GO TO 159
   95 WRITE(6,1095) ZXR,ZX
   96 GO TO 159
   97 WRITE(6,1097) ZXR,ZX
  159 CONTINUE
 1091 FORMAT(1H1,/,/,/,/,/,/,/,/,/,/,
     1                54X,9HRADIATORS,12X,5HSTUBS,/,/,/,15X,37HAVERAGE CH
     2ARACTERISTIC IMPEDANCE     =,F10.3,9X,F10.3,/,/,/,15X,17HAVERAGE RE
     3ACTANCE,19X,1H=,2(F5.2,F10.3,3X),/,/,/,15X,36HREACTANCE ABOVE OR B
     4ELOW THE AVERAGE ,/,/)
 1093 FORMAT(40X,12HAT FEED END=,2(F5.2,F10.3,3X),/)
 1095 FORMAT(40X,12HAT VERTEX  =,2(F5.2,F10.3,3X),/)
 1097 FORMAT(40X,12HAT FAR END =,2(F5.2,F10.3,3X))
      RETURN
      END
```

```
C
C
C
C     SAMPLE PROGRAM SMIGUEL - SUBROUTINE FLORES
C
C
      SUBROUTINE FLORES(EL,R,CAPA,RM)
      DIMENSION RZNEG(50),XZNEG(50), RZPOS(50),XZPOS(50),TRZN(50),
     1TXZN(50),TRZP(50),TXZP(50),ARED(100),AXAD(100),RESD(100),
     1XASD(100),RTOT(100),XTOT(100),RINT(100),XINT(100)
      COMPLEX BZ,BO,BZC,BEL,BRU,BRD,UM,COM,ZNEG,ZPOS,COP,CZ,CO,
     1CL,CRD,CRU,ZTOT
C
C        FLORES COMPUTES THE MUTUAL RESISTANCE BETWEEN
C        TWO PARALLEL WIRES WITH SINUSOIDAL CURRENT DISTRIBUTION
C          THE REQUIRED INPUT DATA ARE
C            -EL   - THE HALF-LENGTH OF THE WIRES
C            -R    - THE DISTANCE BETWEEN WIRES
C            -CAPA- THE FREE SPACE PHASE FACTOR
C          THE OUTPUT IS
C            -RM   - THE MUTUAL RESISTANCE
C
      UM=CMPLX(0.0,1.0)
  123 ARG=EL/50.0
      DO 50 N=1,100
      XN=N
      Z=-EL+(XN-1.0)*ARG
      BUM=SQRT(R**2+(Z+EL)**2)
      BDO=SQRT(R**2+(Z-EL)**2)
      BTR=SQRT(R**2+Z**2)
      RED=30.0*(SIN(CAPA*(EL-Z))/(SIN(CAPA*EL)**2)*(
     1SIN(CAPA*BUM)/BUM+SIN(CAPA*BDO)/BDO+2.0*SIN(CAPA*BTR)*COS(CAPA*
     2EL)/BTR))
      ARED(N)=RED
   50 CONTINUE
      CALL QSF(ARG,ARED,RESD,N)
      RM=RESD(100)
      RETURN
      END
```

```
C
C
C
C     SAMPLE PROGRAM SMIGUEL - SUBROUTINE IMPRAD
C
C
      SUBROUTINE IMPRAD (B,EL,EPSLON,A,GAMA,AMEDA,X,ZXR,ZAVR,AVKR)
      COMPLEX ZXR,ZAVR
C
C        IMPRAD COMPUTES THE IMPEDANCE OF A TRANSMISSION LINE
C          WITH RHOMBIC SHAPE
C        THE DATA REQUIRED ARE
C          THE DIMENSIONS AND ANGLES DEFINING THE LINE
C          THE FREQUENCY
C          THE POINT -X- FOR WHICH THE COMPUTATION IS REQUIRED
C        THE OUTPUT IS
C          AVKR - THE AVERAGE IMPEDANCE
C          ZAVR - THE AVERAGE REACTANCE
C          ZXR  - THE RELATIVE REACTANCE ABOVE OR BELOW THE AVERAGE AS
C                 A FUNCTION OF X
C
      PI=3.14159
      GAMEP=GAMA-EPSLON
      GAPEP=GAMA+EPSLON
      CAPA=2.0*PI/AMEDA
      AL=(EL-2.0*B*SIN(GAMA))*SIN(EPSLON)
      BL=2.0*B*COS(GAMEP)
      CL=2.0*B*COS(GAPEP)
      AE=AL/COS(GAMEP)
      BE=ALOG(2.0*COS(GAMEP)/A)
      CE=ALOG(2.0*COS(GAPEP)/A)
      DE=(AL+2.0*B*(COS(GAMEP)+COS(GAPEP)))/COS(GAPEP)
      AVKR=120.0*(BE+ALOG(AE+2.0*B)-1.0+(AE/(2.0*B))*ALOG(1.0+2.0*B/AE))
      ZAVR=CMPLX(0.0,CAPA*AVKR)
      IF(X-2.0*B) 10,10,15
   10 ZXR=CMPLX(0.0,120.0*CAPA*(BE+ALOG(AE+X)))-ZAVR
      GO TO 16
   15 ZXR=CMPLX(0.0,120.0*CAPA*(CE+ALOG(DE-X)))-ZAVR
   16 CONTINUE
      RETURN
      END
```

```
C
C
C
C     SAMPLE PROGRAM SMIGUEL - SUBROUTINE IMPSTU
C
C
      SUBROUTINE IMPSTU (EL,B,EPSLON,A,GAMA,X,AMEDA,ZAV,AVK,YAV,
     1ZX,YX,TAU,SAN)
      COMPLEX ZAV,YAV,ZX,YX
C
C         IMPSTU COMPUTES THE IMPEDANCE OF TRANSMISSION LINE
C          FORMED BY THE CONNECTING STUBS
C         THE DATA REQUIRED ARE
C           THE DIMENSIONS AND ANGLES DEFINING THE LINE
C           THE FREQUENCY
C           THE POINT -X- FOR WHICH THE COMPUTATION IS REQUIRED
C         THE OUTPUT IS
C           -AVK- THE AVERAGE CHARACTERISTIC IMPEDANCE
C           -ZAV- THE AVERAGE IMPEDANCE
C           -YAV- THE AVERAGE ADMITANCE
C           -ZX - THE IMPEDANCE ABOVE OR BELOW THE AVERAGE
C           -YX - THE ADMITANCE ABOVE OR BELOW THE AVERAGE
C
      PI=3.14159
      CAPA=2.0*PI/AMEDA
      ELL=EL/SQRT(TAU)
      BBL=B*SAN/SQRT(TAU)
      AE=ELL/SIN(GAMA)-2.0*BBL
      BE=ALOG(2.0*SIN(GAMA)*SIN(EPSLON)/A)
      AVK=120.0*(BE+ALOG(AE+4.0*BBL)-1.0+(AE/(4.0*BBL))*ALOG(1.0+4.0*BBL
     1/AE))
      ZAV=CMPLX(0.0,CAPA*AVK)
      ZX=CMPLX(0.0,120.0*CAPA*(BE+ALOG(AE+X)))-ZAV
      YX=ZX/(AVK**2)
      YAV=ZAV/(AVK**2)
      RETURN
      END
```

```
C
C
C
C     SAMPLE PROGRAM SMIGUEL - SUBROUTINE POLAR
C
C
      SUBROUTINE POLAR (A,B,C)
      COMPLEX A
C
C  POLAR TRANSFORMS A COMPLEX IN FORM A=P+JQ
C INTO FORM B*(E**J(ANGLE))   (B=B),(C=ANGLE)
C
      PI=3.14159
      ETETA=AIMAG(A)
      EFI=REAL(A)
   60 B=SQRT(ETETA**2+EFI**2)
      IF(EFI) 63,69,61
   61 PSI=ATAN(ETETA/EFI)
      GO TO 75
   63 IF(ETETA) 64,66,68
   64 PSI=ATAN(ETETA/EFI)-PI
      GO TO 75
   66 PSI=PI
      GO TO 75
   68 PSI=ATAN(ETETA/EFI)+PI
      GO TO 75
   69 IF(ETETA)70,72,74
   70 PSI=-PI/2.0
      GO TO 75
   72 PSI=0.0
      GO TO 75
   74 PSI=PI/2.0
   75 PSI=360.0*PSI/(2.0*PI)
      C=PSI
      RETURN
      END
```

```
C
C
C
C        SAMPLE PROGRAM SMIGUEL - SUBROUTINE QSF                                QSF  003
C
C
C           SUBROUTINE QSF                                                      QSF  004
C                                                                               QSF  005
C           PURPOSE                                                             QSF  006
C              TO COMPUTE THE VECTOR OF INTEGRAL VALUES FOR A GIVEN             QSF  007
C              EQUIDISTANT TABLE OF FUNCTION VALUES.                            QSF  008
C                                                                               QSF  009
C           USAGE                                                               QSF  010
C              CALL QSF (H,Y,Z,NDIM)                                            QSF  011
C                                                                               QSF  012
C           DESCRIPTION OF PARAMETERS                                           QSF  013
C              H      - THE INCREMENT OF ARGUMENT VALUES.                       QSF  014
C              Y      - THE INPUT VECTOR OF FUNCTION VALUES.                    QSF  015
C              Z      - THE RESULTING VECTOR OF INTEGRAL VALUES. Z MAY BE       QSF  016
C                       IDENTICAL WITH Y.                                       QSF  017
C              NDIM   - THE DIMENSION OF VECTORS Y AND Z.                       QSF  018
C                                                                               QSF  019
C           REMARKS                                                             QSF  020
C              NO ACTION IN CASE NDIM LESS THAN 3.                              QSF  021
C                                                                               QSF  022
C           SUBROUTINES AND FUNCTION SUBPROGRAMS REQUIRED                       QSF  023
C              NONE                                                             QSF  024
C                                                                               QSF  025
C           METHOD                                                              QSF  026
C              BEGINNING WITH Z(1)=0, EVALUATION OF VECTOR Z IS DONE BY         QSF  027
C              MEANS OF SIMPSONS RULE TOGETHER WITH NEWTONS 3/8 RULE OR A       QSF  028
C              COMBINATION OF THESE TWO RULES. TRUNCATION ERROR IS OF           QSF  029
C              ORDER H**5 (I.E. FOURTH ORDER METHOD). ONLY IN CASE NDIM=3       QSF  030
C              TRUNCATION ERROR OF Z(2) IS OF ORDER H**4.                       QSF  031
C              FOR REFERENCE, SEE                                               QSF  032
C              (1) F.B.HILDEBRAND, INTRODUCTION TO NUMERICAL ANALYSIS,          QSF  033
C                  MCGRAW-HILL, NEW YORK/TORONTO/LONDON, 1956, PP.71-76.        QSF  034
C              (2) R.ZURMUEHL, PRAKTISCHE MATHEMATIK FUER INGENIEURE UND        QSF  035
C                  PHYSIKER, SPRINGER, BERLIN/GOETTINGEN/HEIDELBERG, 1963,      QSF  036
C                  PP.214-221.                                                  QSF  037
C                                                                               QSF  038
C        ...............................................................QSF  039
C                                                                               QSF  040
C                                                                               QSF  042
C                                                                               QSF  043
C                                                                               QSF  045
```

```
C
C
C
C       SAMPLE PROGRAM SMIGUFL - SUBROUTINE QSF                          QSF  048
C
C
      SUBROUTINE QSF(H,Y,Z,NDIM)                                         QSF  041
      DIMENSION Y(500),Z(500)
      HT=.3333333*H                                                      QSF  046
      IF(NDIM-5)7,8,1                                                    QSF  047
C     NDIM IS GREATER THAN 5. PREPARATIONS OF INTEGRATION LOOP           QSF  049
    1 SUM1=Y(2)+Y(2)                                                     QSF  050
      SUM1=SUM1+SUM1                                                     QSF  051
      SUM1=HT*(Y(1)+SUM1+Y(3))                                           QSF  052
      AUX1=Y(4)+Y(4)                                                     QSF  053
      AUX1=AUX1+AUX1                                                     QSF  054
      AUX1=SUM1+HT*(Y(3)+AUX1+Y(5))                                      QSF  055
      AUX2=HT*(Y(1)+3.875*(Y(2)+Y(5))+2.625*(Y(3)+Y(4))+Y(6))            QSF  056
      SUM2=Y(5)+Y(5)                                                     QSF  057
      SUM2=SUM2+SUM2                                                     QSF  058
      SUM2=AUX2-HT*(Y(4)+SUM2+Y(6))                                      QSF  059
      Z(1)=0.                                                            QSF  060
      AUX=Y(3)+Y(3)                                                      QSF  061
      AUX=AUX+AUX                                                        QSF  062
      Z(2)=SUM2-HT*(Y(2)+AUX+Y(4))                                       QSF  063
      Z(3)=SUM1                                                          QSF  064
      Z(4)=SUM2                                                          QSF  065
      IF(NDIM-6)5,5,2                                                    QSF  066
C                                                                        QSF  067
C     INTEGRATION LOOP                                                   QSF  068
    2 DO 4 I=7,NDIM,2                                                    QSF  069
      SUM1=AUX1                                                          QSF  070
      SUM2=AUX2                                                          QSF  071
      AUX1=Y(I-1)+Y(I-1)                                                 QSF  072
      AUX1=AUX1+AUX1                                                     QSF  073
      AUX1=SUM1+HT*(Y(I-2)+AUX1+Y(I))                                    QSF  074
      Z(I-2)=SUM1                                                        QSF  075
      IF(I-NDIM)3,6,6                                                    QSF  076
    3 AUX2=Y(I)+Y(I)                                                     QSF  077
      AUX2=AUX2+AUX2                                                     QSF  078
      AUX2=SUM2+HT*(Y(I-1)+AUX2+Y(I+1))                                  QSF  079
    4 Z(I-1)=SUM2                                                        QSF  080
    5 Z(NDIM-1)=AUX1                                                     QSF  081
      Z(NDIM)=AUX2                                                       QSF  082
      RETURN                                                             QSF  083
    6 Z(NDIM-1)=SUM2                                                     QSF  084
```

```
C
C
C
C     SAMPLE PROGRAM SMIGUEL - SUBROUTINE QSF
C
C
      Z(NDIM)=AUX1
      RETURN
C
C     END OF INTEGRATION LOOP
C
    7 IF(NDIM-3)12,11,8
C
C     NDIM IS EQUAL TO 4 OR 5
    8 SUM2=1.125*HT*(Y(1)+Y(2)+Y(2)+Y(2)+Y(3)+Y(3)+Y(3)+Y(4))
      SUM1=Y(2)+Y(2)
      SUM1=SUM1+SUM1
      SUM1=HT*(Y(1)+SUM1+Y(3))
      Z(1)=0.
      AUX1=Y(3)+Y(3)
      AUX1=AUX1+AUX1
      Z(2)=SUM2-HT*(Y(2)+AUX1+Y(4))
      IF(NDIM-5)10,9,9
    9 AUX1=Y(4)+Y(4)
      AUX1=AUX1+AUX1
      Z(5)=SUM1+HT*(Y(3)+AUX1+Y(5))
   10 Z(3)=SUM1
      Z(4)=SUM2
      RETURN
C
C     NDIM IS EQUAL TO 3
   11 SUM1=HT*(1.25*Y(1)+Y(2)+Y(2)-.25*Y(3))
      SUM2=Y(2)+Y(2)
      SUM2=SUM2+SUM2
      Z(3)=HT*(Y(1)+SUM2+Y(3))
      Z(1)=0.
      Z(2)=SUM1
   12 RETURN
      END
```

```
C
C
C
C     SAMPLE PROGRAM SMIGUEL - SUBROUTINE RADIA
C
C
      SUBROUTINE RADIA (B,CAPA,GAMA,ZRA)
C
C        RADIA COMPUTES THE RADIATION RESISTANCE OF A
C          RHOMBIC ANTENNA
C          THE DATA REQUIRED ARE
C          B    - THE LENGTH OF A WIRE
C          GAMA - THE HALF-ANGLE FORMED BY THE WIRES
C          CAPA - THE FREE SPACE PHASE VELOCITY
C        THE OUTPUT IS
C          ZRA  - THE RADIATION RESISTANCE IN COMPLEX FORM
C
C        RADIA CALLS SICI THAT COMPUTES SIN AND COS INTEGRALS
C
      PI=3.14159
      D=4.0*B*CAPA
      CALL SICI(D,SD,CD)
      A=PI/2.0-GAMA
      P=D*(SIN(A)**2)
      CALL SICI(P,SP,CP)
      Q=D*(COS(A)**2)
      CALL SICI(Q,SQ,CQ)
      R=D*SIN(A)*(1.0-SIN(A))
      CALL SICI(R,SR,CR)
      T=D*SIN(A)*(1.0+SIN(A))
      CALL SICI(T,ST,CT)
      U=D*SIN(A)
      CALL SICI(U,SU,CU)
      V=D*COS(A)*(1.0+COS(A))
      CALL SICI(V,SV,CV)
      X=D*(1.0+COS(A))
      CALL SICI(X,SX,CX)
      Y=D*(1.0-COS(A))
      CALL SICI(Y,SY,CY)
      Z=D*COS(A)*(1.C-COS(A))
      CALL SICI(Z,SZ,CZ)
      RES=1.1544+2.0*ALOG(P)+2.0*CD-2.0*CU-CX-CY+COS(P)*(CZ+CR+CV+CT-
     12.0*CQ-2.0*CP)+SIN(P)*(SZ-SR-SV+ST+2.0*SQ-2.0*SP)
      ZRA=CMPLX(RES*120.0,0.0)
      RETURN
      END
```

```
C
C
C
C         SAMPLE PROGRAM SMIGUEL - SUBROUTINE SICI
C
C
      SUBROUTINE SICI (X,SI,CI)
      DIMENSION XS(500),YS(500),XC(500),YC(500),S(500),C(500)
C
C        SICI COMPUTES SIN AND COS INTEGRALS
C           THE INPUT DATA IS
C           X  - THE VARIABLE VALUE
C           SICI CALLS QSF THAT COMPUTES INTEGRALS
C
      IF(X-0.0) 3,3,4
    3 X=.000000000001
    4 CONTINUE
      DO  10 I=1,500
      AI=I
      ASG=X/500.0
      XS(I)=ASG*AI
      YS(I)=SIN(XS(I))/XS(I)
      ACG=( 4.0-X)/500.0
      XC(I)=ACG*AI+X
      YC(I)=-COS(XC(I))/XC(I)
   10 CONTINUE
      CALL QSF (ASG,YS,S,500)
      CALL QSF (ACG,YC,C,500)
      SI=S(500)
      CI=C(500)-.14098
      RETURN
      END
```

```
C
C
C
C
C     SAMPLE PROGRAM SMIGUEL - SUBROUTINE SJORGF
C
C
      SUBROUTINE SJORGE (B,EL,EPSLON,A,GAMA,AMEDA,ATT,BETA,MSD,AIN,
     1ARG,AA,BB,CC,DD)
      DIMENSION AIRA(500),AIIA(500),
     1BIRA(500),BIIA(500),AIRT(500),AIIT(500),BIRT(500),BIIT(500)
      COMPLEX AI,BI,AA,BB,CC,DD,Z,AR,BR,ZAVR,ZXR,AT,BT,UM
C
C         SJORGE COMPUTES THE NON-UNIFORM LINE CORRECTIONS
C         FOR A SECTION OF LINE
C           THE REQUIRED INPUT DATA ARE
C             -THE PHYSICAL DESCRIPTION OF LINE
C             --AIN - THE INITIAL POINT OF THE SECTION
C             -ARG  - THE SIZE OF THE INTEGRATION INCREMENT
C             -AMEDA- THE WAVELENGTH
C             -BETA - THE PHASE FACTOR
C           THE OUTPUT IS
C             -AA,BB,CC,DD-THE COEFFICIENTS OF THE LINE EQUATIONS
C         SJORGE USES IMPRAD TO OBTAIN THE LINE COEFFICIENTS
C         AND QSF TO PERFORM INTEGRATIONS
C
      UM=CMPLX(0.0,1.0)
  110 DO 120 MS=1,MSD
      SM=MS
      Y=AIN+(SM-1.0)*ARG
      CALL IMPRAD(B,EL,EPSLON,A,GAMA,AMEDA,Y,ZXR,ZAVR,AVKR)
      Z=ZXR
      X=ARG+(SM-1.0)*ARG
      AI=CMPLX(COSH(2.0*ATT*X)*COS(2.0*BETA*X),SINH(2.0*ATT*X)
     1*SIN(2.0*BETA*X))*Z/AVKR
      BI=    CMPLX(SINH(2.0*ATT*X)*COS(2.0*BETA*X),COSH(2.0*ATT*X)
     1*SIN(2.0*BETA*X))*Z/AVKR
      AIR=REAL(AI)
      AII=AIMAG(AI)
      AIRA(MS)=AIR
      AIIA(MS)=AII
      BIR=REAL(BI)
      BII=AIMAG(BI)
      BIRA(MS)=BIR
      BIIA(MS)=BII
  120 CONTINUE
C
```

```
C
C
C
C      SAMPLE PROGRAM SMIGUEL - SUBROUTINE SJORGE
C
C
      AT=CMPLX(COSH(ATT*X)*COS(BETA*X),SINH(ATT*X)*SIN(BETA*X))
      BT=CMPLX(SINH(ATT*X)*COS(BETA*X),COSH(ATT*X)*SIN(BETA*X))
      CALL  QSF(ARG,AIRA,AIRT,MSD)
      CALL  QSF(ARG,AIIA,AIIT,MSD)
      CALL  QSF(ARG,BIRA,BIRT,MSD)
      CALL  QSF(ARG,BIIA,BIIT,MSD)
      AR=CMPLX(AIRT(MSD),AIIT(MSD))
      BR=CMPLX(BIRT(MSD),BIIT(MSD))
      AA=(1.0+BR)*AT-AR*BT
      BB=AR*AT+(1.0-BR)*BT
      CC=(1.0+BR)*BT-AR*AT
      DD=AR*BT+(1.0-BR)*AT
C
      RETURN
      END
```

```
ALL UNITS ARE MKS

 -INPUT DATA

   ALFAE  =    13.7000
   ALFAS  =     7.5000
   TAU    =     0.8500
   FREQ   =  0.110E 10
   SDF    =     0.1500
   DE     =    12.0000
   EPSLON=      1.5000

 -COMPUTED DATA

   B1     =     0.0126
   L1     =     0.1006
   GAMA   =    12.3518
   SAN    =     0.5401
   LAMEDA=      0.2727

   SRES   =     0.0682
   LENGTH OF WIRES
         0.0251      0.0295      0.0347
         0.0409      0.0481      0.0566
         0.0666      0.0783      0.0921
         0.1084      0.1275      0.1500

MAX. FREQUENCY OF OPERATION  0.299E 10

MIN. FREQUENCY OF OPERATION  0.500E 09

HEIGHT  OF LAST ELEMENT            0.163

OVERALL LENGTH OF STRUCTURE        0.541

HEIGHT OF FEED POINT               0.003
```

```
                                            RADIATORS              STUBS

AVERAGE CHARACTERISTIC IMPEDANCE     =    471.470               292.266

AVERAGE REACTANCE                    = 0.0   10861.883    0.0    6733.305

REACTANCE ABOVE OR BELOW THE AVERAGE

                        AT FEED END= 0.0  -4504.469    0.0     -80.453
                        AT VERTEX  = 0.0   2097.145    0.0       0.422
                        AT FAR END = 0.0  -4209.039    0.0      78.996
```

```
FREQ= 0.110E 10   WITHOUT ACCOUNTING FOR MUTUALS
NOTE - SEE MAIN PROGRAM AFTER STATEMENT 50
       FOR PRINT OUT INTERPRETATION
```

ELEM	POINT	VOLT	VANG	CUR	CANG	Q	ZINR	
1		154.220	-62.315	1.000	0.0	54.593	71.653	-136.564
1	1	373.121	-81.310	0.711	-6.376			
1	2	502.218	-86.833	0.192	-39.929			
2		417.684	-90.132	0.973	-170.803	39.124	69.569	423.477
2	1	47.247	-151.380	1.343	-174.688			
2	2	386.940	99.893	1.021	-177.488			
3		482.781	96.638	0.257	30.812	26.418	770.409	1716.301
3	1	233.420	89.524	0.908	11.069			
3	2	141.623	-67.538	0.934	7.078			
4		301.748	-78.697	0.204	-23.403	17.457	840.897	-1214.140
4	1	223.908	-88.693	0.407	-159.791			
4	2	43.382	177.859	0.583	-171.759			
5		156.689	105.292	0.272	159.606	11.587	336.103	-467.975
5	1	160.861	82.340	0.184	37.511			
5	2	56.228	23.721	0.345	-0.106			
6		92.159	-81.454	0.239	-45.363	7.875	312.130	-227.516
6	1	112.412	-128.910	0.133	-144.926			
6	2	55.847	166.926	0.222	145.407			
7		64.101	57.444	0.195	79.598	5.577	304.928	-124.136
7	1	82.825	-13.506	0.100	-18.800			
7	2	38.943	-88.093	0.158	-107.483			
8		48.799	152.805	0.123	166.108	4.200	386.217	-91.361
8	1	46.596	56.189	0.077	58.143			
8	2	27.537	-33.184	0.085	-53.695			
9		29.379	-170.651	0.077	-155.268	3.453	367.111	-101.129
9	1	24.821	77.955	0.044	73.297			
9	2	14.263	-39.612	0.039	-51.504			
10		14.421	168.375	0.038	178.216	3.220	372.595	-65.116
10	1	11.960	31.167	0.019	26.742			
10	2	5.985	-117.498	0.015	-113.418			
11		5.856	71.915	0.016	82.631	3.594	361.682	-66.237
11	1	4.572	-91.643	0.008	-95.531			
11	2	2.307	100.992	0.007	90.732			
12		2.175	-93.762	0.007	-108.296	5.067	292.359	86.226
12	1	1.336	80.358	0.005	48.284			
12	2	0.082	-134.910	0.006	-137.159			

FREQ= 0.110E 10 ACCOUNTING FOR MUTUALS
NOTE - SEE MAIN PROGRAM AFTER STATEMENT 50
FOR PRINT OUT INTERPRETATION

ELEM	POINT	VOLT	VANG	CUR	CANG	Q	ZINR	
1		516.835	2.210	1.000	0.0	0.600	516.451	19.931
1	1	270.355	-37.428	0.723	-48.493			
1	2	160.055	-107.861	0.484	-74.331			
2		188.707	-130.904	0.342	-131.138	0.719	551.840	2.251
2	1	98.178	-169.366	0.257	172.188			
2	2	50.345	108.918	0.189	145.458			
3		66.744	80.514	0.115	86.137	0.863	577.022	-56.817
3	1	36.773	42.689	0.085	17.359			
3	2	14.359	-45.408	0.071	-13.923			
4		22.407	-85.059	0.040	-71.555	1.038	544.583	-130.673
4	1	13.785	-126.003	0.027	-152.980			
4	2	4.178	150.890	0.025	166.493			
5		7.305	90.870	0.015	109.283	1.242	472.554	-156.621
5	1	5.049	41.725	0.008	19.251			
5	2	1.472	-33.841	0.009	-34.911			
6		2.441	-115.560	0.005	-98.535	1.469	418.392	-136.035
6	1	1.761	-179.338	0.003	168.042			
6	2	0.679	103.363	0.003	95.307			
7		0.789	7.447	0.002	16.252	1.700	398.636	-98.742
7	1	0.840	-79.938	0.001	-68.137			
7	2	0.194	-84.691	0.002	-176.430			
8		0.501	93.721	0.000	-172.531	1.917	410.352	-97.386
8	1	0.291	-152.428	0.001	5.284			
8	2	0.719	-72.245	0.001	135.427			
9		0.626	77.109	0.002	-141.753	2.140	382.519	-99.803
9	1	1.104	178.400	0.002	-0.950			
9	2	1.718	-64.833	0.004	131.209			
10		1.712	91.070	0.004	-105.634	2.478	377.356	-72.696
10	1	3.150	-127.346	0.006	43.735			
10	2	4.261	6.858	0.011	-161.098			
11		4.367	177.648	0.011	2.590	3.228	365.218	-70.620
11	1	8.440	-10.469	0.014	169.959			
11	2	10.449	153.582	0.027	-14.844			
12		9.785	-13.076	0.030	-174.330	4.710	303.633	74.598
12	1	16.877	-168.487	0.035	18.243			
12	2	19.956	28.189	0.060	-141.177			

```
ALL UNITS ARE MKS

 -INPUT DATA

   ALFAE =    13.7000
   ALFAS =     7.5000
   TAU   =     0.8500
   FREQ  = 0.170E 10
   SDE   =     0.1500
   DE    =    12.0000
   EPSLON=     1.5000

 -COMPUTED DATA

   B1    =     0.0126
   L1    =     0.1006
   GAMA  =    12.3518
   SAN   =     0.5401
   LAMEDA=     0.1765

   SRES  =     0.0441
   LENGTH OF WIRES
         0.0251     0.0295     0.0347
         0.0409     0.0481     0.0566
         0.0666     0.0783     0.0921
         0.1084     0.1275     0.1500

MAX. FREQUENCY OF OPERATION  0.299E 10

MIN. FREQUENCY OF OPERATION  0.500E 09

HEIGHT  OF LAST ELEMENT          0.163

OVERALL LENGTH OF STRUCTURE      0.541

HEIGHT OF FEED POINT             0.003
```

```
                                             RADIATORS              STUBS

AVERAGE CHARACTERISTIC IMPEDANCE     =    471.470               292.266

AVERAGE REACTANCE                    = 0.0  16786.551    0.0  10406.020

REACTANCE ABOVE OR BELOW THE AVERAGE

                        AT FEED END= 0.0  -6961.461    0.0   -124.344
                        AT VERTEX  = 0.0   3241.031    0.0      0.648
                        AT FAR END = 0.0  -6504.887    0.0    122.078
```

FREQ= 0.170E 10 WITHOUT ACCOUNTING FOR MUTUALS
NOTE - SEE MAIN PROGRAM AFTER STATEMENT 50
FOR PRINT OUT INTERPRETATION

ELEM	POINT	VOLT	VANG	CUR	CANG	Q	ZINR	
1		2559.156	-39.703	1.000	0.0	19.955	1968.935	-1634.802
1	1	1692.493	-47.881	3.782	-122.958			
1	2	368.463	-170.740	4.858	-131.143			
2		1354.365	144.875	1.927	-157.027	13.196	371.433	-596.685
2	1	1284.409	127.386	1.573	72.710			
2	2	380.514	69.248	2.865	44.847			
3		746.267	-36.271	1.839	7.395	8.884	293.576	-280.211
3	1	913.934	-74.276	0.968	-97.345			
3	2	404.520	-132.213	1.841	-158.683			
4		513.981	116.219	1.487	145.511	6.196	301.484	-169.130
4	1	649.338	56.043	0.782	43.917			
4	2	304.513	-18.984	1.254	-34.734			
5		376.172	-130.716	1.000	-118.269	4.564	367.279	-81.065
5	1	399.225	137.800	0.602	140.699			
5	2	222.539	55.925	0.745	33.977			
6		248.192	-76.540	0.643	-61.001	3.635	371.961	-103.427
6	1	217.420	178.170	0.377	174.461			
6	2	126.228	68.085	0.355	55.815			
7		127.074	-77.722	0.351	-66.378	3.239	354.632	-71.136
7	1	108.053	156.057	0.176	147.104			
7	2	59.345	15.432	0.138	13.825			
8		57.653	-150.126	0.146	-136.374	3.389	383.617	-93.816
8	1	44.532	51.399	0.073	57.589			
8	2	19.721	-114.934	0.064	-100.659			
9		20.265	58.702	0.062	71.787	4.421	319.435	-73.290
9	1	15.984	-129.127	0.034	-121.389			
9	2	7.929	33.487	0.030	54.193			
10		9.640	-179.792	0.023	-170.160	7.016	400.681	-71.534
10	1	8.624	-31.016	0.015	-44.991			
10	2	4.215	107.594	0.017	95.906			
11		4.827	-164.716	0.015	-150.206	8.466	295.352	-76.338
11	1	5.396	-54.727	0.008	-58.038			
11	2	2.487	53.242	0.010	39.584			
12		3.057	102.815	0.008	98.945	6.659	432.994	51.479
12	1	2.967	146.469	0.004	172.387			
12	2	0.398	-169.995	0.006	-139.341			

FREQ= 0.170E 10   ACCOUNTING FOR MUTUALS
NOTE - SEE MAIN PROGRAM AFTER STATEMENT 50
FOR PRINT OUT INTERPRETATION

ELEM	POINT	VOLT	VANG	CUR	CANG	Q	ZINR	
1		572.764	-11.053	1.000	0.0	0.978	562.141	-109.804
1	1	339.030	-50.473	0.694	-77.620			
1	2	109.640	-136.235	0.633	-114.661			
2		187.443	171.124	0.361	-171.533	1.173	496.000	-154.890
2	1	125.298	125.020	0.214	100.853			
2	2	36.357	48.635	0.217	51.062			
3		61.607	-27.631	0.135	-9.078	1.395	432.122	-145.032
3	1	45.497	-85.727	0.069	-101.981			
3	2	14.355	-158.385	0.074	-168.674			
4		21.190	105.963	0.051	121.545	1.627	399.278	-111.386
4	1	16.484	31.311	0.024	24.155			
4	2	5.657	-44.362	0.026	-61.910			
5		7.745	-157.254	0.018	-144.656	1.849	409.997	-91.318
5	1	5.534	108.722	0.009	108.805			
5	2	2.397	23.483	0.008	0.285			
6		2.767	-109.323	0.007	-94.580	2.064	391.987	-103.148
6	1	1.863	142.857	0.003	137.775			
6	2	0.899	29.667	0.002	16.928			
7		0.900	-116.812	0.002	-104.234	2.344	370.022	-78.199
7	1	0.634	118.333	0.001	104.218			
7	2	0.357	-23.834	0.001	-35.160			
8		0.352	166.726	0.001	-174.788	2.909	381.095	-90.801
8	1	0.293	-4.834	0.000	39.011			
8	2	0.160	151.151	0.000	-96.139			
9		0.174	-26.885	0.000	88.068	4.358	319.454	-73.164
9	1	0.264	146.833	0.000	-61.263			
9	2	0.279	-36.898	0.001	145.730			
10		0.236	171.132	0.001	17.877	8.209	403.716	-76.978
10	1	0.325	49.098	0.001	-135.343			
10	2	0.404	-89.957	0.001	85.576			
11		0.329	162.115	0.001	-8.792	11.706	281.609	-78.938
11	1	0.672	74.330	0.001	-123.557			
11	2	0.610	-45.987	0.002	156.825			
12		0.638	-83.013	0.002	78.344	6.451	428.828	43.746
12	1	1.055	-143.177	0.002	32.002			
12	2	1.294	153.643	0.004	-13.723			

```
ALL UNITS ARE MKS
 -INPUT DATA

   ALFAE =    13.7000
   ALFAS =     7.5000
   TAU   =     0.8500
   FREQ  = 0.230E 10
   SDE   =     0.1500
   DE    =    12.0000
   EPSLON=     1.5000

 -COMPUTED DATA

   B1    =     0.0126
   L1    =     0.1006
   GAMA  =    12.3518
   SAN   =     0.5401
   LAMEDA=     0.1304

   SRES  =     0.0326
   LENGTH OF WIRES
         0.0251     0.0295     0.0347
         0.0409     0.0481     0.0566
         0.0666     0.0783     0.0921
         0.1084     0.1275     0.1500

MAX. FREQUENCY OF OPERATION  0.299E 10

MIN. FREQUENCY OF OPERATION  0.500E 09

HEIGHT  OF LAST ELEMENT          0.163

OVERALL LENGTH OF STRUCTURE      0.541

HEIGHT OF FEED POINT             0.003
```

```
                                           RADIATORS              STUBS

AVERAGE CHARACTERISTIC IMPEDANCE     =   471.470             292.266

AVERAGE REACTANCE                    = 0.0  22711.219    0.0  14078.734

REACTANCE ABOVE OR BELOW THE AVERAGE

                          AT FEED END= 0.0  -9418.441    0.0   -168.223
                          AT VERTEX  = 0.0   4384.937    0.0      0.883
                          AT FAR END = 0.0  -8800.723    0.0    165.172
```

FREQ= 0.230E 10   WITHOUT ACCOUNTING FOR MUTUALS
NOTE - SEE MAIN PROGRAM AFTER STATEMENT 50
FOR PRINT OUT INTERPRETATION

ELEM	POINT	VOLT	VANG	CUR	CANG	Q	ZINR	
1		428.855	-47.221	1.000	0.0	9.374	291.269	-314.768
1	1	512.211	-80.898	0.532	-109.131			
1	2	212.429	-137.887	1.043	-164.892			
2		287.973	110.902	0.804	142.345	6.499	305.676	-186.899
2	1	355.897	54.278	0.434	40.048			
2	2	169.656	-20.371	0.691	-35.261			
3		205.739	-129.633	0.564	-116.867	4.744	355.472	-80.539
3	1	229.276	141.669	0.330	144.482			
3	2	124.175	62.761	0.431	40.169			
4		141.605	-67.754	0.363	-51.879	3.731	375.158	-106.687
4	1	124.841	-170.403	0.218	-173.713			
4	2	74.232	83.143	0.208	69.507			
5		74.583	-60.979	0.206	-47.930	3.264	352.463	-81.686
5	1	62.673	176.950	0.106	168.063			
5	2	35.475	41.788	0.084	35.633			
6		34.871	-121.336	0.087	-109.176	3.327	392.341	-84.523
6	1	27.513	83.965	0.043	88.701			
6	2	12.435	-80.227	0.037	-64.298			
7		12.581	97.354	0.036	112.415	4.197	333.657	-89.636
7	1	9.994	-85.987	0.019	-77.037			
7	2	5.003	82.312	0.017	101.641			
8		5.657	-125.359	0.014	-120.668	6.569	406.613	-32.957
8	1	4.760	27.066	0.009	11.555			
8	2	2.249	165.772	0.010	160.522			
9		2.862	-96.390	0.008	-83.230	8.590	341.422	-77.109
9	1	2.882	18.239	0.005	14.445			
9	2	1.620	127.331	0.005	118.881			
10		1.633	-178.431	0.005	-170.469	6.830	312.042	-50.147
10	1	1.561	-108.605	0.002	-114.386			
10	2	0.709	-55.325	0.002	-42.168			
11		0.683	-46.356	0.002	-32.517	7.178	310.435	-83.529
11	1	0.464	-36.405	0.001	-29.144			
11	2	0.127	-19.171	0.001	-23.850			
12		0.289	-98.345	0.001	-47.451	9.756	450.431	-190.014
12	1	0.422	-118.631	0.000	173.289			
12	2	0.182	-91.447	0.001	145.456			

FREQ= 0.230E 10 ACCOUNTING FOR MUTUALS
NOTE - SEE MAIN PROGRAM AFTER STATEMENT 50
FOR PRINT OUT INTERPRETATION

ELEM	POINT	VOLT	VANG	CUR	CANG	Q	ZINR	
1		463.548	-18.689	1.000	0.0	1.363	439.105	-148.536
1	1	338.683	-74.827	0.521	-92.296			
1	2	105.104	-147.306	0.554	-156.515			
2		158.313	119.261	0.378	135.525	1.595	401.602	-117.164
2	1	122.778	47.346	0.182	38.662			
2	2	41.490	-28.128	0.193	-44.191			
3		57.389	-138.001	0.137	-125.551	1.819	408.014	-90.082
3	1	41.826	130.200	0.069	130.234			
3	2	17.466	47.805	0.064	24.201			
4		20.775	-82.826	0.051	-68.127	2.033	396.334	-104.007
4	1	13.890	171.222	0.026	167.462			
4	2	6.730	63.465	0.019	47.158			
5		6.918	-81.651	0.018	-68.819	2.295	369.699	-84.491
5	1	4.805	153.516	0.008	145.500			
5	2	2.330	16.471	0.006	11.215			
6		2.285	-146.314	0.006	-134.280	2.797	387.960	-84.125
6	1	1.646	59.459	0.003	61.013			
6	2	0.711	-104.795	0.002	-93.584			
7		0.717	72.800	0.002	82.978	4.057	336.470	-90.335
7	1	0.559	-107.317	0.001	-109.610			
7	2	0.268	68.684	0.001	63.541			
8		0.259	-149.206	0.001	-149.078	7.472	415.667	-23.379
8	1	0.242	-19.648	0.001	2.949			
8	2	0.227	119.027	0.000	160.711			
9		0.167	-92.222	0.001	-143.281	11.719	348.281	-82.410
9	1	0.230	-59.101	0.001	18.764			
9	2	0.278	115.026	0.000	14.616			
10		0.227	110.553	0.001	-152.224	10.939	295.141	-44.468
10	1	0.159	-20.361	0.001	-161.602			
10	2	0.327	-62.631	0.001	143.810			
11		0.335	-66.572	0.000	123.007	5.789	318.920	-72.609
11	1	0.603	-69.298	0.001	110.226			
11	2	0.717	-80.722	0.002	106.929			
12		0.580	-31.607	0.002	160.290	9.773	450.730	-190.470
12	1	1.240	35.192	0.002	-156.796			
12	2	1.497	79.964	0.004	-92.820			

INITIAL DISTRIBUTION LIST

		No. Copies
1.	Defense Documentation Center Cameron Station Alexandria, Virginia 22314	20
2.	Library Naval Postgraduate School Monterey, California 93940	2
3.	Naval Ship Systems Command Department of the Navy Washington, D. C. 20360	1
4.	Estado Maior da Armada Ministerio da Marinha P. do Comercio Lisboa Portugal	10
5.	Professor Paul E. Cooper Department of Electrical Engineering Naval Postgraduate School Monterey, California 93940	1
6.	Granger Associates 1601 California Avenue Palo Alto, California 94304	1
7.	Dr. John W. Greiser 11400 Alford Avenue Los Altos, California	1
8.	Ten. Victor M. Novais Gonsalves Direccao do Servico de Pessoal Ministerio da Marinha P. do Comercio Lisboa Portugal	1

Unclassified
Security Classification

DOCUMENT CONTROL DATA - R&D

(Security classification of title, body of abstract and indexing annotation must be entered when the overall report is classified)

1. ORIGINATING ACTIVITY *(Corporate author)* Naval Postgraduate School Monterey, California 93940	2a. REPORT SECURITY CLASSIFICATION Unclassified 2b. GROUP

3. REPORT TITLE

The Analysis of a Log-Periodic Zig-Zag Antenna

4. DESCRIPTIVE NOTES *(Type of report and inclusive dates)*

5. AUTHOR(S) *(Last name, first name, initial)*

Gonsalves, Victor Manuel Nogueira Novais

6. REPORT DATE	7a. TOTAL NO. OF PAGES	7b. NO. OF REFS
September, 1967	134	25

8a. CONTRACT OR GRANT NO. N/A b. PROJECT NO. c. d. Distribution unlimited	9a. ORIGINATOR'S REPORT NUMBER(S) 9b. OTHER REPORT NO(S) *(Any other numbers that may be assigned this report)*

10. AVAILABILITY/LIMITATION NOTICES

~~This document is subject to special export controls and each transmittal to foreign governments or foreign nationals may be made only with prior approval of the Naval Postgraduate School.~~

11. SUPPLEMENTARY NOTES	12. SPONSORING MILITARY ACTIVITY Naval Ship Systems Command Department of the Navy Washington, D. C. 20360

13. ABSTRACT

During recent years, logarithmically periodic antennas have been widely used due to their frequency response characteristics, simplicity of design and directivity. However, their theory of operation still is in a development phase, and very few models have been fully analyzed. The present paper is an attempt to analyze the operation of a zig-zag model that has the property of being symmetrical, and suitable for operation against ground. The radiation pattern of the antenna is obtained for different models of current distribution, and, finally, the impedance characteristics and an approximate current distribution are obtained, using non-uniform transmission line theory. The results obtained show reasonable agreement with experimental data, and confirm conclusions drawn from physical considerations.

DD FORM 1 JAN 64 1473

Unclassified
Security Classification

Unclassified
Security Classification

14 KEY WORDS	LINK A		LINK B		LINK C	
	ROLE	WT	ROLE	WT	ROLE	WT
Antenna						
Log-Periodic						
Zig-Zag						
Bent Zig-Zag						

DD FORM 1 NOV 65 1473 (BACK)
S/N 0101-807-6821

Unclassified
Security Classification

A-31409